

UNIVERSITAT ROVIRA I VIRGILI

Application of Advanced Oxidation Processes in the Reclamation of Wastewaters from the Oil
& Gas Sector

Hande Demir Duz

UNIVERSITAT ROVIRA I VIRGILI

Application of Advanced Oxidation Processes in the Reclamation of Wastewaters from the Oil
& Gas Sector

Hande Demir Duz

Hande Demir Duz

**Application of Advanced Oxidation Processes in the
Reclamation of Wastewaters from the Oil & Gas Sector**

Doctoral Thesis

Supervised by:

Dr. Sandra Contreras Iglesias

Dr. Mayra García Álvarez

Departament d'Enginyeria Química



UNIVERSITAT ROVIRA i VIRGILI

Tarragona (Spain)

2020

UNIVERSITAT ROVIRA I VIRGILI

Application of Advanced Oxidation Processes in the Reclamation of Wastewaters from the Oil
& Gas Sector

Hande Demir Duz



UNIVERSITAT ROVIRA I VIRGILI

DEPARTMENT OF CHEMICAL ENGINEERING
ESCOLA TÈCNICA SUPERIOR D'ENGINYERIA QUÍMICA

Av. Països Catalans, 26, 43007, Tarragona (Spain)

Tel. +34 977 55 96 03 / 04 Fax +34 977 55 96 21

e-mail: secdeq@etseq.urv.es

<http://www.etseq.urv.es/DEQ/>

I STATE that the present study, entitled “Application of Advanced Oxidation Processes in the Reclamation of Wastewaters from the Oil & Gas Sector”, presented by Hande Demir Duz for the award of the degree of Doctor, has been carried out under my supervision at the Chemical Engineering Department of this university.

Tarragona, 6th of July 2020

Doctoral Thesis Supervisor/s

A handwritten signature in black ink, appearing to read "Sandra Contreras Iglesias". The signature is written in a cursive style and is enclosed within a faint, hand-drawn oval.

Dr. Sandra Contreras Iglesias

A handwritten signature in blue ink, appearing to read "Mayra García Álvarez". The signature is written in a cursive style and is enclosed within a faint, hand-drawn oval.

Dr. Mayra García Álvarez

UNIVERSITAT ROVIRA I VIRGILI

Application of Advanced Oxidation Processes in the Reclamation of Wastewaters from the Oil
& Gas Sector

Hande Demir Duz

ACKNOWLEDGEMENTS

I would like to express my deepest gratitude to all who made this thesis possible with their professional and personal supports. Thank you very much!

First of all, I would like to present my special thanks and gratitude to my supervisors, Dr. Sandra Contreras and Dr. Mayra García Álvarez, for giving me the opportunity to involve in the projects that formed this thesis, also, for their limitless supports that contributed to my personal and professional improvements, always keeping my motivation high during this Ph.D.

I would like to thank to Dr. Francisco Medina Cabello for letting me be the part of CATHETER research group that provides any source and support made my Ph.D. completed smoothly. Also, I would like to present my gratitude to Vanessa, Sandra, Anton, Abel and especially to Susana for all their administrative and technical helps during the evolution of my Ph.D. from the beginning to the end and for their friendship.

At the University of Alberta, firstly, I would like to thank to Dr. Mohamed Gamal El-Din for accepting me to his research group that allowed me to be part of his projects that improved my knowledge on my profession. I also would like to thank to Pamela, Selamawith, Lingling for their support to accommodate myself to the working area fast and for their guidance that helped me to obtain many results in a short time. Specially, I also would like to present my thankfulness to my colleagues, Mirna, Abdulrahim, Rui, Lingjun and Shailesh for their help in the laboratory and for their friendship during my stay in Canada.

I also would like to acknowledge Marti-Franques Research Grant (2016PMF-PIPF-30) given by Universitat Rovira I Virgili, the funding from the European Union's Horizon 2020 research and innovation program under grant agreement No 688989 and Agència de Gestió d'Ajuts Universitaris i de Recerca (AGAUR, 2017SGR01516) that supported the research within this thesis financially. In addition, I would like to acknowledge the financial support provided during my research stay in Canada by Natural Sciences and Engineering Research Council of Canada (NSERC), Senior Industrial Research Chair (IRC) in Oil Sands Tailings Water Treatment and, as a part of the University of Alberta's Future Energy Systems research initiative, the funding from the Canada First Research Excellence Fund.

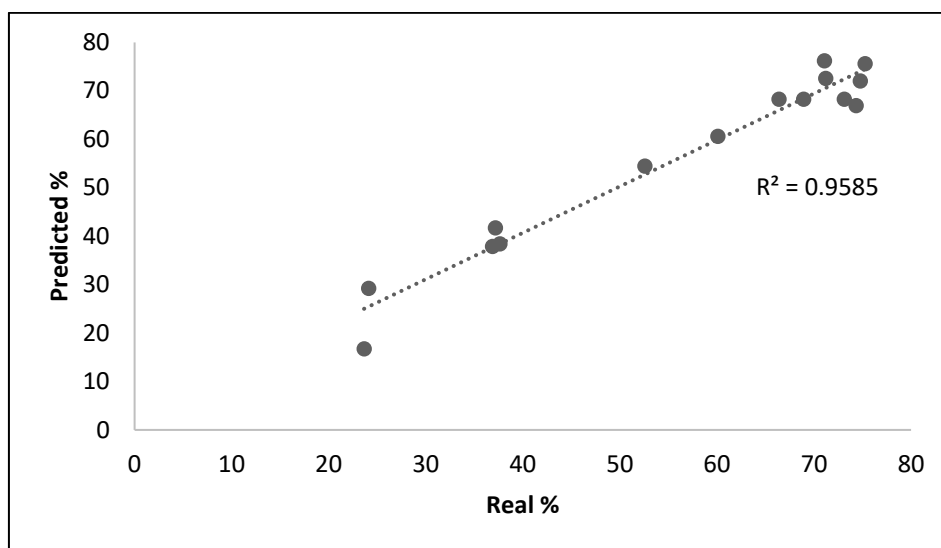


Figure 4.5 Experimental responses versus predicted responses by Box-Behnken design applied for RRW2.

According to **Table 4.6**, the quadratic model obtained by the Box-Behnken design (*eq. 3*) with a Model F-value of 34.61 was considered significant. The lack of fit of 2.13 indicates that there is a good fit of the model relative to pure error. This is seen, in addition, with the regression coefficient (R^2) of 97.19%, adjusted R^2 of 94.38% and predicted R^2 of 82.43% that presents the adequate match of the model and the response. Therefore, the model was used to determine the optimized parameters for the current process. **Table 4.6** also presents the optimum conditions predicted by the model with the desirability of 1 and their responses either the observed or the predicted ones which had low standard deviation (SD) as expected.

4.3.3 Treatment assessment by TOC

Considering the feasibility of the ozone-based treatment for the treatment of RRW2, the boundaries that were determined for the response surface methodology were kept reasonable in terms of the costs of the operation and the resources.

According to the optimized parameters presented in **Table 4.6**, it is possible to reach the final TOC requirements with the H_2O_2 amount down to 47 mg/L when the treatment lasts 60 min keeping the O_3 feed rate at 0.9 g/h. However, considering the cost of O_3 production, it can be more realistic to apply the parameters given in Run 15 in **Table 4.5**, which could reduce the operation time down to 37.5 min rather than 60 min while increasing the H_2O_2 amount to 80 mg/L. Thus, some of the energy requirement for the O_3 formation from O_2 and for other operations could be saved by

increasing the consumption of the reagent. A comparison between these two cases was performed in terms of energy and reagent consumptions (**Table 4.7**). The calculation of electrical energy per order (EEO) for O₃ treatment was reported before by Jiménez et al. by the *eq. 4*, where the P is rated power, V is the volume of effluent treated, t is the treatment duration and TOC_i and TOC_f is initial and final TOC values [24].

$$EEO \left(\frac{kWh}{m^3} \right) = \frac{P(kW) * t(h) * 1000}{V(L) * \log \left(\frac{TOC_i}{TOC_f} \right)} \quad (4)$$

The rated power (P) was calculated as 0.19 kW including 0.002 kW of stirring, 0.008 kW for ozone measurer with O₃ destruction catalyst and 0.009 kW for ozone generator, which was calculated by for the constant O₃ production of 0.9 kg/h that was used for the optimum conditions obtained by the model (ozone generator consumed around 10 kW/Kg O₃ according to the supplier). As the reagents, 38,57 m³/h of oxygen (with a unit price of 3 Eur/m³ [31]) gas for O₃ generation and H₂O₂ with a unit price of 346 Eur/m³ were consumed. Thus, 37% of total cost could be saved by changing parameters. Also, since the operation and reagent costs of the large-scale operations are lower than those of laboratory scale operations, the saving can be higher for scaled-up operations.

In accordance with the treatment conditions and response of RRW2, RRW3 was treated within the parameter boundaries that were considered for RRW2 to compare the treatment impact depending on the changing characteristics. The initial treatment of RRW3 conducted with the optimized parameters of RRW2 (**Table 4.6**) resulted in an average TOC removal of 67%, by which final TOC reached ca. 9 mg C/L. Thus, although the boundaries for H₂O₂ and O₃ were kept at the same range, treatment time was enlarged up to 90 min rather than 60 min to check whether the target final TOC can be reached.

Table 4.7 Energy consumption comparison of different operation parameters.

		Treatment Conditions				Costs per unit		
Required		O ₃ (kg)	Time (h)	EEO (kWh/m ³)	O ₂ (Eur/m ³)	35% H ₂ O ₂ (Eur/m ³)	Cost of energy (Eur/kWh)	
C _{H2O2} (g/m ³)	35% H ₂ O ₂ (L/m ³)							
Case 1	47	0.9	1	95.1	3	346	0.148	
Case 2	80	0.56	0.625	67.1				
Calculated cost per treatment								
				Case 2				
35% H ₂ O ₂ (Eur/m ³)	Energy (Eur/m ³)	O ₂ (Eur/m ³)	Total (Eur/m ³)	35% H ₂ O ₂ (Eur/m ³)	Energy (Eur/m ³)	O ₂ (Eur/m ³)	Total (Eur/m ³)	Cost save
0.025	14	116	130	0.042	10	72	82	37%

Figure 4.6 presents the effect of H_2O_2 addition to the system. For all cases, most of the total organic carbon was removed in 30 min in the presence of H_2O_2 . However, in the absence of H_2O_2 (**Figure 4.6a**), TOC removal reached up to 56% with an O_3 dosing of 2.7 g/h after 90 min treatment, while the treatment efficiency of 1.8 g O_3 /h was already 54%. Ozone depletion (calculated by residual O_3 measured during both experiments) was higher at the highest feed rate, indicating that even if ozone dissolved in RRW3 can be increased, reacted ozone does not increase, which showed the unnecessary of excessive amount of O_3 feed for the treatment. In the presence of H_2O_2 , even with small addition of H_2O_2 (**Figure 4.6b**), TOC removal efficiency was slightly increased in 30 min (10% more than the treatment without H_2O_2). When the H_2O_2 /COD ratio (w/w) was increased to 1.05 (**Figure 4.6c**), 30-min treatment efficiency reached around 60% regardless to the O_3 feed amount, while that of the H_2O_2 /COD ratio (w/w) 2 (**Figure 4.6d**) varied between 55% to 75% depending on the O_3 feed ratio. This behavior could be explained by the changes in radicals that competed to attack the organic contaminants faster than the other while changing the intermediate product. Thus, the reaction pathway may change depending on the by-products occurred during the treatment. Bourgin et al. explained the similar behavior of the selectivity of direct reaction of ozone and the $\text{O}_3/\text{H}_2\text{O}_2$ treatment due to the hydroxyl radicals on the abatement of some micropollutants from water [32].

In the best of the cases giving the maximum removal, the final TOC reached for RRW3 was 5.15 mg C/L. This value was obtained by using the highest amounts of reagents after 90-min treatment, which were H_2O_2 /COD ratio (w/w) of 2 and 2.7 g O_3 /h. On the other hand, the target TOC (4 mg C/L) could only be reached by discontinuous addition of H_2O_2 rather than its initial addition at once. When the required amount of H_2O_2 (160 mg/L for the H_2O_2 /COD ratio (w/w) of 2) was added at 4 times (40 mg/L for each addition in every 15 min), final TOC of 3.32 mg C/L was reached after 90-min treatment. This suggests that, in those cases where the H_2O_2 is added at once for RRW3 treatment, there is an excessive H_2O_2 present in the solution which likely acts as a scavenger, thus consuming the $\text{HO}\cdot$ generated. Although the O_3 depletion (measured as the difference between feed rate and residual rate) is higher at higher concentrations of H_2O_2 (because of the interactions between them), the rate may vary due to the scavenging effect of excessive H_2O_2 (and hydroxyl ion) in reacting with hydroxyl radical, which negatively affects the organics degradation/mineralization.

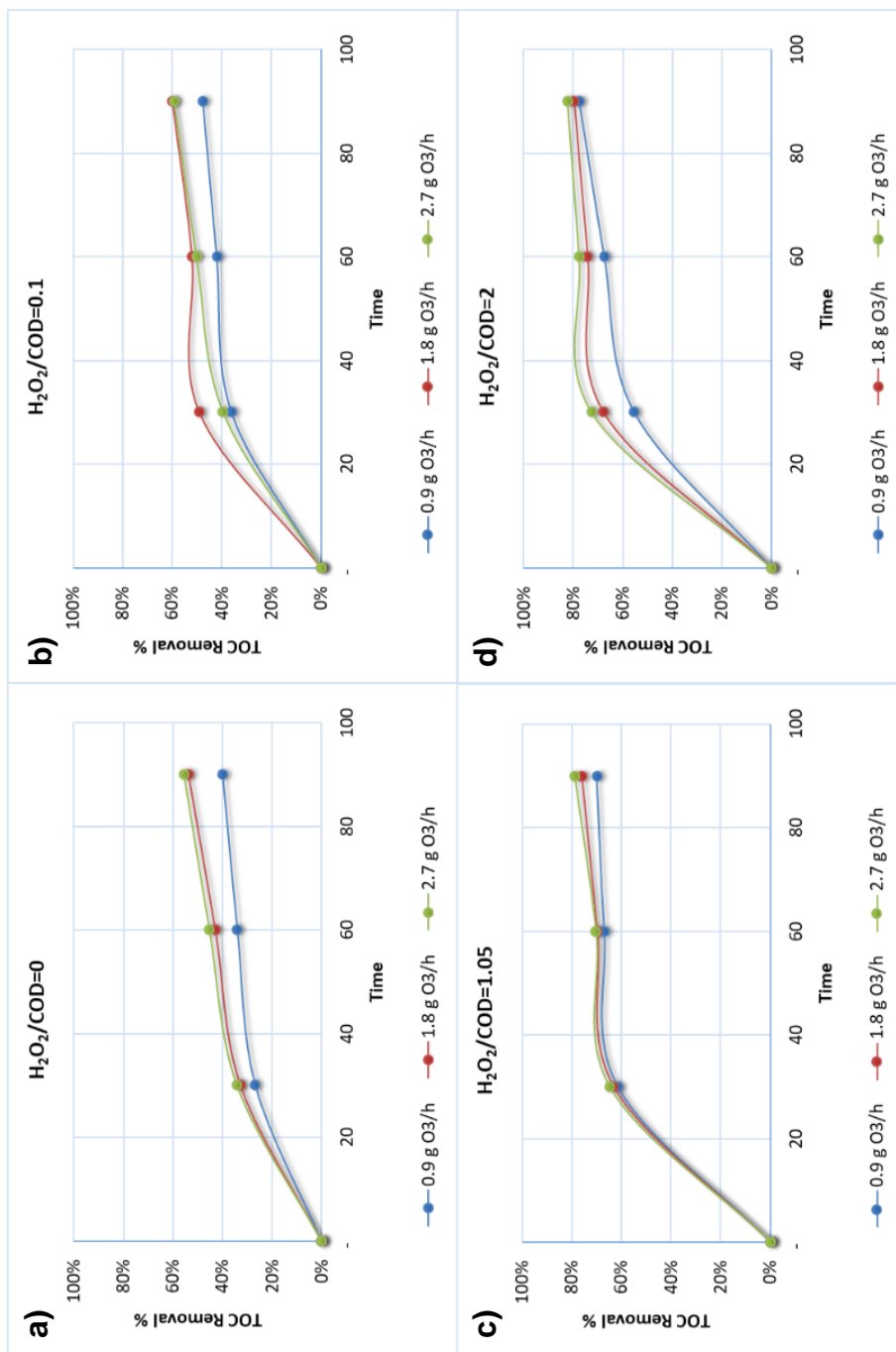


Figure 4.6 RRW3 Treatment efficiencies of ozone-based studies depending on the varied H_2O_2/COD ratios (w/w) between 0-2.

CHAPTER 4: Reuse and Recycle Solutions in Refineries by Ozone-Based Advanced Oxidation Processes: A Statistical Approach

Then, the compositional difference between RRW2 and RRW3 affects to the treatment efficiencies or required amounts of reagents. In this case, RRW3 present higher amount of recalcitrant products (likely saturated alkanes) than RRW2 having an inhibiting effect on the ozonation treatment. Thus, fluctuations in the water properties and components that can occur either during the production or in the different points of each plant pretreatment may affect to the ozonation efficiency to achieve the water requirements to reuse.

4.3.4 Oxidant consumption

The contour plots present a relationship between H_2O_2 and O_3 (**Figure 4.4**), which motivates further attention to oxidant consumption behavior during the treatments. Thus, initially, ozone consumption (calculated from residual monitored during the reactions) has been considered as a significant indicator to find the optimized amount of oxidant to be fed into the system. **Figure 4.7** shows the importance of the initial O_3 feed rate recorded during the experiments conducted with RRW2. The time factors have been selected according to the case of reaching to 0.9 g feed (Feed(g) = O_3 dose (g/h)*t (h)). Thus, O_3 dosing was performed during 60 min, 30 min and 20 min for 0.9 g/h, 1.8 g/h and 2.7 g/h O_3 feed, respectively. According to the obtained results, when the feed rate was kept at 0.9 g/h, increasing H_2O_2 amount did not change the O_3 consumption rate, which reached only up to 9% of the feed amount. However, when the feed rate increased to 1.8 g/h and 2.7 g/h, consumed amount of O_3 increased to 25% when the O_3 feed reached to 0.9 g. Besides, increasing the feed rate from 1.8 g/h to 2.7 g/h did not change either the O_3 consumption or the TOC removal significantly, which presented the high amount of O_3 feed to be redundant. Khuntia et al., reported the similar consumption increase with increasing O_3 dose [33].

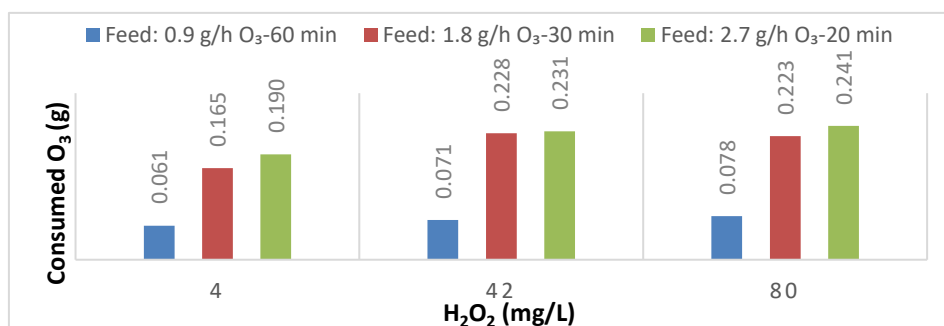


Figure 4.7 Ozone consumption (reacted + dissolved) at the time that reached to the same O_3 feed amount of 0.9 g by different feed rate.

CHAPTER 4: Reuse and Recycle Solutions in Refineries by Ozone-Based Advanced Oxidation Processes: A Statistical Approach

Figure 4.8 exhibits the significance of the optimum oxidant feed for the maximum TOC removal for the experiments conducted with RRW2 during 37.5 min. The number of run represents the conditions of the experiments given in **Table 4.5** previously. The green data present the ratio of consumed O_3 amount calculated based on the *eq. 1* to remove TOC (mole/mole), while the purple data present the ratio between consumed O_3 and consumed H_2O_2 (mole/mole). The consumed amount of H_2O_2 was determined by the semi-quantitative strips that gives a range of concentration in mg/L. In case of any detected H_2O_2 amount in the samples, calculations were made based on the lower scale of the range assuming the higher amount of reagent consumption. Notably, when an insufficient amount of H_2O_2 was added to the reactor (i.e. 4 mg/L) as in the case of Run 2 and 4, most of the O_3 seems not to react with the organic matter, reaching a low %TOC removal and, therefore, being ineffective treatment conditions. On the other hand, when higher amount of H_2O_2 (i.e. 80 mg/L) was fed as in the cases of Run 1 and Run 15, the oxidants resulted more efficient in removing the carbon content. In these cases, both the O_3 cons/TOC and O_3 cons/ H_2O_2 cons ratios decrease compared to the former cases. Indeed, conditions used in Run 15 were markedly more efficient in terms of effective consumption of oxidants reaching the higher TOC removal while reducing the unreacted oxidant amount. This result totally agrees with the optimized conditions found previously through box-Behnken response surface methodology to achieve lower costs maintaining high TOC removal, as presented in this chapter, **section 4.3.3**.

In case of the treatment of RWW3, similar consumption behavior was obtained. When the treatment ends in 30 min (**Figure 4.9a**), the most effective reagent consumption was achieved with 160 mg/L of H_2O_2 and 0.9 g/h O_3 (E7) reaching 55% of TOC removal. The increase in O_3 dose resulted in higher TOC removal; however, this also cause an increase in O_3 wastage. On the other hand, increasing the reaction time to 90 min (**Figure 4.9c**) led to higher TOC removals still preserving the effective consumption of the reagents. Nevertheless, again the optimum conditions can be determined according to the cost analysis for each case.

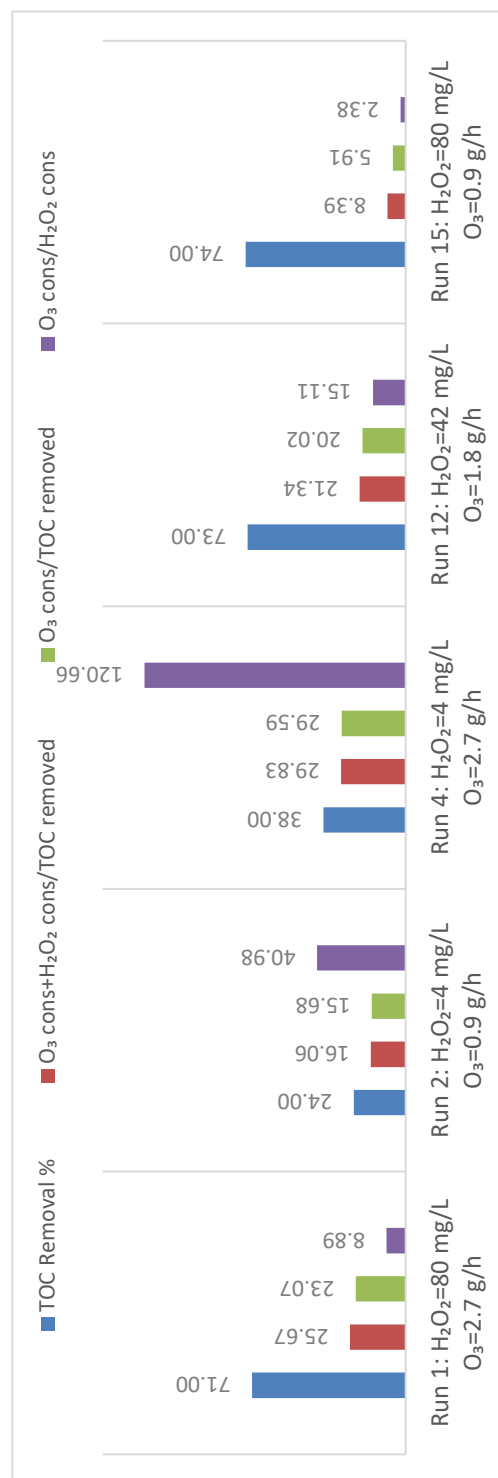


Figure 4.8 The oxidant consumption ratios (mole/mole) compared to TOC removal % for RRW2 treatment during 37.5 min.

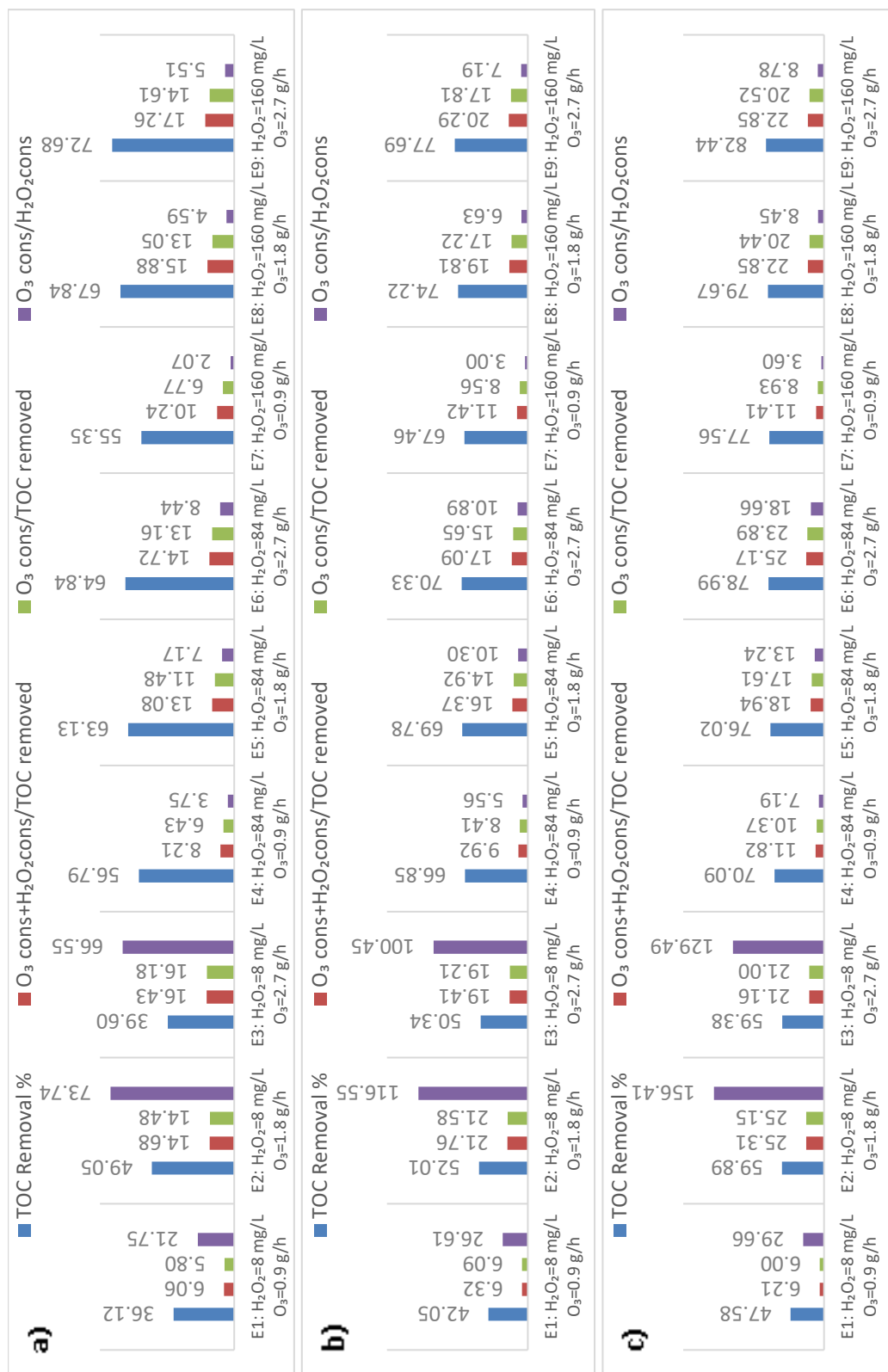


Figure 4.9 The oxidant consumption ratios (mole/mole) compared to TOC Removal % for RRW3 treatment a) 30 min, b) 60 min, c) 90 min.

4.4 Conclusions

The selection of optimal conditions for effective degradation of two wastewater effluents from a refinery in Turkey collected after biological treatment was studied using fractional factorial design; whereas, the optimization of the significant parameters was performed by Box-Behnken response surface methodology.

According to the screening results obtained by the fractional factorial design, it was found that both the reagents concentration used for the treatment and the time were very significant for the treatment efficiency, while pH was found insignificant in terms of its effect on TOC removal. The optimized parameters by Box-Behnken design indicated that it is possible to reach the TOC requirements for reuse purposes by adjusting the amount of H_2O_2 and reaction time at low feed O_3 rates. Thus, optimization allows reducing operational costs maintaining the process effectiveness to reach the established target. The ratio between consumed O_3 and H_2O_2 played a crucial role for an optimum treatment either in terms of efficiency or for the operation costs. However, the effect of initial characteristics of the effluents must be taken into account to determine the appropriate oxidant feed.

According to local water specifications for reclamation, peroxone treatment appears as a promising technique for water polishing allowing water recycling in refineries. The final characteristics of the treated water make it suitable to be reused in the plant's cooling towers or stored for fire extinction or cleaning purposes, which are the major water consumption sources of a refinery. This allows decreasing substantially the raw water consumption and generates a positive impact at different levels: social, economic and environmental.

An important point concerns to the fluctuation in the characteristics of the effluent, which was found rather significant in the treatment efficiency and the operational conditions that should be adjusted. This is especially important for real applications in situ, since the water variability in the refinery is highly expected with time and season. However, we have shown here that this problem may be overcome by means of detailed statistical approaches, which may be extrapolated to a refinery scenario through the development of a decision support system.

References

- [1] I.N. Dias, A.C. Cerqueira, G.L. Sant'Anna Jr., M. Dezotti, Oil refinery wastewater treatment in biofilm reactor followed by sand filtration aiming water reuse, *J. Water Reuse Desalin.* 2

CHAPTER 4: Reuse and Recycle Solutions in Refineries by Ozone-Based Advanced Oxidation Processes: A Statistical Approach

- (2012) 84–91. doi:10.2166/wrd.2012.022.
- [2] C.J. Escudero, O. Iglesias, S. Dominguez, M.J. Rivero, I. Ortiz, Performance of electrochemical oxidation and photocatalysis in terms of kinetics and energy consumption. New insights into the p-cresol degradation, *J. Environ. Manage.* 195 (2017) 117–124. doi:10.1016/j.jenvman.2016.04.049.
- [3] G. Boczkaj, A. Fernandes, Wastewater treatment by means of advanced oxidation processes at basic pH conditions: A review, *Chem. Eng. J.* 320 (2017) 608–633. doi:10.1016/j.cej.2017.03.084.
- [4] M.H. El-Naas, M.A. Alhaija, S. Al-Zuhair, Evaluation of a three-step process for the treatment of petroleum refinery wastewater, *J. Environ. Chem. Eng.* 2 (2014) 56–62. doi:10.1016/j.jece.2013.11.024.
- [5] A.L.N. Mota, L.F. Albuquerque, L.T.C. Beltrame, O. Chiavone-Filho, A. Machulek Jr., C.A.O. Nascimento, Advanced oxidation processes and their application in the petroleum industry: a review, *Brazilian J. Pet. Gas.* 2 (2008) 122–142. doi:10.5419/bjpg.v2i3.57.
- [6] M. Al Zarooni, W. Elshorbagy, Characterization and assessment of Al Ruwais refinery wastewater, *J. Hazard. Mater.* 136 (2006) 398–405. doi:10.1016/j.jhazmat.2005.09.060.
- [7] S. Srikanth, M. Kumar, S.K. Puri, Bio-electrochemical system (BES) as an innovative approach for sustainable waste management in petroleum industry, *Bioresour. Technol.* 265 (2018) 506–518. doi:https://doi.org/10.1016/j.biortech.2018.02.059.
- [8] IFP Energies nouvelles, Water in fuel production, *Panorama* 2011. (2010) 1–10. https://www.researchgate.net/publication/276292861_Water_in_fuel_production_Oil_production_and_refining (accessed September 28, 2019).
- [9] S. Jafarinejad, S.C. Jiang, Current technologies and future directions for treating petroleum refineries and petrochemical plants (PRPP) wastewaters, *J. Environ. Chem. Eng.* 7 (2019) 103326. doi:https://doi.org/10.1016/j.jece.2019.103326.
- [10] C.F. Bustillo-Lecompte, M. Knight, M. Mehrvar, Assessing the performance of UV/H₂O₂ as a pretreatment process in TOC removal of an actual petroleum refinery wastewater and its inhibitory effects on activated sludge, *Can. J. Chem. Eng.* 93 (2015) 798–807. doi:10.1002/cjce.22180.
- [11] X. Jia, Z. Li, R.R. Tan, D.C.Y. Foo, T. Majozzi, F. Wang, Interdisciplinary contributions to sustainable water management for industrial parks, *Resour. Conserv. Recycl.* 149 (2019) 646–648. doi:https://doi.org/10.1016/j.resconrec.2019.06.034.
- [12] S.S.H. Ziabari, S.M. Khezri, R.R. Kalantary, Ozonation optimization and modeling for treating diesel-contaminated water, *Mar. Pollut. Bull.* 104 (2016) 240–245. doi:10.1016/j.marpolbul.2016.01.017.
- [13] V.S.R. Rajasekhar Pullabhotla, C. Southway, S.B. Jonnalagadda, Ozone initiated oxidation of hexadecane with metal loaded γ -Al₂O₃ catalysts, *Catal. Lett.* 124 (2008) 118–126. doi:10.1007/s10562-008-9434-4.

CHAPTER 4: Reuse and Recycle Solutions in Refineries by Ozone-Based Advanced Oxidation Processes: A Statistical Approach

- [14] C. Chen, H. Chen, X. Guo, S. Guo, G. Yan, Advanced ozone treatment of heavy oil refining wastewater by activated carbon supported iron oxide, *J. Ind. Eng. Chem.* 20 (2014) 2782–2791. doi:10.1016/j.jiec.2013.11.007.
- [15] A. Coelho, A. V. Castro, M. Dezotti, G.L. Sant’Anna Jr., Treatment of petroleum refinery sourwater by advanced oxidation processes, *J. Hazard. Mater.* 137 (2006) 178–184. doi:10.1016/j.jhazmat.2006.01.051.
- [16] B.M. Souza, B.S. Souza, T.M. Guimarães, T.F.S. Ribeiro, A.C. Cerqueira, G.L. Sant’Anna, M. Dezotti, Removal of recalcitrant organic matter content in wastewater by means of AOPs aiming industrial water reuse, *Environ. Sci. Pollut. Res.* 23 (2016) 22947–22956. doi:10.1007/s11356-016-7476-5.
- [17] G. Boczkaj, A. Fernandes, P. Makos, Study of different advanced oxidation processes for wastewater treatment study of different advanced oxidation processes for wastewater treatment from petroleum bitumen production at basic pH, *Ind. Eng. Chem. Res.* 56 (2017) 8806–8814. doi:10.1021/acs.iecr.7b01507.
- [18] S.T. Narendran, S.N. Meyyanathan, V.V.S.R. Karri, Experimental design in pesticide extraction methods: A review, *Food Chem.* 289 (2019) 384–395. doi:10.1016/j.foodchem.2019.03.045.
- [19] P.K. Sahu, N.R. Ramiseti, T. Cecchi, S. Swain, C.S. Patro, J. Panda, An overview of experimental designs in HPLC method development and validation, *J. Pharm. Biomed. Anal.* 147 (2018) 590–611. doi:10.1016/j.jpba.2017.05.006.
- [20] D.C. Montgomery, *Design and analysis of experiments*, Eighth, John Wiley & Sons, Inc., Hoboken, 2017. <https://lccn.loc.gov/2017002355>.
- [21] M. Jamshidnezhad, *Experimental design in petroleum reservoir engineering*, in: *Exp. Des. Pet. Reserv. Stud.*, Gulf Professional Publishing, Waltham, 2015.
- [22] J. Rodríguez-Chueca, C. Amor, J.R. Fernandes, P.B. Tavares, M.S. Lucas, J.A. Peres, Treatment of crystallized-fruit wastewater by UV-A LED photo-Fenton and coagulation-flocculation, *Chemosphere* 145 (2016) 351–359. doi:10.1016/j.chemosphere.2015.11.092.
- [23] A.R. Ribeiro, O.C. Nunes, M.F.R. Pereira, A.M.T. Silva, An overview on the advanced oxidation processes applied for the treatment of water pollutants defined in the recently launched Directive 2013/39/EU, *Environ. Int.* 75 (2015) 33–51. doi:10.1016/j.envint.2014.10.027.
- [24] S. Jiménez, M. Andreozzi, M.M. Micó, M.G. Álvarez, S. Contreras, Produced water treatment by advanced oxidation processes, *Sci. Total Environ.* 666 (2019) 12–21. doi:10.1016/j.scitotenv.2019.02.128.
- [25] F.J. Beltran, *Ozone reaction kinetics for water and wastewater systems*, Lewis Publishers, Boca Raton, 2004.
- [26] A. Deligiorgis, N.P. Xekoukoulotakis, E. Diamadopoulou, D. Mantzavinos, Electrochemical oxidation of table olive processing wastewater over boron-doped diamond electrodes: Treatment optimization by factorial design, *Water Res.* 42 (2008) 1229–1237.

CHAPTER 4: Reuse and Recycle Solutions in Refineries by Ozone-Based Advanced Oxidation Processes: A Statistical Approach

doi:10.1016/j.watres.2007.09.014.

- [27] G. Hayder, M.Z. Ramli, M.A. Malek, A. Khamis, N.M. Hilmin, Prediction model development for petroleum refinery wastewater treatment, *J. Water Process Eng.* 4 (2014) 1–5. doi:10.1016/j.jwpe.2014.08.006.
- [28] S. Shafiei, A. Ebadi, A.D. Kiadehi, A. Aghaeinejad-Meybodi, A. Khataee, Degradation of Fluoxetine using catalytic ozonation in aqueous media in the presence of nano- γ -alumina catalyst: Experimental, modeling and optimization study, *Sep. Purif. Technol.* 211 (2018) 551–563. doi:10.1016/j.seppur.2018.10.020.
- [29] P. Stepnowski, E.M. Siedlecka, P. Behrend, B. Jastorff, Enhanced photo-degradation of contaminants in petroleum refinery wastewater, *Water Res.* 36 (2002) 2167–2172. doi:10.1016/S0043-1354(01)00450-X.
- [30] R. de Abreu Domingos, F.V. da Fonseca, Evaluation of adsorbent and ion exchange resins for removal of organic matter from petroleum refinery wastewaters aiming to increase water reuse, *J. Environ. Manage.* 214 (2018) 362–369. doi:10.1016/j.jenvman.2018.03.022.
- [31] Boconline, Boconline, (2019). <https://www.boconline.co.uk/shop/en/uk/gas-a-z/oxygen/oxygen-cylinder> (accessed October 3, 2019).
- [32] M. Bourgin, E. Borowska, J. Helbing, J. Hollender, H. Kaiser, C. Kienle, C.S. Mcardell, E. Simon, U. Von Gunten, Effect of operational and water quality parameters on conventional ozonation and the advanced oxidation process O₃/H₂O₂: Kinetics of micropollutant abatement, transformation product and bromate formation in a surface water, *Water Res.* 122 (2017) 234–245. doi:http://dx.doi.org/10.1016/j.watres.2017.05.018.
- [33] S. Khuntia, M. Kumar Sinha, B. Saini, An approach to minimize the ozone loss in a series reactor: A case of peroxone process, *J. Environ. Chem. Eng.* 6 (2018) 6916–6922. doi:10.1016/j.jece.2018.10.069.

5

Comparison of Catalytic Ozone, UV/H₂O₂, UV/PMS and UV/Fenton in Degrading the Naphthenic Acids in Oil Sands Process Water

UNIVERSITAT ROVIRA I VIRGILI

Application of Advanced Oxidation Processes in the Reclamation of Wastewaters from the Oil
& Gas Sector

Hande Demir Duz

5.1 Introduction

Northern Alberta has the third largest oil reserves in the world after Venezuela and Saudi Arabia in the form of oil sands, which cover more than 140.000 km² of surface area [1]. Oil sands are a mixture of sand, clay and water that contain an extra heavy crude oil variant known as bitumen. Bitumen is extracted by warm water and upgraded into synthetic crude oil [2,3]. The extraction process is the most water demanding part of the production requiring water approximately 2-5 times of processed crude oil [4,5]. Consequently, an alkaline and relatively brackish water called oil sands process water (OSPW) is generated and stored in tailing ponds for its reuse such as in the bitumen extraction process, process cooling and material hydro-transport due to the zero discharge policy [5,6]. OSPW contains a variety of metal cations, anions, organic matters and suspended particles. Naphthenic acids (NAs) are the main compounds of the organic fraction, which are naturally generated in crude oils and oil sands bitumen [7,8]. Particularly in Canada, NAs are of concern because of their high concentrations in tailing ponds and also their detrimental effects, especially to the aquatic environment [8].

Advanced oxidation processes (AOPs) are considered clean technologies for the treatment of contaminated waters that apply produced hydroxyl radicals (HO•), which will attack the organic contaminants. The efficiency of AOPs is based on the generation of these highly reactive radicals that are unselective oxidizing species ($E^0=2.80$ V) [9].

Ozone-based technologies are one of those AOPs which can degrade organic contaminants by both direct and indirect reactions under mild conditions by means of strong oxidation potential of ozone (O₃) and hydroxyl radicals, respectively [10,11]. π -bonds containing hydrocarbons such as aromatics can be oxidized by direct reactions in few minutes while indirect reactions can take place in case of the ozone-resistant components that cannot be degraded by direct reactions [12]. Previous studies showed the advantage of ozone-based processes on NAs molecules with higher molecular weights and numbers of rings and are more bio-recalcitrant. Thus, bio-recalcitrant NAs can be transformed into biodegradable compounds, so that the ozonation process can be followed by the biological treatment to remove the remaining contaminants [13]. However, by now, the operation costs of ozone-based processes compared to traditional treatment techniques restrict their full-scale operations especially when high ozone concentrations are needed. Therefore, there

CHAPTER 5: Comparison of Catalytic Ozone, UV/H₂O₂, UV/PMS and UV/Fenton in Degrading the Naphthenic Acids in Oil Sands Process Water

is a gap to decrease the operation costs in terms of the amount of the reactants and the operation time, while increasing the degradation efficiency.

Other promising techniques to treat OSPW could be photocatalytic AOPs. In the presence of UV irradiation and H₂O₂ as an oxidant, photons produced by UV light generate hydroxyl radicals ($\bullet\text{OH}$) by means of homolytic cleavage of H₂O₂. $\bullet\text{OH}$ is a strong oxidant with a redox potential of 2.6 - 2.9 V at acidic pH and 1.8 - 1.9 V at basic pH [7]. As an alternative to H₂O₂, Oxone[®], which is known as potassium peroxymonosulfate (PMS), has been stated as a common oxidizing agent in many studies [14,15]. Its environmentally friendly properties, stability and commercial availability increase the interest of its use as an oxidant instead of H₂O₂. PMS provides HSO₅⁻ anions susceptible of being activated to a strong oxidant, SO₄^{-•}, by either transferring one electron from a metal such as Fe²⁺, Co²⁺ and Ag⁺ or by direct photolysis under proper reaction conditions [16].

AOPs are widely used as pre-treatment or post-treatment for the treatment of industrial effluents. However, recently heterogeneous catalytic AOPs were considered as powerful treatment methods increasing the efficiencies of classical AOPs and decreasing their drawbacks. Activated carbon (AC) is commonly used especially for the adsorption treatment of OSPW. However, there are very few studies that dealt with the AC catalyzed ozonation process [13]. Similarly, only few studies tried to examine the treatment efficiency of Fe-based catalysts on petroleum related components/wastewater and none of them dealt with oil sands related wastewater. Although iron species can be used themselves as catalyst, different kinds of materials such as AC, Al₂O₃ and SiO₂ have been used as support in order to prevent from clustering, especially for the magnetic particles [17–19]. Shahamat et al removed 70% of chemical oxygen demand (COD) from phenol contaminated water by 60-min magnetic carbon (Fe₃O₄/AC) catalyzed ozonation at neutral pH [20]. Mehdi et al. obtained 50% of COD removal from high saline petrochemical wastewater by catalytic ozonation with a magnetic catalyst (powdered AC/Fe₃O₄) at pH 5, while that of pH 7 was 48% [19].

Thus, this study presents the performances of granular activated carbon (GAC)-based catalysts to treat OSPW by catalytic AOPs in order to enhance the treatment efficiencies and reduce toxicity to reach discharging or even reusing limits. GAC-based materials were chosen as support due to their high surface area and excellent adsorption abilities. Iron (III) was selected as metal dopant to obtain magnetic particles while preventing from clustering of the magnetic particles by means of GAC as a support material [19]. Also, possible advantages of Fe doped materials in

Fenton-like treatment and PMS activation was of interest. Thus, photo-based AOPs with the same catalysts were investigated in detail to compare different AOPs. UV-based treatments were also compared with homogeneous photo-catalysis (photo-Fenton) using the same nominal amount of Fe doped in GAC-based catalysts.

5.2 Materials and Methods

5.2.1 OSPW and reagents

Raw OSPW was collected from an oil sands tailings pond in northern Alberta and stored at 4 °C until being used. Before the treatments, OSPW was filtered using a 0.45µm nylon membrane in order to remove suspended solids that could increase the consumption of reagents and decrease the light transmittance in those cases where the light-based treatments are applied. The general specifications of the OSPW after filtration are given in *Table 5.1*.

Table 5.1 General specifications of the OSPW.

DOC (mg C/L)	COD (mg O ₂ /L)	O ₂ -NAs Conc. (mg/L)	pH
86	245	26.4	8.45

Initial ozone treatments were performed on a synthetic water to compare the catalyst performances on the same conditions for all treatment parameters. 1-adamantane carboxylic acid (ACA, >98%, TCI) was chosen as the model compound. ACA is a diamond-structured compound commonly found in OSPW [21]. It is reported as one of the most recalcitrant compounds found in OSPW which cannot be degraded simply by biological treatment [22]. The 200 mg/L stock solution of ACA was buffered by 20 mmol sodium bicarbonate (NaHCO₃) and pH was adjusted to 9 to mimic the pH and alkalinity of OSPW. For the applied experiments, corresponding dilutions were done to reach initial ACA concentration of 50 mg/L. This final concentration was aimed to mimic the typical NAs concentration in OSPW, which generally ranges 40-70 mg/L and could reach up to 130 mg/L [22].

For the catalyst preparation, GAC was purchased from Calgon Carbon Corporation (Pittsburgh, PA, USA) and was modified for further use. Nitric acid (68-70%) was purchased from Fischer Scientific. Urea and melamine (99%, Sigma-Aldrich) were used as the nitrogen (N) doping sources while thiourea (99%, Alfa Aesar) was used for nitrogen/sulphur (N/S) doping. Fe (III) nitrate nonahydrate (Fe(NO₃)₃·9H₂O,

99%, Sigma-Aldrich) was used as the Fe (III) precursor for the catalyst modification step.

FeSO₄·7H₂O (99%, Sigma-Aldrich) was used as Fenton reagent. H₂O₂ (30%, Fisher) and potassium peroxymonosulfate (PMS, 99%, Alfa Aesar) were used as the oxidizing agents in different treatments.

5.2.2 Catalyst preparation procedure

Prior to use, GAC was sieved to a particle size between 0.6-1.4 mm, then washed by Milli-Q water and dried at 110 °C to be used as the starting material labelled as GAC0. The modification procedure of GAC was composed of several steps according to previous studies [23,24]. In brief, GAC was washed by 6M nitric acid solution via Soxhlet system for 3 h to remove the accumulated impurities such as N, P, K, Ca, Al, Si and Fe from the surface of the material [25]. Also, it may increase the surface area as well as improving the surface chemistry by hydrophilic functional group introduction [26]. The obtained material was washed by Milli-Q water several times until neutral pH to remove excessive acid, then filtered and dried in an oven at 110 °C (labeled as GAC1). Afterwards, N (by urea or melamine) or N/S (by thiourea) functional groups were introduced into GAC1. To do so, 2 g of GAC1 was added into 1 M of either 100 mL urea or thiourea solution and shaken at 200 rpm by New Brunswick™ Innova® 2100 platform shaker (Eppendorf Inc., USA) for 24 h at room temperature followed by filtration and drying at 110 °C. The obtained materials were calcined at 450 °C under N₂ atmosphere and denominated as GAC-U and GAC-TU depending on the doping source, urea and thiourea, respectively. For the material prepared with melamine (GAC-M), the method previously reported by Messele et al. was followed [23]. Briefly, 2 g of GAC1 was added into 1 M of melamine suspension in 80% ethanol (100 ml) and stirred at 70°C for 5 h. Afterwards, the mixture was boiled to evaporate the solvent. Obtained slurry was dried at 110 °C and later calcined at 450 °C under N₂ atmosphere. As the last step, the obtained materials were impregnated with 5% Fe (III) with the aim of obtaining magnetic properties after calcination at 600 °C under N₂ atmosphere. For the impregnation, required amount of Fe(NO₃)₃·9H₂O was dissolved in 15 mL of Milli-Q water. Then, 2 g of the selected material was added into the solution to be ultrasonicated for 1 h at 60 °C [20]. Obtained materials were labeled as GAC0-Fe, GAC1-Fe, GAC-UFe, GAC-MFe and GAC-TUFe. **Table 5.2** summarizes the nomenclature of the catalysts with their main preparation features.

Table 5.2 Nomenclature and descriptions of original and modified catalysts.

Material Name	Pre-treatment of GAC support	Heteroatom doping	Nominal	
			1 st Cal.	Fe (III) doping (wt%) 2 nd Cal.
1 GAC0	Milli-Q water	-	-	-
2 GAC1	6M HNO ₃	-	-	-
3 GAC-U	6M HNO ₃	N doping by Urea	450°C	-
4 GAC-M	6M HNO ₃	N doping by Melamine	450°C	-
5 GAC-TU	6M HNO ₃	N/S doping by Thiourea	450°C	-
6 GAC0-Fe	Milli-Q water	-	-	5% 600°C
7 GAC1-Fe	6M HNO ₃	-	-	5% 600°C
8 GAC-UFe	6M HNO ₃	N doping by Urea	450°C	5% 600°C
9 GAC-MFe	6M HNO ₃	N doping by Melamine	450°C	5% 600°C
10 GAC-TUFe	6M HNO ₃	N/S doping by Thiourea	450°C	5% 600°C

5.2.3 Preliminary selection of catalysts on ACA removal by catalytic ozonation

Statistical approach in experimental studies plays an important role in planning and performing the experiments, analysing and interpreting the results efficiently and economically in terms of the experimental costs and time consumption [27]. In this part of the study, this approach has been used to select the most efficient catalysts for the ACA removal based on its quantification by liquid chromatography–mass spectrometry (LC-MS) analysis. The set of experiments for 2-level fractional factorial were designed by Minitab 17 software considering the effects of the catalyst amount, O₃ dose, pH and time. Fractional factorial design is a very useful tool to screen the effects of the variable on the response [28]. **Table 5.3** presents the boundaries of the design and the experimental plan that was performed for the treatment of synthetic water. For each catalyst, 11 experiments were conducted including 3 repetitions at the center points of each variable. The low and high levels of the parameters were decided considering the possible working range of each for the treatment of OSPW based on the previous experience of the authors [29,30]. In the case of O₃ dose, the high level was limited at 25 mg/L since the maximum O₃ concentration in the stock solution that could be reached with the current system was 42 mg/L.

Table 5.3 Experimental conditions and experimental plan.

		Levels			
Independent Variables		Low	High		
A: Amount of Catalyst (mg/L)		100	1000		
B: O ₃ dose (mg/L)		5	25		
C: pH		3	9		
D: Reaction time (min)		15	90		
Run	StdOrder	A	B	C	D
1*	11	550	15	6	52.5
2	3	100	25	3	90
3	4	1000	25	3	15
4*	10	550	15	6	52.5
5	8	1000	25	9	90
6	5	100	5	9	90
7	6	1000	5	9	15
8	1	100	5	3	15
9*	9	550	15	6	52.5
10	2	1000	5	3	90
11	7	100	25	9	15

*Center points

5.2.4 Ozone treatment procedure

Ozone treatments were conducted in 30 ml batch reactors with an ozone dose ranged from 10 to 25 mg/L. O₃ gas was produced by an O₃ generator (PCI-Wedeco, Water Technology, Herford, Germany) from pure O₂. Required ozone was supplied from an O₃ stock solution that was prepared by bubbling the ozone gas through a fine-pore diffuser into Milli-Q water, which was placed in an ice-bath to decrease the O₃ decomposition rate by time. The concentration of O₃ stock solution was monitored by a spectrophotometer at 260 nm, which was also confirmed by indigo method. At the time that the concentration reached the desired level, a dilution was made with the O₃ containing stock solution to supply the required ozone dose for treatment. For the catalytic ozone treatments, required catalyst amount that ranged between 0.1 g/L and 1 g/L was added to the reactors before O₃ addition. The reactors were kept closed without headspace during the treatment. The operation pH was varied from 3 to 9 for the treatment of ACA while it was kept at its natural value (pH 8.45) for OSPW treatment. Ultrasonication was used instead of mixing, which was also recommended for enhancing the reaction efficiency while reducing the reagent and time requirements by means of increased mass transfer [31]. Adsorption tests and single ozonation tests were performed as control experiments.

5.2.5 UV-based treatment procedures

UV-based treatments were studied only for OSPW in order to compare the treatment efficiencies of UV-based processes to those of ozonation. Experiments were carried out with a quasi-collimated beam UV apparatus equipped with a 1 kW medium pressure mercury lamp (Model PSI-I-120, Calgon Carbon Corporation, PA, USA). The treatments were performed in a glass beaker with a volume of 60 ml for 90 min. The irradiance was measured as 4.5 mW/cm² by a calibrated UV detector (Model SED 240, International Light, MA, USA) connected to a radiometer (Model IL 1400 A, International Light, USA). The effect of different oxidants was investigated with the presence of 0.1 g/L catalyst at different pH (3 and natural pH of OSPW). Treatment efficiencies of the H₂O₂-applied heterogeneous oxidation processes were compared to those of homogeneous process, which was UV/Fenton in this study.

90-min UV/Fenton experiments were conducted at pH 3, which was reported as the optimum pH in many studies [32,33]. The amount of Fe²⁺ was kept at 5 mg/L avoiding an excessive use of reagent and not to form any sludge to be managed further. The ratio of H₂O₂/COD (w/w) was varied between 1 and 5. Remained H₂O₂

detected by semi-quantitative H₂O₂ strips was quenched by sodium bisulphite solution after the treatment.

Catalytic UV/oxidant experiments were carried out during 90 min with two sorts of oxidants (e.g., H₂O₂ and PMS) to compare the activation efficiency of different oxidants for this type of effluent and catalysts. The weight ratio of oxidant/COD was kept at 2.5. The catalyst amount used in the experiments was 0.1 g/L. The working pH was kept as the initial pH of the effluent for both two oxidants. Additionally, pH 3 treatment was studied for H₂O₂ to be considered as Fenton-like treatment comparing with the classical photo-Fenton experiments. All the samples have been quenched by sodium bisulphite after the treatments conducted with PMS. In the case of H₂O₂, only the samples containing H₂O₂ after treatment were quenched. The remained H₂O₂ in the samples was determined using semi-quantitative H₂O₂ strips.

5.2.6 Analytical methods

5.2.6.1 Characterization of catalysts

X-ray diffraction (XRD) analysis using a Rigaku XRD Ultima IV diffractometer with Cu K α source radiation with an angular 2 θ -diffraction range between 10° and 80° was employed to determine the crystal structure and crystallinity of the catalyst.

N₂ physisorption was performed at -196 °C using a surface area analyzer (Autosorb-1MP Quantachrome, USA) in order to obtain textural properties of the catalysts. Specific surface areas were calculated according to BET method. Microporosity was assessed by the t-plot method.

Fourier transform infrared (FT-IR) attenuated total reflectance (ATR) analysis was carried out using a Jasco FT-IR 6700 Spectrometer to determine the functional groups on the catalysts. Germanium crystal was employed in ATR. All spectra were recorded from 4000 to 450 cm⁻¹ at a scan rate of 2 mm/s.

The morphology of the catalysts was examined by an environmental scanning electron microscopy (ESEM). Energy dispersive X-Ray (EDX) was performed on the samples in ESEM using a FEI Quanta 600 microscope equipped with energy dispersive X-ray microanalysis from Oxford Instruments operating at high vacuum with an accelerating voltage of 20 kV.

5.2.6.2 Evaluation of treatments

The fluorescent organic compounds in raw/treated OSPW were analysed using Fluorescence Spectrophotometer (Varian Cary Eclipse, Ontario, Canada). Synchronous fluorescence spectroscopy (SFS) analysis is a semi-quantitative analysis that gives the ring structure information of the effluent as the group of one-ring, two-rings and so on [34]. The analysis method was previously reported by Abdalrhman et al., for analysing fluorescent aromatic species. The excitation wave lengths ranged from 200 to 600 nm while emission wavelengths ranged from 218 to 618 nm. Scanning speed was set to 600 nm/min and the photomultiplier (PMT) voltage was set at 800 mV [35].

Dissolved organic carbon (DOC) of the samples was measured by a total organic carbon analyzer (Shimadzu TOC-V CHS/CSN).

Classical NAs concentrations of raw/treated OSPW was determined by ultra-performance liquid chromatography coupled with a time-of-flight mass spectrometer (UPLC-TOF-MS) using a UPLC Phenyl BEH column (Waters, MA, USA) in high resolution mode. The injection solution was prepared with 500 µL of the sample, 100 µL of internal standard (4.0 mg/L of myristic acid-1-¹³C in methanol), and 400 µL methanol reaching a final sample volume of 1 mL as reported before [36]. The removal efficiency results were presented based on the carbon number of the compounds and the double bond equivalence (DBE) number which refers to the hydrogen deficiency (DBE= $-z/2$) [37].

The concentration change of model compound, ACA, was monitored by liquid chromatography coupled with a mass spectrometer (LC-MS, Waters Acquity, USA). The column used for NAs analysis was a C18 (1.7 µm, 50 mm × 2.1 mm) and column temperature was set at 40°C. The analyses were carried out with a mobile phase of 4 mM ammonium acetate with 0.1% acetic acid and 100% acetonitrile. Flow rate and injection volume were 0.4 mL/min and 2 µL, respectively.

Microtox® acute toxicity of the treated/untreated OSPW on *V. fischeri* bacteria was investigated using 81.9% screening test standard protocol using Microtox® 500 Analyzer. The inhibition effect of the samples on *V. fischeri* was measured after 5 min and 15 min cultivation based on the change in the luminescence intensity. Suitable osmotic pressure of the samples was ensured before cultivation. Phenol standard (100 mg/L) was used to check the sensitivity of the *V. fischeri* before the analyses [35].

5.3 Results and Discussions

5.3.1 Initial catalyst selection and effects of selected parameters

The initial selection of the catalysts was made based on the removal efficiency of the model compound (ACA) obtained by the set of experiments indicated in **Table 5.3**, which consists of 11 runs for each catalyst. **Figure 5.1a** and **Figure 5.1b** present the responses over the runs for the catalysts without and with Fe, respectively. It was found that GAC0 (i.e., without Fe) was highly effective by itself in the ACA removal and better than most of the other catalysts prepared without Fe. Several researches reported previously catalytic activity of activated carbon in the ozonation process through enhanced decomposition of dissolved ozone on the carbon surface into OH and O-radicals [38–40]. This result was also supported by the DOC removal levels presented in **Figure 5.1c** and **Figure 5.1d**. Lower removal efficiencies obtained by DOC than LC-MS indicated the transformation of ACA component into other by-products rather than total mineralization. Additionally, the adsorption tests conducted with 1000 mg/L catalysts for 90 min (**Figure 5.2**) showed that ACA was highly adsorbed by the catalysts at acidic pH (pH 3) while its adsorption was quite low at pH 9, except by GAC0, which adsorbed 36% of ACA after 90 min conduction time.

Metal supported carbon could enhance the catalyst efficiency through the creation of new surface active centers; however, in general, the catalysts doped with Fe exhibited less efficiency than the ones without Fe loading. In both cases either being doped by Fe or not, the catalysts N-doped by melamine exhibited in general the lowest ACA removal efficiency. Thus, only GAC0 (as initial catalyst), GAC-U, GAC-TU, GAC-UFe and GAC-TUFe were selected to be studied further.

The main effect plots obtained by the software for each catalyst (given in **Appx. B**) show that an increase in the amount of catalyst, ozone dose and time led to an increase in removal efficiency for all catalysts. However, change in pH influenced negatively on the efficiency of catalysts doped with Fe. This could be due to different form of Fe deposited on the material at acidic and alkaline pH. For the catalysts without Fe, increasing pH increased the removal efficiency having positive effect except from GAC-U and GAC-TU.

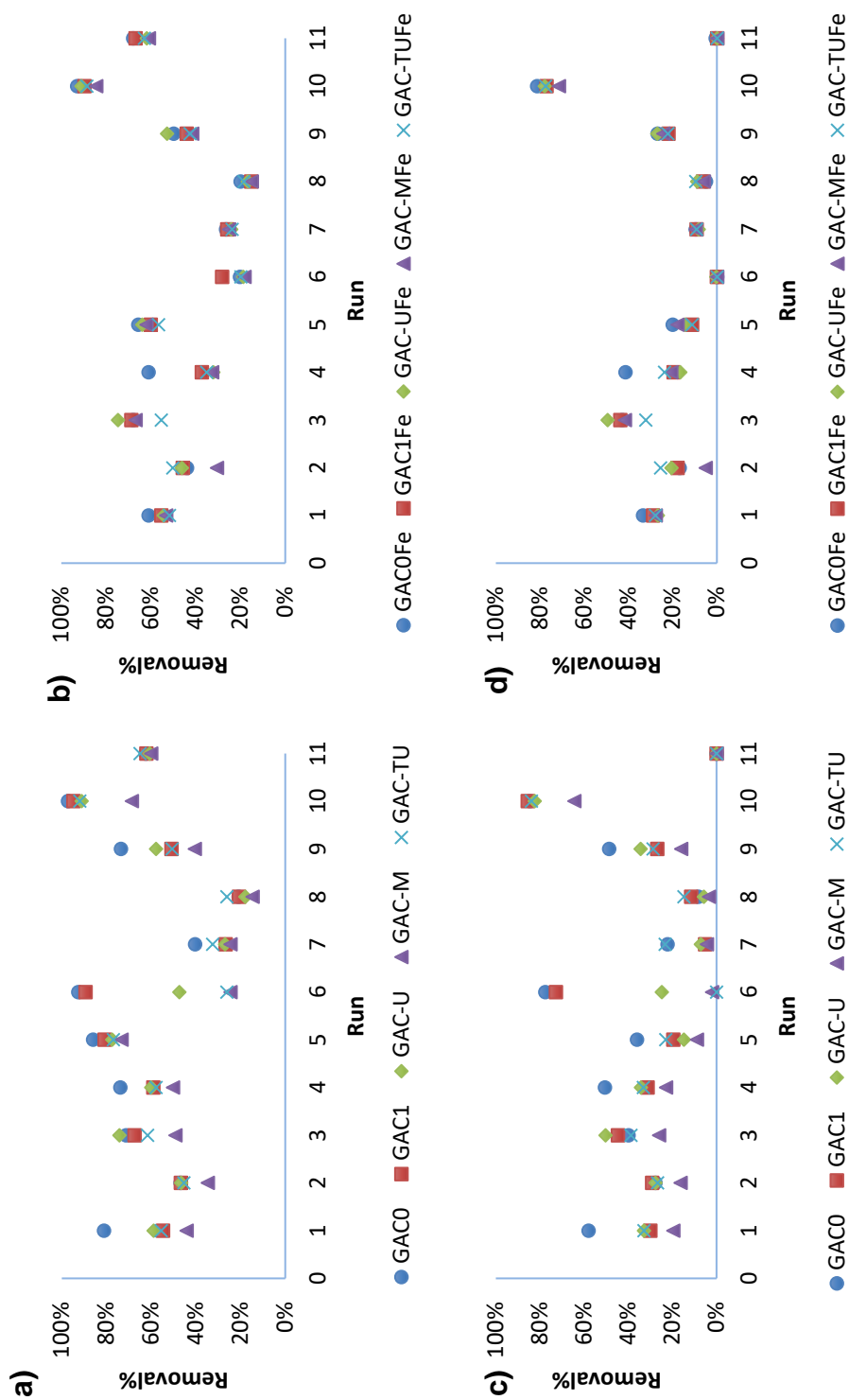


Figure 5.1 Removal efficiencies of different catalysts in experimental runs obtained by LC-MS: a) catalysts without Fe, b) catalysts with Fe; obtained by DOC; c) catalysts without Fe, d) catalysts with Fe.

CHAPTER 5: Comparison of Catalytic Ozone, UV/H₂O₂, UV/PMS and UV/Fenton in Degrading the Naphthenic Acids in Oil Sands Process Water

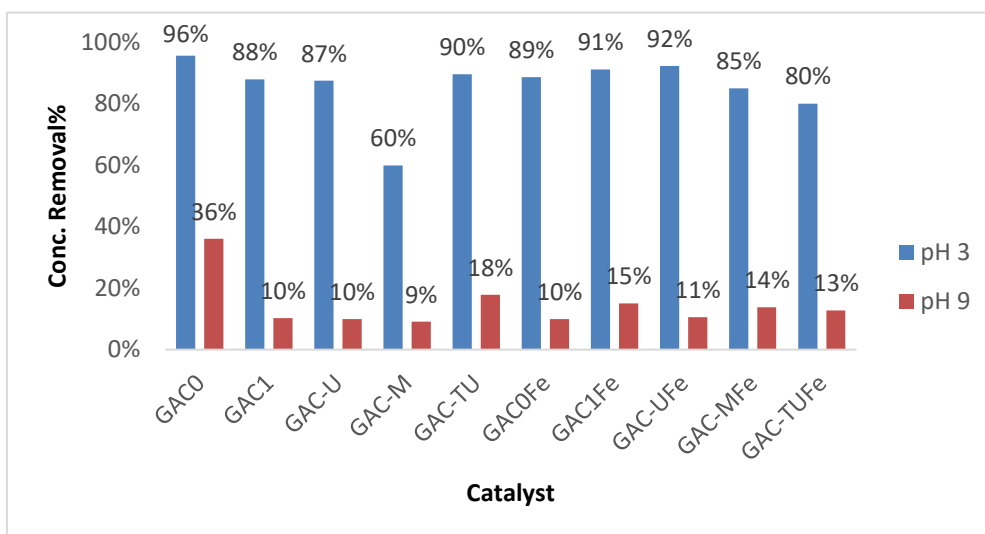


Figure 5.2 90-min adsorption of ACA by 1 g/L catalysts at varied pH.

5.3.2 Characterization of the selected catalysts

Textural properties obtained by N₂ physisorption (*Table 5.4*) revealed that GAC0 was highly microporous with 954 m²/g of BET surface area and total pore volume of 0.57 cm³/g. Nitrogen doping by urea (GAC-U) and later Fe impregnation (GAC-UFe) did not cause any change on the surface area, while N/S doping by thiourea (GAC-TU) resulted in a decrease of surface area at expenses of microporosity, likely due to the blockages in the pore structure caused by N/S penetration to the pores [24]. Later Fe doping on GAC-TU caused an increase on surface area of GAC-TUFe, similarly to that observed in the study of M.-X. Liu et al, where authors reported a N/S doped magnetic catalyst [41].

Table 5.4 Textural properties of the catalysts analyzed by N₂ adsorption.

	GAC0	GAC-U	GAC-TU	GAC-UFe	GAC-TUFe
S (BET) (m ² /g)	954	951	811	953	901
S (micro) (m ² /g)	842	827	695	806	775
S (meso) (m ² /g)	112	124	116	147	126
V (total) (cm ³ /g)	0.57	0.58	0.51	0.59	0.56
V (micro) (cm ³ /g)	0.38	0.38	0.32	0.37	0.35
V (meso) (cm ³ /g)	0.19	0.20	0.19	0.22	0.20

The XRD patterns of all the catalysts (*Figure 5.3*) presented broad diffraction peaks in the 24° and 44° two theta range which correspond to the (002) and (101) diffraction

peaks of carbon materials with low graphitization [24,42]. Only GAC-UFe displayed the diffraction peaks of Fe₃O₄ at 2θ 30.2°, 35.5°, 54°, 57.3° and 62.7°, which correspond to (022), (131), (242), (151) and (044) planes, respectively (JCPDS file no. 96-100-1033). Diffraction peak corresponding to (040) plane was not observed due to overlapping with amorphous carbon diffraction lines. The pattern of GAC-TUFe was similar to those of initial materials, although (131) plane with very low intensity of Fe₃O₄ could be identified. Given that both materials contain similar amount of Fe (as will be discussed later), the differences between both Fe-supported samples can be explained by a better Fe dispersion on the GAC-TUFe catalyst surface [24].

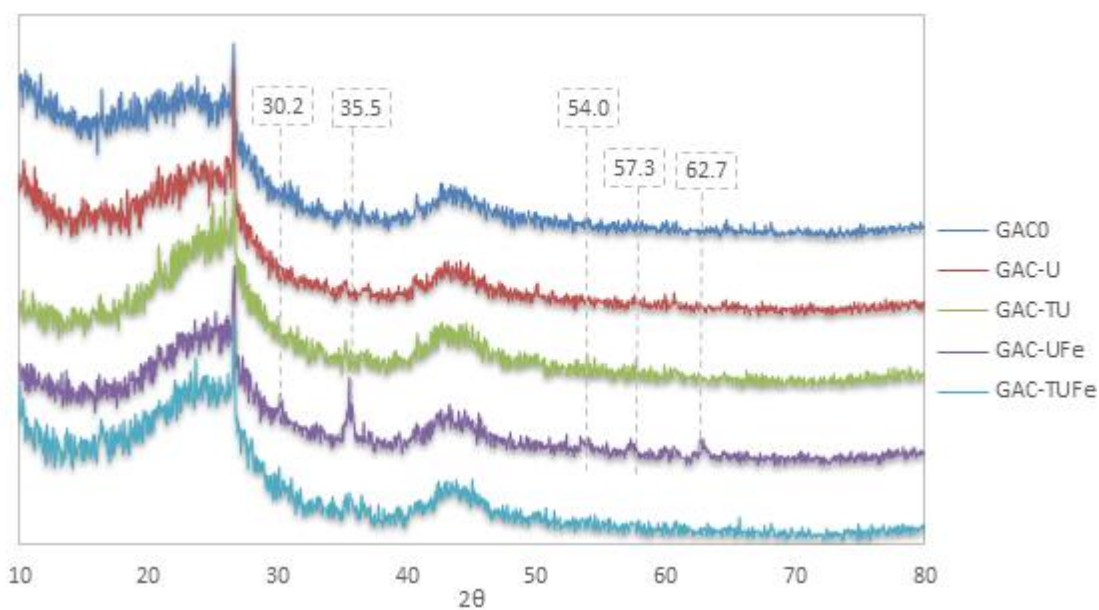


Figure 5.3 XRD patterns for GAC based catalysts.

The functional groups of the catalysts were investigated by FTIR (**Figure 5.4**). The IR bands at 1586 cm⁻¹ correspond to C=C/C=N functional groups [43]. The bands at 1080 cm⁻¹ and 1040 cm⁻¹ are assigned to the asymmetric stretching C-O vibration of the ether and C-O groups linked to aromatic carbons, respectively [44]. These bands are both more intense in all the catalysts except mere GAC0, indicating higher concentration of oxygen atoms than GAC0 in modified catalysts, as also found by EDX analyses [45]. At 1720 cm⁻¹, the absorption band detected for GAC-UFe was assigned to the C=O stretching [45].

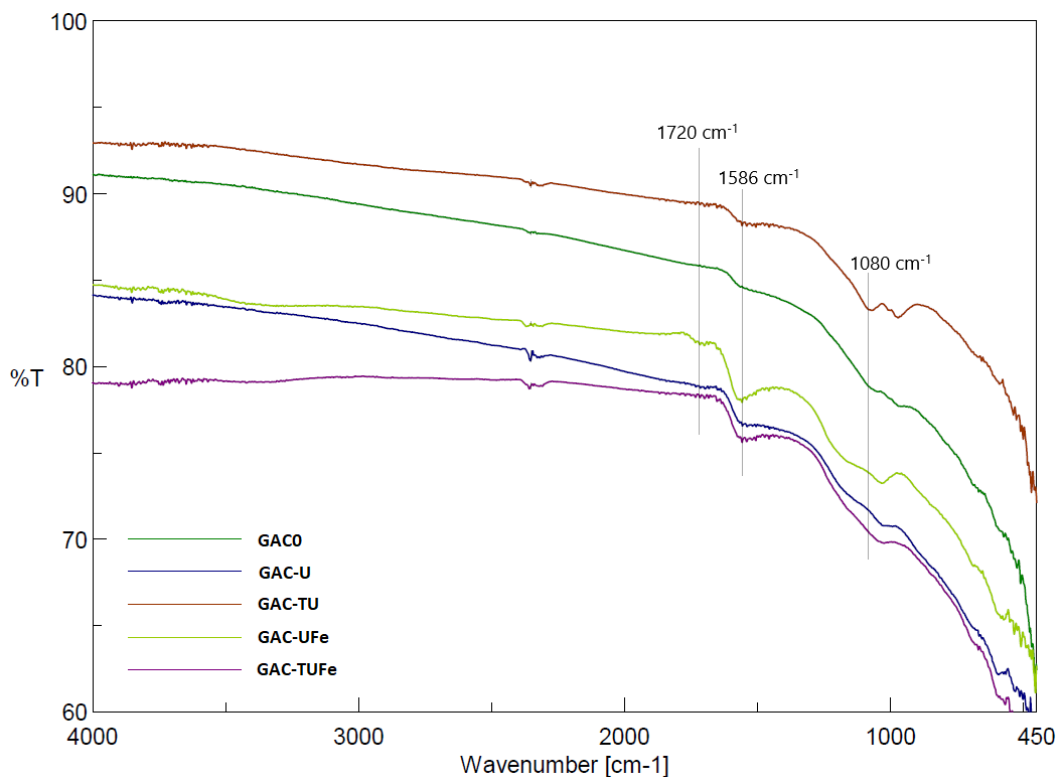
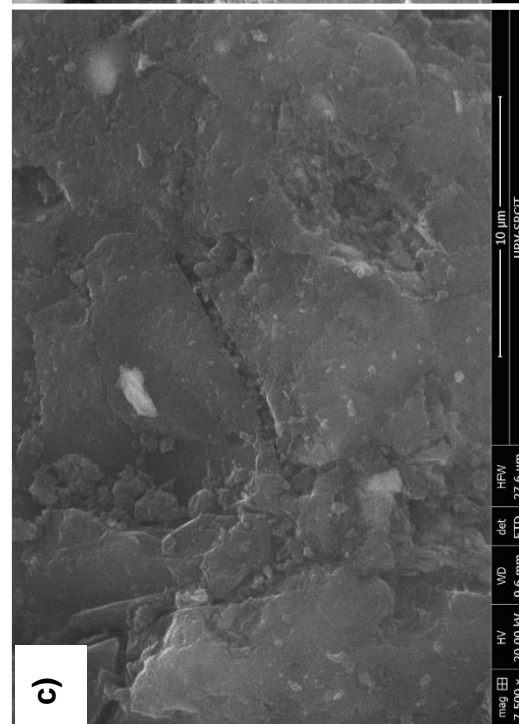
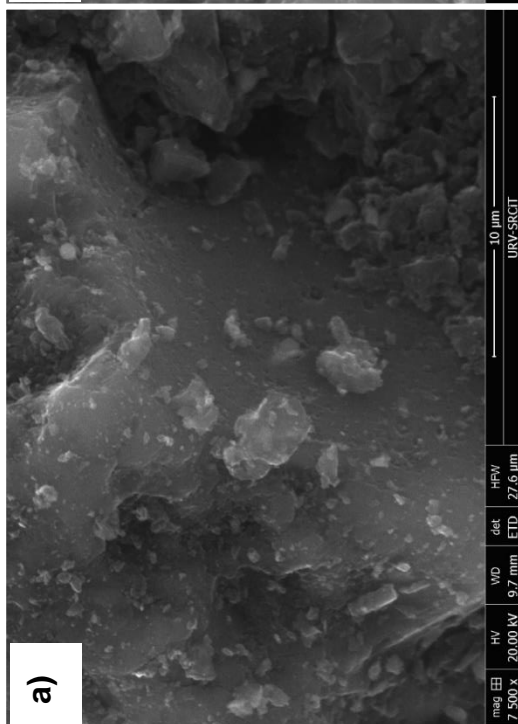
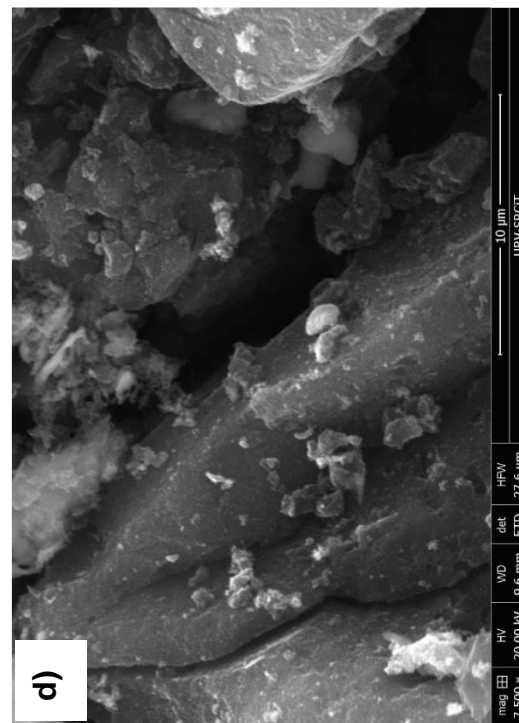
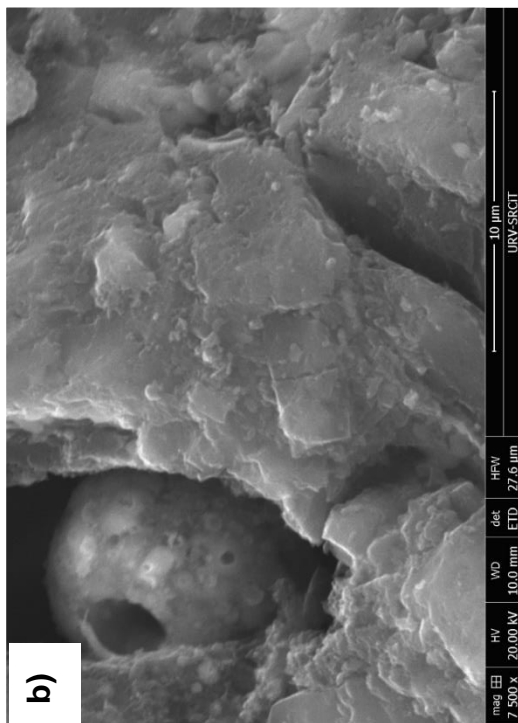


Figure 5.4 FTIR spectra of the catalysts.

Environmental scanning electron microscopy technique (ESEM) was used to investigate the surface physical morphology of the materials (*Figure 5.5a-5.5e* and EDX elemental micro-analyses are given in *Table 5.5*). At a first glance, no great differences were found among the different materials. *Figures 5.5a, 5.5c* show that GAC0 and GAC-TU have a relatively smoother surface if compared with GAC-U and Fe-modified carbon materials (*Figures 5.5b, 5.5d, 5.5e*), which present more caverns on the surface. This fact is also in agreement with the BET surface area results, which decreased significantly in GAC-TU, being similar for the rest of materials. Additionally, the introduction of hydrophilic functional groups by nitric acid wash can be observed by the increased O atoms in the modified catalysts (*Table 5.5*). Besides, sulphur was found in GAC-TU and GAC-TUFe samples (*Table 5.5*). Around a 7 wt% and 9 wt% of Fe was detected on the surface of GAC-UFe (*Figure 5.5d*) and GAC-TUFe (*Figure 5.5e*), respectively, which were well spread on the GAC support as found by EDX analysis (*Figure Appx. B1*).



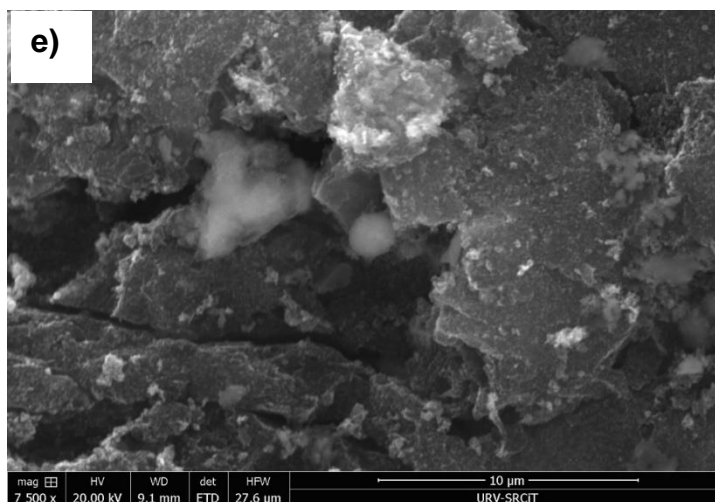


Figure 5.5 Morphology of the catalysts a) GAC0, b) GAC-U, c) GAC-TU, d) GAC-UFe, e) GAC-TUFe.

Table 5.5 EDX elemental micro-analyses.

Element	GAC0		GAC-U		GAC-TU		GAC-UFe		GAC-TUFe	
	Wt%	At%	Wt%	At%	Wt%	At%	Wt%	At%	Wt%	At%
C	84.62	89.92	83.41	88.52	84.39	90.71	72.79	82.9	65.3	77.69
O	9.77	7.79	12.05	9.6	6.88	5.55	15.28	13.06	18.21	16.27
Al	1.26	0.6	1.16	0.55	1.38	0.66	1.61	0.82	2.3	1.22
Si	2.01	0.92	1.98	0.9	2.11	0.97	2.24	1.09	2.8	1.42
S	1.4	0.56	0.69	0.27	5.24	2.11	0.83	0.35	2.56	1.14
Fe	0.94	0.22	0.71	0.16			7.25	1.78	8.83	2.26

5.3.3 Degradation efficiency of OSPW by SFS and DOC

5.3.3.1 Ozone-based treatments

SFS is known to be a powerful tool for simultaneous analysis of multi-component medium without any pre-treatment of samples. It is a simple, selective and sensitive analysis that can detect single-ring and fused-ring aromatics in OSPW, rapidly [7,46]. Compounds with a low energy $\pi \rightarrow \pi^*$ transition or $n \rightarrow \pi^*$ transition are required to be detected via fluorescing under UV irradiation [7]. For ozone-based treatments, as given in **Figure 5.6**, initial composition labelled as OSPW-D (D=diluted) exhibited three peaks at 270 nm, 300 nm and 330 nm, which corresponded to one aromatic ring, two fused aromatic rings and three fused aromatic rings, respectively.

Adsorption tests conducted with 0.5 g of catalyst (**Figure 5.6a**) revealed that all the catalysts, except for GAC-UFe, presented similar adsorption behaviour, which were effective on adsorbing two and three fused rings aromatic components completely. The lower adsorption of two and three fused ring aromatics by GAC-UFe may be because of the changes on the surface properties of the materials upon modifications, such as surface charge that may change the adsorption efficiency of different components existing in OSPW.

Single O₃ treatment (25 mg/L O₃) without catalyst (**Figure 5.6b**), was effective to remove the aromatic rings completely, as expected, since ozone can react with aromatic components directly and rapidly. To observe the effect of the presence of catalyst on the treatment, O₃ concentration was decreased to 10 mg/L (**Figure 5.6c-5.6d**). Single ozonation in this case did not lead to complete removal of aromatic rings, but when using a catalyst, the removal was significantly enhanced, especially for one ring aromatics. This, on the one hand, suggests the generation of more highly oxidative species, which, together with components adsorption on the catalyst surface favour the organics oxidation. On the other hand, the presence of the catalyst allows decreasing the O₃ concentration needed for the treatment.

Although the efficiency of catalysts before and after surface modification was similar, a slight enhancement on the removal of fluorescent organic compounds was observed with the modified catalysts compared to GAC0. Besides, decreasing the catalyst amount to 0.1 g/L resulted in a decrease in the removal of aromatic components.

The results obtained by SFS analysis were in agreement with the DOC removal occurred by ozone-based treatments (**Figure 5.7**). DOC removal increased when using a catalyst; whereas, no DOC removal was obtained by single ozonation either with 10 mg/L or 25 mg/L O₃ dose, which would be explained by transformation of components rather than mineralization. In the case of 0.5 g/L catalyst use, highest DOC removal took place by adsorption (without O₃ feed), which was averagely 28%. In the presence of O₃, DOC removal was decreased to 16% and 10% in average for the O₃ dose of 10 mg/L and 25 mg/L, respectively. This adverse effect between adsorption and O₃ addition could be because of the formation of smaller molecules by O₃, decreasing their adsorption comparing to bigger size molecules initially present in OSPW [36]. In the case of low catalyst amount with 10 mg/L O₃, DOC removal could not be achieved.

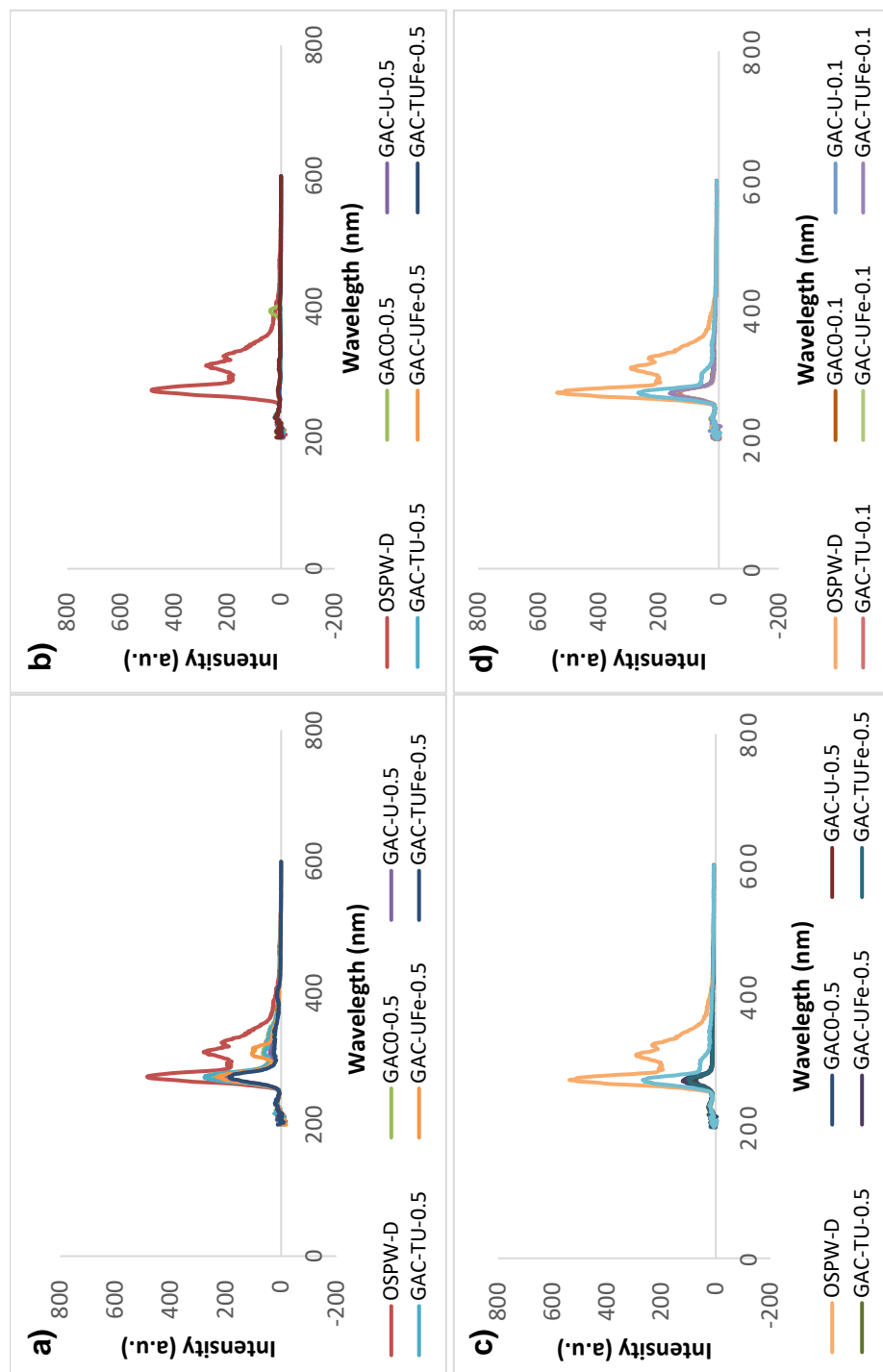


Figure 5.6 SFS analysis for 90 min of ozone-based treatment conducted at its natural pH with and without the use of catalyst: a) only adsorption with 0.5 g/L catalysts, b) ozonation with 25 mg/L O_3 and 0.5 g/L catalyst, c) ozonation with 10 mg/L O_3 and 0.5 g/L catalyst, d) ozonation with 10 mg/L O_3 and 0.1 g/L catalyst.

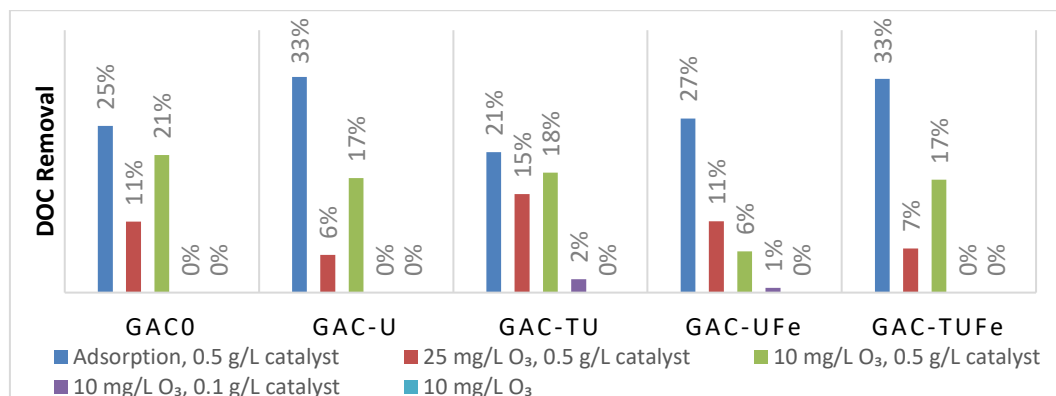


Figure 5.7 DOC removal occurred by ozone-based treatments.

5.3.3.2 UV-based treatments

UV-based homogeneous and heterogeneous photo-catalysis treatments with H₂O₂ and PMS were also studied to treat OSPW being inspired of promising results obtained for the treatment of a petroleum refinery effluent by photo-Fenton with very low Fe²⁺ amount reported recently [30]. It is well known that among AOPs, Fenton process is preferred more frequently because of their relatively simple and economic applicability. However, its drawbacks such as limited pH range and large sludge production are always of concern [47]. Photo-Fenton treatment was considered as a solution to avoid any sludge production using lower amounts of Fe species than discharging limits [30,48]. Even so, the limitation caused by the pH range is still a drawback that could be achieved by Fenton-like processes using other kinds of catalysts that may be active at higher pH. Thus, first intention for the application of UV-based treatments in this study was to examine the effectiveness of photo-Fenton process at pH 3 with 5 mg/L Fe²⁺ and optimize the applied oxidant amount for the treatment of OSPW. Then, second aim was to investigate the activity of produced catalysts with the same oxidant amount (H₂O₂ or PMS) of optimized photo-Fenton treatment and varied pH (pH 3 and pH 8.45, which is the natural pH of OSPW) The amount of catalyst used in the experiments was chosen as 0.1 g/L for two reasons: i) the nominal Fe amount doped on the GAC support was 5 mg/L for the Fe doped catalysts, which was also the same Fe²⁺ amount used for homogeneous treatment. Thus, heterogeneous and homogeneous photo-based treatments could be compared for the same scale of Fe content. ii) using this amount also enable to compare the UV-based treatments and O₃-based treatment for the same scale of catalyst amount.

According to SFS analyses of UV-based treatment, **Figure 5.8** revealed that only adjusting the pH into 3 decreased the aromatics concentration of OSPW

CHAPTER 5: Comparison of Catalytic Ozone, UV/H₂O₂, UV/PMS and UV/Fenton in Degrading the Naphthenic Acids in Oil Sands Process Water

significantly. A decrease in intensity by 75% for the first peak was observed, corresponding to single ring aromatics. The behaviour was similar for two fused and three fused ring peaks. This could be due to the poor solubility of NAs in acidic or neutral pH [4], which was also observed visually with color change from light yellow to darker yellow with newly formed suspended solids. However, in terms of DOC, the decrease in the initial carbon concentration due to the pH adjustment was 23%. Thus, DOC removal efficiencies at varied pH were calculated accordingly by taking into consideration the initial DOC change by pH.

UV/Fenton treatment at pH 3 was firstly investigated with 5 mg/L Fe²⁺, and varied H₂O₂/COD ratios from 1 to 5. **Figure 5.9a** presents the DOC removal efficiencies versus the different H₂O₂/COD ratios (w/w). The optimum ratio found was H₂O₂/COD=2.5 based on DOC removal (63% compared to 51% or 26% for H₂O₂/COD=2 and 1, respectively) reaching a final DOC value of 24 mg/L. The use of higher oxidant amount did not lead to an increase of DOC removal. Besides, SFS analysis given in **Figure 5.8a** confirmed the effectiveness of photo-Fenton treatment on removing fluorescent compounds. Low dose of H₂O₂ led to a decrease in the removal of those compounds with fused rings ≥ 2 . Ultimately, oxidant/COD=2.5 ratio (w/w) was chosen for further treatments performed with the produced catalysts.

Using any of the prepared catalysts (0.1 g/L) under the same conditions (i.e, pH 3 and oxidant/COD=2.5) resulted in lower activity than UV-Fenton treatment according to DOC analysis. This may be due to the light absorptive property of GAC based materials presenting low photocatalytic activity, which might have decreased the reaction efficiency compared to homogeneous UV/Fenton treatment, although some studies presented the synergetic effect of carbon materials in degradation of contaminants in water by photocatalysis [49,50]. Also, it was expected that the efficiencies of homogeneous catalysis would be higher than heterogeneous catalysis due to better contact with the target compounds and faster reaction rates. Averagely 29% and 14% DOC removals were achieved by heterogeneously catalyzed UV/H₂O₂ process at pH 8.45 and pH 3, respectively, presenting similar removal efficiencies by all the catalysts (**Figure 5.9b-5.9c**). However, here it should be considered that adjusting the pH to 3 already removes 23% of the DOC. The efficiency of only the photocatalysis treatment is 14% for pH 3. Considering the total removal, the final DOC reached at pH 8.45 and pH 3 is almost the same, which should be overthought to decide the best operating pH. Additionally, the treatments conducted with PMS revealed much lower DOC removal efficiency than the other treatments with H₂O₂

reaching averagely 10% for all catalysts (**Figure 5.9d**). Thus, the treatments with PMS were not examined further by the other analytical techniques.

Blank experiments including only UV, only oxidant and UV/oxidant were also performed at pH 3 and 8.45. When single UV treatment either at pH 3 or pH 8.45 was applied, although the fluorescent compounds decreased significantly, their complete removal did not take place. After 90-min UV exposure, although a visible color change from light yellow to darker was observed, there was no DOC change. Therefore, the decrease in the fluorescent compound concentration and the color change could be due to the transformation of the compounds by UV irradiation. When an oxidant was added in the presence of UV irradiation, the SFS peaks decreased almost totally; whereas, DOC removal by UV/H₂O₂ was 29% and 11% for pH 8.45 and pH 3, respectively. The DOC removal of the UV/PMS at pH 8.45 was only 7%. The effect of the catalyst type could not be assessed by SFS analysis.

5.3.4 Quantification of NAs

Detailed analyses of NAs in raw and treated effluents play an important role to evaluate the success of the treatment. NAs are considered as the main components of OSPW that contributes to acute and chronic toxicity of various aquatic organisms [3]. Therefore, detailed examination of NAs during the treatments could clarify the changes in toxicity as well as the treatment efficiency.

NAs are a complex mixture of alkyl-substituted acyclic and cycloaliphatic carboxylic acids with a general chemical formula C_nH_{2n+z}O_x, where n, z and x indicate the number of carbon atoms, the hydrogen deficiency arising from double bonds and/or rings and the number of oxygen atoms, respectively [7]. C_nH_{2n+z}O₂ classical formula represents the NAs that are in high concentrations initially, while C_nH_{2n+z}O_x x>2 NAs are formed after oxidation [51]. Due to the wide range of NAs present in OSPW, their detection can be accomplished relating with the n and z numbers as a general profile instead of individual identification [8]. Semi-quantification of detected NAs is made with internal standard calibration where the signal of NAs are compared to the signal of the internal standard, myristic acid-1-¹³C [6]. Initial classical NAs concentration of raw OSPW used in this study was 26.4 mg/L according to UPLC-TOF-MS quantification, which was in the similar ranges reported before [52].

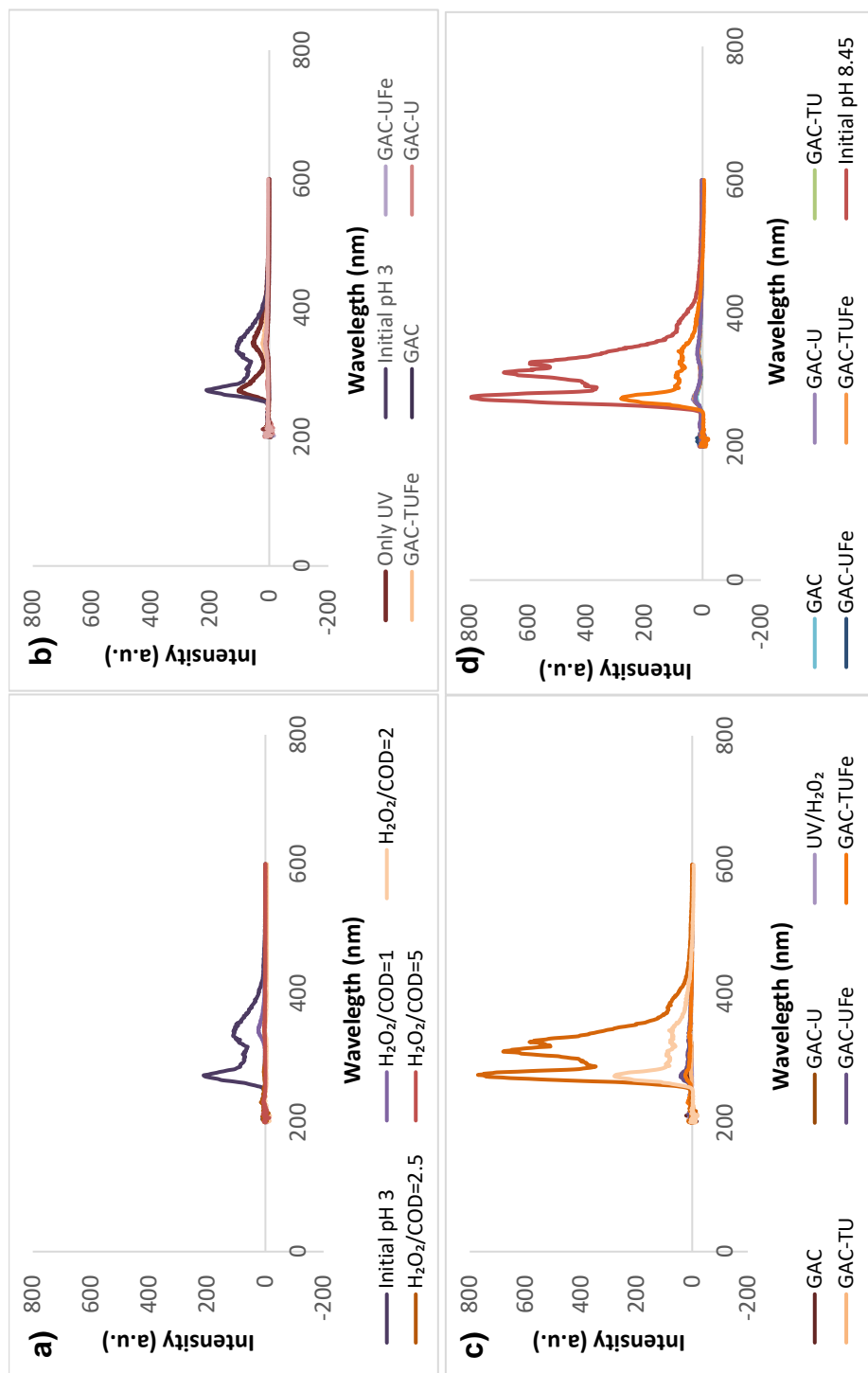


Figure 5.8 SFS analysis for UV-based treatment with and without the use of catalyst: a) UV/Fenton with 5 mg/L Fe and variable H_2O_2/COD from 1 to 5 at pH 3, b) UV/ H_2O_2 /Catalyst (0.1 g/L cat. and $H_2O_2/COD=2.5$) at pH 3, c) UV/ H_2O_2 /Catalyst (0.1 g/L cat. and $H_2O_2/COD=2.5$) at pH 8.45, d) UV/PMS/Catalyst (0.1 g/L cat. and PMS/ $COD=2.5$) at pH 8.45.

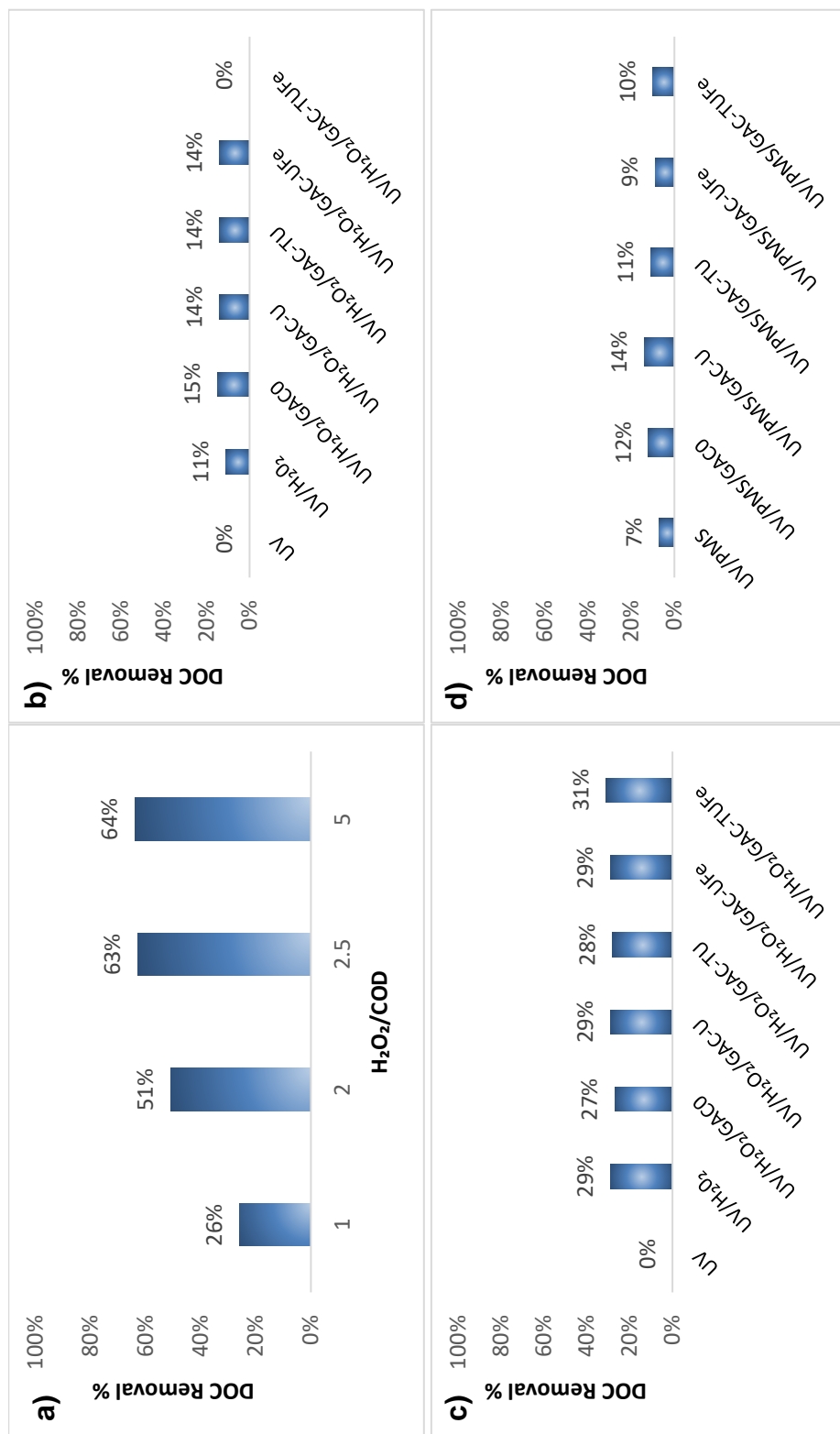


Figure 5.9 DOC removal by 90 min of a) photo-Fenton conducted with 5 mg/L Fe^{2+} and variable H_2O_2/COD ratios at pH 3, b) UV/ H_2O_2 /catalyst (0.1 g/L cat. and $H_2O_2/COD=2.5$) at pH 3, c) UV/ H_2O_2 /catalyst (0.1 g/L cat. and $H_2O_2/COD=2.5$) at pH 8.45, d) UV/PMS/catalyst (0.1 g/L cat. and PMS/ $COD=2.5$) at pH 8.45.

5.3.4.1 Ozone-based treatments

Quantification of NAs in raw and O₃ treated (with/without catalyst) samples collected at the end of treatment (i.e., 90 min) were performed to compare the effect of O₃ dose and catalyst amount on the removal efficiency of NAs in OSPW. The adsorption capacity of the produced materials in terms of NAs concentration removal was also discussed.

O₂-NAs removal percentage based on the carbon number and DBE number of the present compounds after 90-min O₃ treatment with 25 mg/L O₃ and 0.5 g/L of catalysts are shown in **Figure 5.10a-5.10b**. At least 92% of C14-C18 compounds were removed either by catalytic or single ozonation, while complete removal of C19-C21 was achieved in all the cases. The removal efficiency of those components with lower carbon number is difficult to establish accurately due to the formation of low carbon components as by-products from the oxidation of the higher number carbon components. Both the oxidation/removal and production of low carbon components occur at the same time. However, the impact of the catalytic processes rather than single ozonation is significant. Thus, it was observed an increased removal efficiency for the C9-C15 compounds when a catalyst was used, which could be due to the enhanced adsorption presented by the materials. Although the set of catalysts presented similar performance, the highest performance was achieved by GAC-TU for the removal of C11-C13 compounds. Notably, GAC0 presented significant removal capacity for C9-C10 compounds suggesting more economic catalytic application avoiding catalyst modification costs. The increase in the C9 concentration presented in **Figure 5.10a** accounts for the formation of small molecules from bigger molecules by bond breaking. This could also be seen from the removal of DBE number in **Figure 5.10c** which demonstrated almost total removal of π bonds producing saturated molecules (DBE=0). The 90 min of adsorption tests performed with 0.5 g/L catalysts (**Figure 5.10c-5.10d**) revealed that the higher the carbon number and DBE value of the compounds, the higher the removal% by adsorption occurred. Nevertheless, the total NAs concentration after adsorption ranged between 9.7-15.6 mg/L, while that of ozone applied treatments ranged between 1.0-2.3 mg/L indicating need of O₃ use to enhance the efficiency of the treatment. Additionally, GAC-TU catalyst combined with O₃ presented slightly higher efficiencies compared to the rest of catalysts tested. This could be because of the S atom embedded in the material that causes better activation of ozone although its adsorption ratio was lower than the other catalysts [53]. However, it should be noted that the adsorption capacity of the materials could be different in the

presence/absence of oxidant, which may change the porosity and surface chemistry of the material [54].

The effect of decreasing the O₃ dose (10 mg/L) is presented in **Figure 5.11a-5.11b**. The removal efficiency of the compounds regarding to their carbon number and DBE value was decreased significantly as compared with those of higher O₃ dose treatments (**Figure 5.10a-5.10b**). At this O₃ dose (10 mg/L), the catalytic treatments resulted in higher removal of the compounds with high carbon number than single ozonation, which is in agreement with the SFS results given in **Figure 5.6c-5.6d**. However, the increase in C8-C10 compounds and lower removal efficiency of DBE confirmed the partial oxidation of π bonds, as also seen by SFS analysis. Thus, O₃ was found to be the main responsible of the oxidation, and it needs to be dosed sufficiently for a possible complete mineralization. Additionally, the use of lower amounts of catalysts (**Figure 5.11c-5.11d**) resulted in decreasing the NAs removal efficiency. Considering the total removal of NAs summarized in **Table Appx. B1**, proper treatment method and the most economic treatment conditions can be decided depending on the objective of the treatment of OSPW, which was obtaining a treated effluent appropriate for discharging in this chapter. When the O₃ feeding dose was 25 mg/L, high removal of NAs up to 96% was achieved by catalytic applications. However, single ozonation also removed 92% of NAs at this O₃ concentration. Thus, only ozonation rather than catalytic treatment could be an option to reduce the cost of catalyst production, its recovery and regeneration after treatment. As the second option, O₃ dose could be reduced down to 10 mg/L. However, in this case, a catalytic treatment must be applied to reach high NAs removal efficiencies (up to 92%) since the NAs removal efficiency of single ozonation with 10 mg/L O₃ was only 63%.

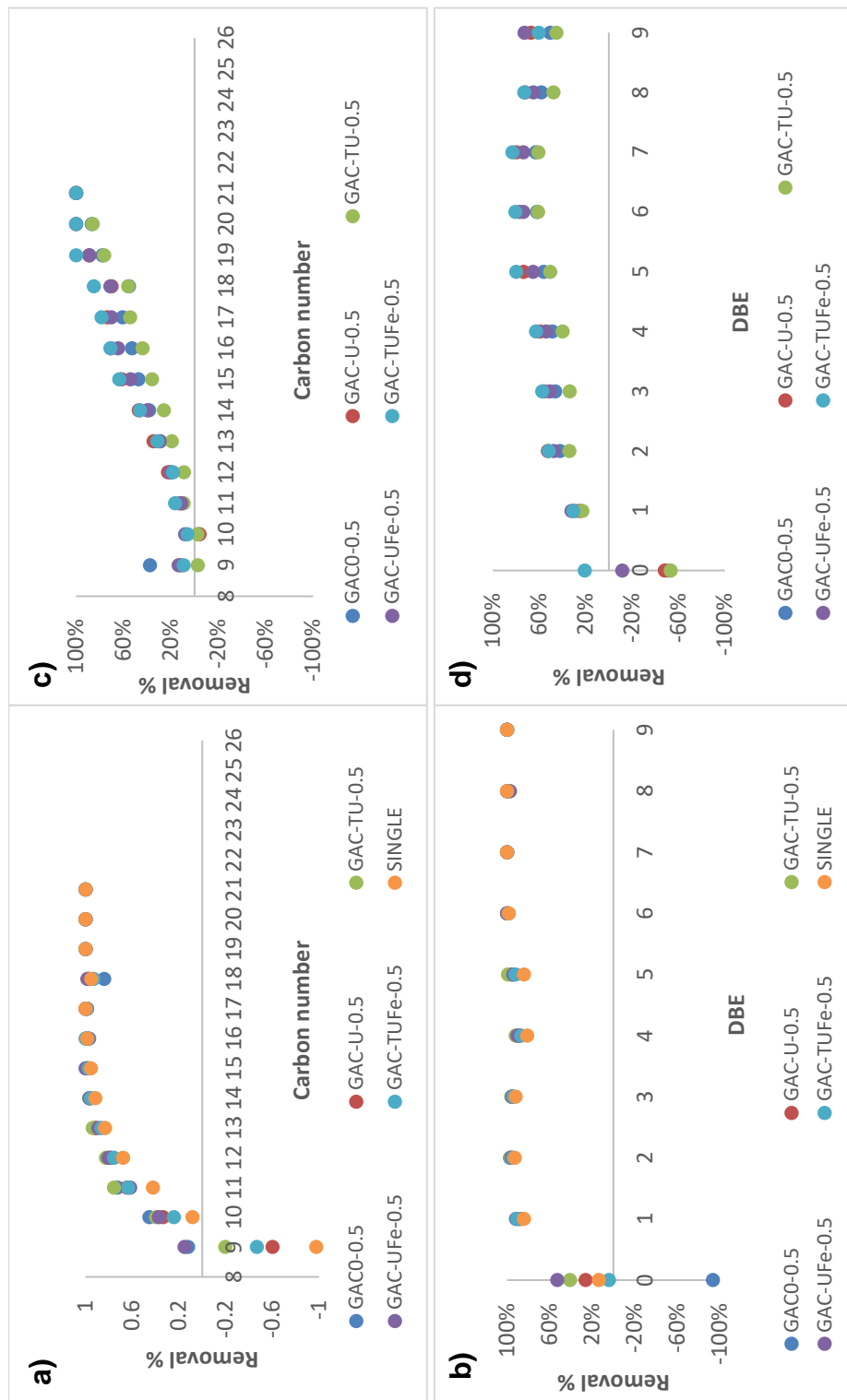
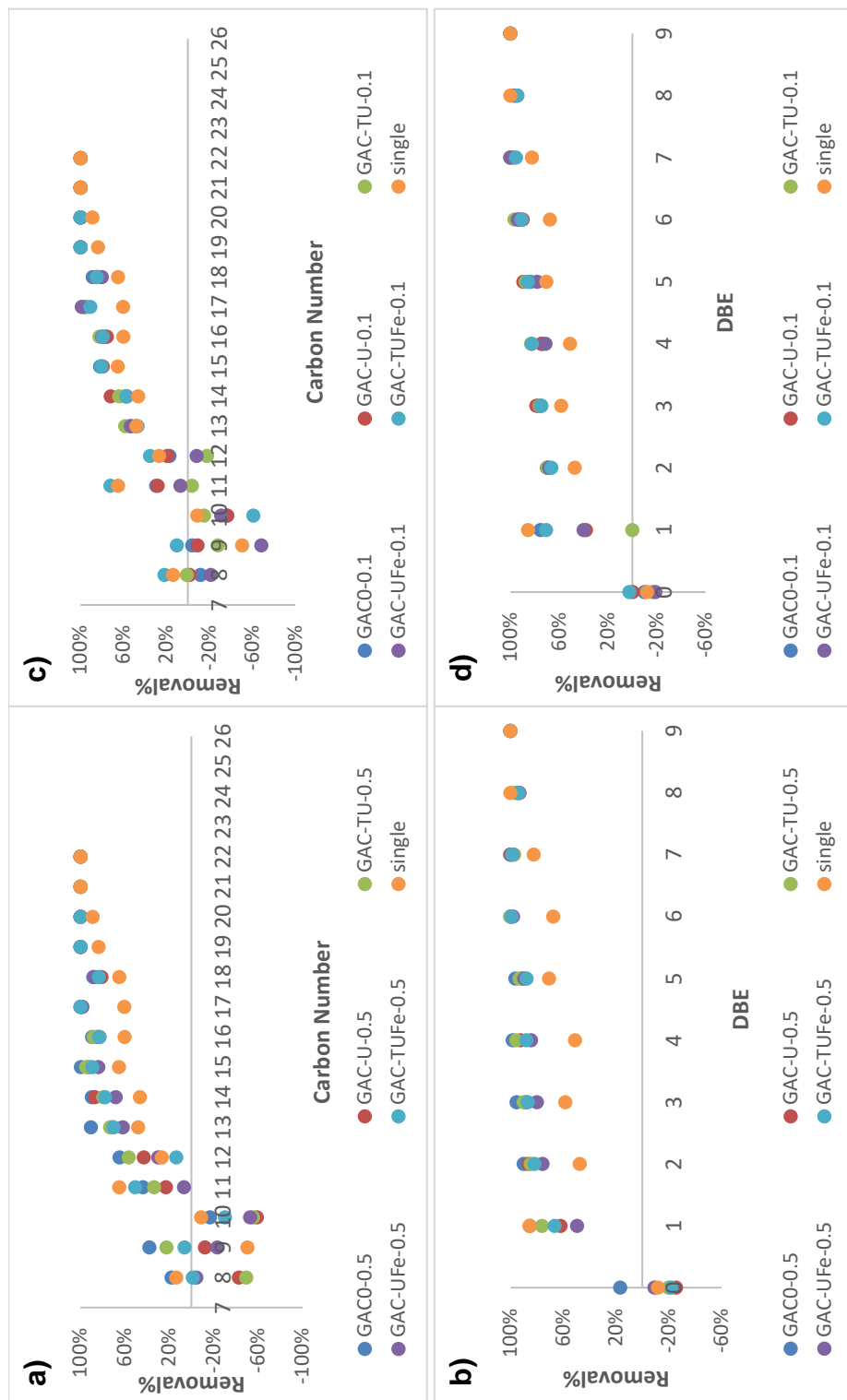


Figure 5.10 Removal of O₂-NAs by 90-min catalytic O₃ treatment with 25 mg/L O₃ and 0.5 g/L catalyst with respect to a) carbon number and b) DBE number. Removal of O₂-NAs by 90-min adsorption with respect to c) carbon number and d) DBE number.



5.3.4.2 UV-based treatments

The NAs concentration change after treatment by UV/Fenton was first examined since the degradation efficiencies with regards to SFS and DOC analyses were quite promising by this treatment although the acidic operation pH was still a challenge. Later, NAs after other UV-based treatments applied using H₂O₂ were compared with those of UV/Fenton. Since the degradation efficiencies by PMS discussed in section 3.3 were not promising enough, those samples were not included to study further.

The quantified O₂-NAs in raw OSPW drastically decreased from 26 mg/L to 1.7 mg/L after pH adjustment to 3 although the DOC removal was only 23%. This concentration difference could be because of the presented form of NAs at different pH values. At natural form of OSPW (pH≈8.5), NAs are present as a mixture of ions and neutral molecules depending on their pK_a values and they are mostly in neutral form at acidic pH [55]. Thus, the concentration removal of the samples treated at pH 3 are presented in *Figure 5.12* calculated accordingly.

Among the UV-based processes performed at pH 3, photo-Fenton treatments exhibited the best NAs removal efficiency resulting in up to 99% of O₂-NAs removal depending on the applied H₂O₂ dose. The most efficient O₂-NAs removal was obtained with the H₂O₂/COD ratio of 2. Higher dose of H₂O₂ resulted in lower removal of O₂-NAs, contrarily to that observed with DOC removal, which resulted better at higher H₂O₂ dose. This suggests the production of new O₂-NAs rather than total mineralization to CO₂ and H₂O at the lower H₂O₂/COD ratios. The blank experiments conducted with only UV light removed just 36% of O₂-NAs, which could be the transformation of O₂-NAs to another compound since the DOC did not change after UV exposure.

In the case of the catalytic UV-based treatments performed at pH 8.45, UV/H₂O₂ treatment either with or without catalyst led to 98% of O₂-NAs removal. Hereby, any positive effect of catalysts on removal efficiency was not observed either by UPLC-TOF-MS or SFS and DOC for the treatments at pH 8.45. The current removals were so as to UV/H₂O₂.

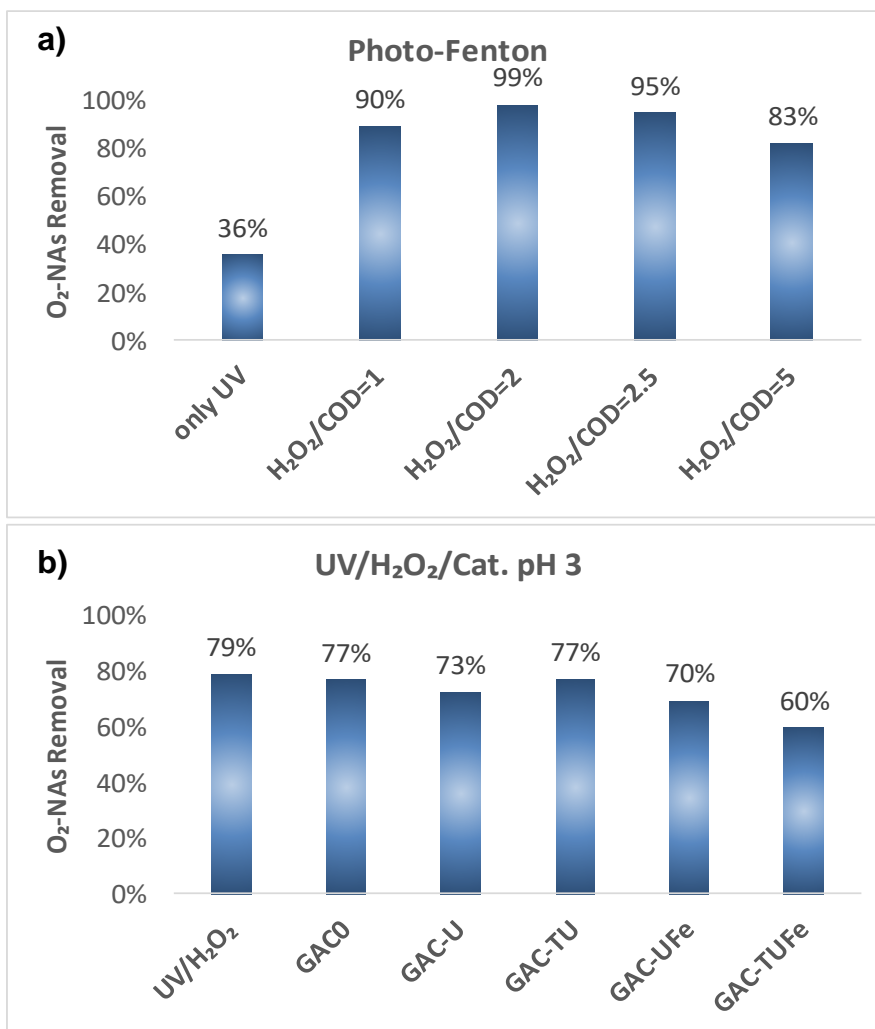


Figure 5.12 Removal of O₂-NAs by 90-min treatments at pH 3 a) Photo-Fenton with 5 mg/L Fe²⁺ and variable H₂O₂ dose b) UV/H₂O₂/Catalysts (0.1 g/L) with H₂O₂/COD=2.5 dose.

5.3.5 Toxicity

It is often reported that the presence of NAs in OSPW is the main reason of its acute toxicity, although their toxic effect could vary depending on the NAs structure (alicyclic or aromatic) and their molecular weight [56]. Based on the preliminary toxicity tests performed by Microtox using *V. fischeri*, the toxicity of the samples after adsorption decreased significantly, suggesting that the compounds with bigger molecule size including ring structures may be responsible for the acute toxicity, as they were adsorbed by the catalysts according to both SFS analysis and NAs quantification by UPLC-TOF-MS. The same behaviour was observed in those O₃-based treated samples. This can also demonstrate that complete mineralization is not

necessary to reduce toxicity of the effluent, considering the low DOC removals achieved by adsorption and applied O₃-based treatments. However, the highest toxicity reduction rates were observed for the photo-Fenton treatments. Nevertheless, these results need further confirmation, therefore details are not provided.

5.4 Conclusions

This study compared different catalytic AOPs for the reclamation of OSPW using granular activated carbon-based materials. A compilation of the results is presented in *Tables Appx. B1-Appx. B2*. From the point of prepared catalysts, the selected materials for the experiments done with real OSPW were found more suitable for the ozone-based treatments in general considering mineralization, NAs removal and mild operation parameters including natural pH and room temperature. However, a cost and sustainability study for the production of the catalysts should be considered, since there was no significant difference between the efficiencies of the treatments conducted with the modified and non-modified GAC, although it was enhanced slightly by modified catalysts.

Concerning the mineralization, which may allow the discharge or reuse of the effluent after treatment, UV/Fenton process was found the best method to achieve higher removal ratios reaching up to 64% with a very low Fe²⁺ concentration, that may be appropriate to discharge after treatment without further sludge removal or reuse it in the plant either for general purposes or for the process units. Also, 99% of NAs was removed, which could reduce the corrosion of the process units caused by NAs, in case of it is reused in the plant. However, the main drawback of this treatment method would be the operating pH, which must be around 3 that would increase the cost of the material used for the treatment units and also the reagent used for regulating the pH around 7 after treatment.

References

- [1] C. Li, L. Fu, J. Stafford, M. Belosevic, M. Gamal El-Din, The toxicity of oil sands process-affected water (OSPW): A critical review, *Sci. Total Environ.* 601–602 (2017) 1785–1802. doi:10.1016/j.scitotenv.2017.06.024.
- [2] T. Leshuk, T. Wong, S. Linley, K.M. Peru, J. V. Headley, F. Gu, Solar photocatalytic degradation of naphthenic acids in oil sands process-affected water, *Chemosphere* 144 (2016) 1854–1861. doi:10.1016/j.chemosphere.2015.10.073.
- [3] C. Benally, M. Li, M. Gamal El-Din, The effect of carboxyl multiwalled carbon nanotubes content on the structure and performance of polysulfone membranes for oil sands process-

CHAPTER 5: Comparison of Catalytic Ozone, UV/H₂O₂, UV/PMS and UV/Fenton in Degrading the Naphthenic Acids in Oil Sands Process Water

- affected water treatment, *Sep. Purif. Technol.* 199 (2018) 170–181. doi:10.1016/j.seppur.2018.01.030.
- [4] X. Xu, G. Pliego, J.A. Zazo, S. Sun, P. García-Muñoz, L. He, J.A. Casas, J.J. Rodriguez, An overview on the application of advanced oxidation processes for the removal of naphthenic acids from water, *Crit. Rev. Environ. Sci. Technol.* 47 (2017) 1337–1370. doi:10.1080/10643389.2017.1348113.
- [5] E.W. Allen, Process water treatment in Canada's oil sands industry: I. Target pollutants and treatment objectives, *J. Environ. Eng. Sci.* 7 (2008) 123–138. doi:10.1139/S07-038.
- [6] R. Huang, Y. Chen, M.N.A. Meshref, P. Chelme-Ayala, S. Dong, M.D. Ibrahim, C. Wang, N. Klammerth, S.A. Hughes, J. V. Headley, K.M. Peru, C. Brown, A. Mahaffey, M. Gamal El-Din, Characterization and determination of naphthenic acids species in oil sands process-affected water and groundwater from oil sands development area of Alberta, Canada, *Water Res.* 128 (2018) 129–137. doi:10.1016/j.scitotenv.2018.07.111.
- [7] C. Wang, N. Klammerth, S.A. Messele, A. Singh, M. Belosevic, M. Gamal El-Din, Comparison of UV/hydrogen peroxide, potassium ferrate(VI), and ozone in oxidizing the organic fraction of oil sands process-affected water (OSPW), *Water Res.* 100 (2016) 476–485. doi:10.1016/j.watres.2016.05.037.
- [8] J.S. Clemente, P.M. Fedorak, A review of the occurrence, analyses, toxicity, and biodegradation of naphthenic acids, *Chemosphere* 60 (2005) 585–600. doi:10.1016/j.chemosphere.2005.02.065.
- [9] A.R. Ribeiro, O.C. Nunes, M.F.R. Pereira, A.M.T. Silva, An overview on the advanced oxidation processes applied for the treatment of water pollutants defined in the recently launched Directive 2013/39/EU, *Environ. Int.* 75 (2015) 33–51. doi:10.1016/j.envint.2014.10.027.
- [10] V.S.R. Rajasekhar Pullabhotla, C. Southway, S.B. Jonnalagadda, Ozone initiated oxidation of hexadecane with metal loaded γ -Al₂O₃ catalysts, *Catal. Lett.* 124 (2008) 118–126. doi:10.1007/s10562-008-9434-4.
- [11] J. Wang, Z. Bai, Fe-based catalysts for heterogeneous catalytic ozonation of emerging contaminants in water and wastewater, *Chem. Eng. J.* 312 (2017) 79–98. doi:10.1016/j.cej.2016.11.118.
- [12] F.J. Beltran, *Ozone reaction kinetics for water and wastewater systems*, Lewis Publishers, Boca Raton, 2004.
- [13] A.K.H. Al jibouri, J. Wu, S.R. Upreti, Heterogeneous catalytic ozonation of naphthenic acids in water, *Can. J. Chem. Eng.* 97 (2018) 67–73. doi:10.1002/cjce.23209.
- [14] K.Y.A. Lin, Z.Y. Zhang, Metal-free activation of Oxone using one-step prepared sulfur-doped carbon nitride under visible light irradiation, *Sep. Purif. Technol.* 173 (2017) 72–79. doi:10.1016/j.seppur.2016.09.008.
- [15] K.Y.A. Lin, Y.C. Chen, Accelerated decomposition of Oxone using graphene-like carbon nitride with visible light irradiation for enhanced decolorization in water, *J. Taiwan Inst. Chem. Eng.* 60 (2016) 423–429. doi:10.1016/j.jtice.2015.10.046.
- [16] H.L. So, W. Chu, Y.H. Wang, Naphthalene degradation by Fe²⁺/Oxone/UV – Applying an unconventional kinetics model and studying the reaction mechanism, *Chemosphere* 218 (2019) 110–118. doi:10.1016/j.chemosphere.2018.11.091.
- [17] H. Park, J. Kim, H. Jung, J. Seo, H. Choi, Iron oxide nanoparticle-impregnated alumina for

- catalytic ozonation of para-chlorobenzoic acid in aqueous solution, *Water Air Soil Pollut.* 225 (2014) 1975. doi:10.1007/s11270-014-1975-0.
- [18] J. Bing, C. Hu, Y. Nie, M. Yang, J. Qu, Mechanism of catalytic ozonation in Fe₂O₃/Al₂O₃@SBA-15 aqueous suspension for destruction of ibuprofen, *Environ. Sci. Technol.* 49 (2015) 1690–1697. doi:10.1021/es503729h.
- [19] M. Ahmadi, B. Kakavandi, N. Jaafarzadeh, A.A. Babaei, Catalytic ozonation of high saline petrochemical wastewater using PAC @ FeII/FeIII/O₂; Optimization, mechanisms and biodegradability studies, *Sep. Purif. Technol.* 177 (2017) 293–303. doi:10.1016/j.seppur.2017.01.008.
- [20] S. Nasserli, A. Mahvi, Y. Shahamat, A. Esrafil, M. Farzadkia, M. Gholami, Magnetic heterogeneous catalytic ozonation: a new removal method for phenol in industrial wastewater, *J. Environ. Heal. Sci. Eng.* 12 (2014) 50. doi:10.1186/2052-336x-12-50.
- [21] A. Dissanayake, A.G. Scarlett, A.N. Jha, Diamondoid naphthenic acids cause in vivo genetic damage in gills and haemocytes of marine mussels, *Env. Sci Pollut Res.* 23 (2016) 7060–7066. doi:10.1007/s11356-016-6268-2.
- [22] S.S. Tiwari, O.T. Iorhemen, J.H. Tay, Aerobic granular sludge and naphthenic acids treatment by varying initial concentrations and supplemental carbon concentrations, *J. Hazard. Mater.* 362 (2019) 348–357. doi:https://doi.org/10.1016/j.jhazmat.2018.09.043.
- [23] S.A. Messele, O.S.G.P. Soares, J.J.M. Órfão, F. Stüber, C. Bengoa, A. Fortuny, A. Fabregat, J. Font, Zero-valent iron supported on nitrogen-containing activated carbon for catalytic wet peroxide oxidation of phenol, *Appl. Catal. B Environ.* 154–155 (2014) 329–338.
- [24] H. Qin, R. Xiao, J. Chen, Catalytic wet peroxide oxidation of benzoic acid over Fe/AC catalysts: Effect of nitrogen and sulfur co-doped activated carbon, *Sci. Total Environ.* 626 (2018) 1414–1420. doi:10.1016/j.scitotenv.2018.01.206.
- [25] E. Bouleghimat, P.R. Davies, R.J. Davies, R. Howarth, J. Kulhavy, D.J. Morgan, The effect of acid treatment on the surface chemistry and topography of graphite, *Carbon N. Y.* 61 (2013) 124–133. doi:10.1016/j.carbon.2013.04.076.
- [26] A. Allwar, R. Hartati, I. Fatimah, Effect of nitric acid treatment on activated carbon derived from oil palm shell, *AIP Conf. Proc.* 1823 (2017). doi:10.1063/1.4978202.
- [27] J. Anthony, *Design of Experiments for Engineers and Scientists*, Elsevier Ltd, Oxford, 2003. doi:https://doi.org/10.1016/B978-0-7506-4709-0.X5000-5.
- [28] D.C. Montgomery, *Design and analysis of experiments*, Eighth, John Wiley & Sons, Inc., Hoboken, 2017. https://lccn.loc.gov/2017002355.
- [29] H. Demir-Duz, A.S. Aktürk, O. Ayyildiz, M.G. Alvarez, S. Contreras, Reuse and recycle solutions in refineries by ozone-based advanced oxidation processes : A statistical approach, *J. Environ. Manage.* 263 (2020) 110346. doi:https://doi.org/10.1016/j.jenvman.2020.110346.
- [30] H. Demir-Duz, O. Ayyildiz, A.S.A.S. Aktürk, M.G.M.G. Álvarez, S. Contreras, Approaching zero discharge concept in refineries by solar-assisted photo-Fenton and photo-catalysis processes, *Appl. Catal. B Environ.* 248 (2019) 341–348. doi:10.1016/j.apcatb.2019.02.026.
- [31] S.M. Joshi, P.R. Gogate, Treatment of landfill leachate using different configurations of ultrasonic reactors combined with advanced oxidation processes, *Sep. Purif. Technol.* 211 (2019) 10–18. doi:10.1016/j.seppur.2018.09.060.
- [32] A. Rubio-Clemente, E. Chica, G.A. Peñuela, Petrochemical wastewater treatment by photo-fenton process, *Water. Air. Soil Pollut.* 226 (2015). doi:10.1007/s11270-015-2321-x.

CHAPTER 5: Comparison of Catalytic Ozone, UV/H₂O₂, UV/PMS and UV/Fenton in Degrading the Naphthenic Acids in Oil Sands Process Water

- [33] N. Wang, T. Zheng, G. Zhang, P. Wang, A review on Fenton-like processes for organic wastewater treatment, *J. Environ. Chem. Eng.* 4 (2016) 762–787. doi:10.1016/j.jece.2015.12.016.
- [34] P. Pourrezaei, A. Alpatova, K. Khosravi, P. Drzewicz, Y. Chen, P. Chelme-Ayala, M. Gamal El-Din, Removal of organic compounds and trace metals from oil sands process-affected water using zero valent iron enhanced by petroleum coke, *J. Environ. Manage.* 139 (2014) 50–58. doi:10.1016/j.jenvman.2014.03.001.
- [35] A.S. Abdalrhman, Y. Zhang, M. Gamal El-Din, Electro-oxidation by graphite anode for naphthenic acids degradation, biodegradability enhancement and toxicity reduction, *Sci. Total Environ.* 671 (2019) 270–279. doi:10.1016/j.scitotenv.2019.03.262.
- [36] R. Qin, D. Lillico, Z. Tong, R. Huang, M. Belosevic, J. Stafford, M.G. El-din, Separation of oil sands process water organics and inorganics and examination of their acute toxicity using standard in-vitro bioassays, *Sci. Total Environ.* 695 (2019) 133532.
- [37] Z. Fang, R. Huang, P. Chelme-Ayala, Q. Shi, C. Xu, M. Gamal El-Din, Comparison of UV/Persulfate and UV/H₂O₂ for the removal of naphthenic acids and acute toxicity towards *Vibrio fischeri* from petroleum production process water, *Sci. Total Environ.* 694 (2019) 1–10. doi:10.1016/j.scitotenv.2019.133686.
- [38] M. Sanchez-Polo, U. Von Gunten, J. Rivera-Utrilla, Efficiency of activated carbon to transform ozone into OH radicals: Influence of operational parameters, *Water Res.* 39 (2005) 3189–3198. doi:10.1016/j.watres.2005.05.026.
- [39] J. Riviera-Utrilla, M. Sanchez-Polo, Ozonation of 1,3,6-naphthalenetrisulphonic acid catalysed by activated carbon in aqueous phase, *Appl. Catal. B Environ.* 39 (2002) 319–329.
- [40] C.A. Guzman-Perez, J. Soltan, J. Robertson, Kinetics of catalytic ozonation of atrazine in the presence of activated carbon, *Sep. Purif. Technol.* 79 (2011) 8–14. doi:10.1016/j.seppur.2011.02.035.
- [41] M. Liu, X. Deng, D. Zhu, H. Duan, W. Xiong, Magnetically separated and N, S co-doped mesoporous carbon microspheres for the removal of mercury ions, *27* (2016) 795–800.
- [42] W. Da Oh, S.K. Lua, Z. Dong, T.T. Lim, Performance of magnetic activated carbon composite as peroxymonosulfate activator and regenerable adsorbent via sulfate radical-mediated oxidation processes, *J. Hazard. Mater.* 284 (2015) 1–9. doi:10.1016/j.jhazmat.2014.10.042.
- [43] R. Atchudan, T.N.J.I. Edison, S. Perumal, P. Thirukumaran, R. Vinodh, Y.R. Lee, Green synthesis of nitrogen-doped carbon nanograss for supercapacitors, *J. Taiwan Inst. Chem. Eng.* 102 (2019) 475–486. doi:10.1016/j.jtice.2019.06.020.
- [44] O. Guo-Li, G. Jian-Feng, H. Tuo-Ping, A. Fu-Qiang, W. Yu, W. Yan-Jun, Z. Dong, Synthesis of an activated carbon based urea formaldehyde resin and its adsorption and recognition performance towards Fe(III), *RSC Adv.* 5 (2015) 71878–71882. doi:10.1039/c5ra11795j.
- [45] M. Pedrosa, L.M. Pastrana-Martínez, M.F.R. Pereira, J.L. Faria, J.L. Figueiredo, A.M.T. Silva, N/S-doped graphene derivatives and TiO₂ for catalytic ozonation and photocatalysis of water pollutants, *Chem. Eng. J.* 348 (2018) 888–897. doi:10.1016/j.cej.2018.04.214.
- [46] G. Hua, J. Broderick, K.T. Semple, K. Killham, I. Singleton, Rapid quantification of polycyclic aromatic hydrocarbons in hydroxypropyl-β-cyclodextrin (HPCD) soil extracts by synchronous fluorescence spectroscopy (SFS), *148* (2007) 176–181. doi:10.1016/j.envpol.2006.10.040.

CHAPTER 5: Comparison of Catalytic Ozone, UV/H₂O₂, UV/PMS and UV/Fenton in Degrading the Naphthenic Acids in Oil Sands Process Water

- [47] Y. Pan, M. Zhou, X. Li, L. Xu, Z. Tang, M. Liu, Novel Fenton-like process (pre-magnetized Fe₀/H₂O₂) for efficient degradation of organic pollutants, *Sep. Purif. Technol.* (2016). doi:10.1016/j.seppur.2016.06.011.
- [48] Y. Abdulaziz Mustafa, A. Ibrahim Alwared, M. Ebrahim, Removal of oil from wastewater by advanced oxidation process/homogeneous process, *J. Eng.* 19 (2013) 686–694.
- [49] E.M. Saggiaro, A.S. Oliveira, T. Pavesi, J.C. Moreira, Effect of Activated Carbon and Titanium Dioxide on the Remediation of an Indigoid Dye in Model Waters, *Rev. Chim.* 65 (2014) 237–241.
- [50] I.V. Gala, j. j. López-Penalver, M. Sánchez-Polo, J. Rivera-Utrilla, Activated carbon as photocatalyst of reactions in aqueous phase, *Appl. Catal. B Environ.* 142–143 (2013) 694–704. doi:10.1016/j.apcatb.2013.06.003.
- [51] M.N.A. Meshref, N. Klammerth, M.S. Islam, K.N. McPhedran, M. Gamal El-Din, Understanding the similarities and differences between ozone and peroxone in the degradation of naphthenic acids: Comparative performance for potential treatment, *Chemosphere* 180 (2017) 149–159. doi:10.1016/j.chemosphere.2017.03.113.
- [52] J. Xue, Y. Zhang, Y. Liu, M. Gamal El-Din, Dynamics of naphthenic acids and microbial community structures in a membrane bioreactor treating oil sands process-affected water: impacts of supplemented inorganic nitrogen and hydraulic retention time, *RSC Adv.* 7 (2017) 17670–17681. doi:10.1039/c7ra01836c.
- [53] Y. Guo, Z. Zeng, Y. Li, Z. Huang, Y. Cui, In-situ sulfur-doped carbon as a metal-free catalyst for persulfate activated oxidation of aqueous organics, *Catal. Today.* 307 (2018) 12–19. doi:http://dx.doi.org/10.1016/j.cattod.2017.05.080.
- [54] X. Liu, H. Yin, A. Lin, Z. Guo, Effective removal of phenol by using activated carbon supported iron prepared under microwave irradiation as a reusable heterogeneous Fenton-like catalyst, *J. Environ. Chem. Eng.* (2017). doi:10.1016/j.jece.2017.01.010.
- [55] R. Huang, K.N. McPhedran, N. Sun, P. Chelme-Ayala, M. Gamal El-Din, Investigation of the impact of organic solvent type and solution pH on the extraction efficiency of naphthenic acids from oil sands process-affected water, *Chemosphere* 146 (2016) 472–477. doi:10.1016/j.chemosphere.2015.12.054.
- [56] A.G. Scarlett, H.C. Reinardy, T.B. Henry, C.E. West, R.A. Frank, L.M. Hewitt, S.J. Rowland, Acute toxicity of aromatic and non-aromatic fractions of naphthenic acids extracted from oil sands process-affected water to larval zebrafish, *Chemosphere* 93 (2013) 415–420. doi:10.1016/j.chemosphere.2013.05.020.

6

Synergetic Effect of O_3/H_2O_2 and UV-C Light Irradiation for the Treatment of Oil Sands Process Water



UNIVERSITAT ROVIRA I VIRGILI

Application of Advanced Oxidation Processes in the Reclamation of Wastewaters from the Oil
& Gas Sector

Hande Demir Duz

6.1 Introduction

Bitumen obtained from oil sands is an unconventional fossil fuel that became important in the market due to increasing global demand for oil [1]. However, processing bitumen produces several wastes including produced waste gases or produced water that cause several environmental problems [2]. Regarding produced water, bitumen extraction from oil sands by caustic hot water forms nine cubic meters of raw tailings called oil sands process water (OSPW) per a cubic meter of produced oil [3]. OSPW consisting of water, sand, clay, unrecovered bitumen and other organics including naphthenic acids (NAs) is stored in tailing ponds because of the zero-discharge policy. Typically, a 80% of OSPW is reused in subsequent extraction processes, while the rest must be further managed [3,4]. As a part of the industry's reclamation plan, OSPW in tailings ponds needs to be treated and eventually be discharged into terrestrial and/or aquatic habitat [5]. Particularly, the major concern in OSPW treatment is the abatement of naphthenic acids (NAs) because of their high concentration (20-80 mg/L) and their acute and subchronic toxic effects on aquatic organisms compared to other organic compounds [6].

Naphthenic acids are natural components of bitumen that solubilize during the extraction process. The term of NAs includes mainly alkyl substituted cycloaliphatic carboxylic acids with lower amounts of acyclic aliphatic, aromatic olefinic, hydroxy, and dibasic acids [7]. NAs are expressed by the general formula of $C_nH_{2n+z}O_x$ where n represents the number of carbon atoms, Z is a negative even integer associated with the ring structure and double bonds existing in the component, and x stands for the number of oxygen atoms [8,9]. Due to the complex nature of NAs mixture, the analytical methods developed up to now allow solely the detection of general profile of the mixture related to their carbon content and Z number instead of the detection of the individual components [10].

The environmental management of OSPW could be done cost effectively by biological treatment to reduce the toxicity in some sort. However, in terms of accomplishing with the discharging policies, biological treatment is a very slow process with low efficiency because of the bio-recalcitrant characteristics of NAs in general [11]. Likewise, adsorption by different adsorbents including organic-rich soil, biochar and activated carbon has been reported because of its high efficiency in NAs removal. However, an extra cost is required for regeneration of the adsorbent or its disposal after use [12]. Thus, advanced oxidation processes (AOPs) are getting

essential to reach a balance between cost and treatment efficiency avoiding further disposal managements after treatment.

Among AOPs, ozone has wide range of applications in various kinds of effluents from different sectors and its application is not limited to wastewater treatment but also for potable water disinfection, air cleaning, food processing and preserving and health sector due to the high reactivity of ozone [13,14]. Indeed, ozonation is currently used at a large-scale as a stage of municipal wastewater treatment facilities because of its disinfection, decolorization and deodorization power and degradation of micropollutants and organic compounds. In terms of investment and operational costs, which was stated as 0.02-0.07 Eur/m³ of treated wastewater, it was found feasible to be operated [15]. However, the efficiency of the treatment would depend on the complexity of the wastewater. The presence of components that easily react with O_3 can be removed in few seconds to 2 min. by direct reaction of O_3 . Once they are removed completely or their concentration decreases, the O_3 decomposition gets slower and, indirect reactions gain importance for the removal of recalcitrant components so as to achieve higher treatment efficiencies depending on the type of organic molecules and medium pH [16].

In case of OSPW, several studies have been focused on the potential decrease of NAs concentration in OSPW rather than aiming at mineralization, in order to reduce the toxicity of the effluent and/or increase the biodegradability by either ozone or O_3/H_2O_2 treatment. In some cases, applied ozone treatments were in batch mode, i.e., O_3 was fed into water to form a stock solution of O_3 in order to be added to batch reactor at once [8]. The studies performed by semi-batch mode, where O_3 was bubbled into a batch reactor with a constant volume of OSPW, applied very low amounts of oxidants only enough to transform contaminants into other compounds improving the toxicity. In this case, no mineralization was observed after treatment, but this was not the objective of these studies. [17,18]. In other studies, it has been reported higher toxicity after ozone treatment caused by the generated by-products [19].

Optimised amounts of oxidants are crucial to increase treatment efficiency achieving the mineralization of the by-products and consequently, the reduction in toxicity. This optimized parameters and the systems are specific to the configurations of the units [20]. Furthermore, the feeding methods including batch, semi-batch and continuous modes, and the design of the reactor are also critical for a successful treatment. Especially for the treatments where O_3 was bubbled into the effluent, the effect of the size of the O_3 bubbles has been reported [21,22]. The study of Chu et

al., where the performance difference between a microbubble generator and a conventional bubble contactor was investigated, confirmed the enhancement in mass transfer improving the removed total organic carbon (TOC) per gram of ozone consumed by accelerated formation of hydroxyl radicals (OH•) when microbubble generator was used [22].

Thus, this study explores the efficient treatment of OSPW aiming at mineralization rather than transformation of contaminants by semi-batch ozone-based AOPs, where O₃ was fed into the reactor by a microporous diffuser, combined with H₂O₂ and/or ultraviolet C irradiation (UV-C) looking for increasing the concentration of available radicals to boost the effectiveness in the degradation of recalcitrant contaminants. Here and to the best of our knowledge, the combined O₃-based treatments in the presence of UV-C irradiation are studied for the first time to treat OSPW. The optimum amounts of reactants, reaction time and the effect of UV-C application have been systematically studied, and the feasibility of the applied processes, including an economic comparison is also discussed. This will allow a possible reusing and/or discharging solution to the sector, where current zero-discharge policy causes a decrease in the quality of the OSPW recycled to processing unit; and thus, an increase in the volume of the effluent stored in tailing ponds by time due to the lack of an established method to treat OSPW.

6.2 Experimental

6.2.1 Materials and methods

Raw OSPW was collected from an oil sands tailing pond in northern Alberta and stored at 4 °C until being used. Main parameters were measured periodically to confirm its stability. Only insignificant differences between the measurements have been observed. Before the treatments, OSPW was filtered using a 0.45 µm nylon membrane to remove suspended solids that could increase the consumption of reagents and decrease the light transmittance (important parameter in case of the light-based treatments). **Table 6.1** presents the initial characteristics of OSPW used in this study, after filtration.

Hydrogen peroxide (H₂O₂, 35 wt%, Acros Organic) was used as the oxidant in the ozone-based treatments while potassium iodide (KI, Sigma-Aldrich) were used as a trap to destroy residual O₃ after treatments. Sulfuric acid and sodium hydroxide solutions (1M) were used for pH adjustment of the samples collected for biological

based analyses when needed, while sodium bisulfite (NaHSO₃, 40%, Panreac) was used for quenching remained H₂O₂ in the samples and stopping the reaction.

Table 6.1 Initial characteristics of raw OSPW.

DOC (mg C/L)	COD (mg O ₂ /L)	pH	Conductivity (mS/cm)
100	270	8.5	4.6

Ozone (O₃) based experiments were performed in a laboratory scale semi-batch system consisting of an ozone generator, a quartz reactor, a residual ozone measurer and an ozone trap. In the case of UV-C combined treatments, the reactor was surrounded by 4 UV-C low pressure lamps (15W each) that emit mostly at 254 nm. Ozone was produced from pure oxygen by an ozone generator and fed into the quartz reactor containing 300 mL of effluent by an inert, porous diffuser. The outlet gas stream of the reactor was connected to an ozone analyzer to measure residual O₃ during the treatment. In the case of tests involving H₂O₂, desired amounts of H₂O₂ were added into the effluent at once just before starting the O₃ feed. Blank experiments were also conducted to establish the effectiveness of the single processes.

Applied O₃ production rates were 0.9 g/h, 1.8 g/h and 2.7 g/h while varied doses of H₂O₂ were tested (calculated based on the weight/weight ratio of H₂O₂ to initial chemical oxygen demand (COD) and ranged between 0.1 and 5). All the treatments took place during 90 min at natural pH conditions. Samples were collected every 30 min for detailed analysis.

6.2.2 Analytical methods

Dissolved Organic Carbon (DOC) was measured by Shimadzu TOC-L (CSN 638-91109-48) analyzer. Microtox[®] acute toxicity of the treated/untreated OSPW on *V. fischeri* bacteria was investigated using 81.9% screening test standard protocol with a Microtox[®]500 Analyzer. The inhibition effect of the samples on *V. fischeri* was measured after 15 min cultivation based on the change in the luminescence intensity. The results were expressed by EC₅₀ concentration, defined as the effective nominal concentration of raw/treated OSPW by volume percent that caused reduction in the intensity of light emission by 50%.

6.3 Results and Discussions

6.3.1 Dissolved organic carbon (DOC) removal

DOC analysis is a fast and easy technique to evaluate the treatment efficiencies, which gains importance especially for the treatment of real effluents with complex organic composition like OSPW. For this, the effect of combining H₂O₂ and UV-C to single O₃ treatment was assessed initially by DOC removal. The initial tests of OSPW were focused on single ozonation, conducted with O₃ production rates of 0.9 g/h, 1.8 g/h and 2.7 g/h, which removed 33%, 45% and 53% of DOC, respectively after 90 min treatment. Scott et al. previously reported approximately 25% of TOC removal after 130 min ozone treatment of OSPW, where ozone was fed to the system continuously reaching 35 mg/L of dissolved ozone in the reactor [17]. Thus, single ozonation seems not to be effective enough to mineralize the recalcitrant components present in OSPW. The introduction of promoters of the ozone decomposition to increase the concentration of OH• radicals, consequently the occurrence of indirect reactions, can favour the mineralization of those recalcitrant components present in OSPW.

Introducing H₂O₂ into the system led to a significant increase of the DOC removal efficiency (**Figure 6.1**), as expected. It is frequently reported that in the presence of H₂O₂, the conversion rate of O₃ to HO• and dissolved O₃ amount increases. Besides, the generation of HO• and HO₂• radicals from the activation of H₂O₂ by O₃ or O₃ decomposition promoted by H₂O₂ can take place [23]. Thus, 71% of DOC removal was achieved after 90 min of O₃/H₂O₂ treatment with 0.9 g/h O₃ production rate and H₂O₂/COD=2. Whereas, increasing the O₃ production rate to 1.8 g/h and 2.7 g/h O₃ (maintaining the H₂O₂/COD ratio) led to a DOC removal of 84% and 86%, respectively, indicating that higher production rates of O₃ than 1.8 g/h, in the presence of H₂O₂, do not lead to significant changes in the DOC removal. Thus, UV-C combined treatments were performed only with O₃ production rates of 0.9 g/h and 1.8 g/h.

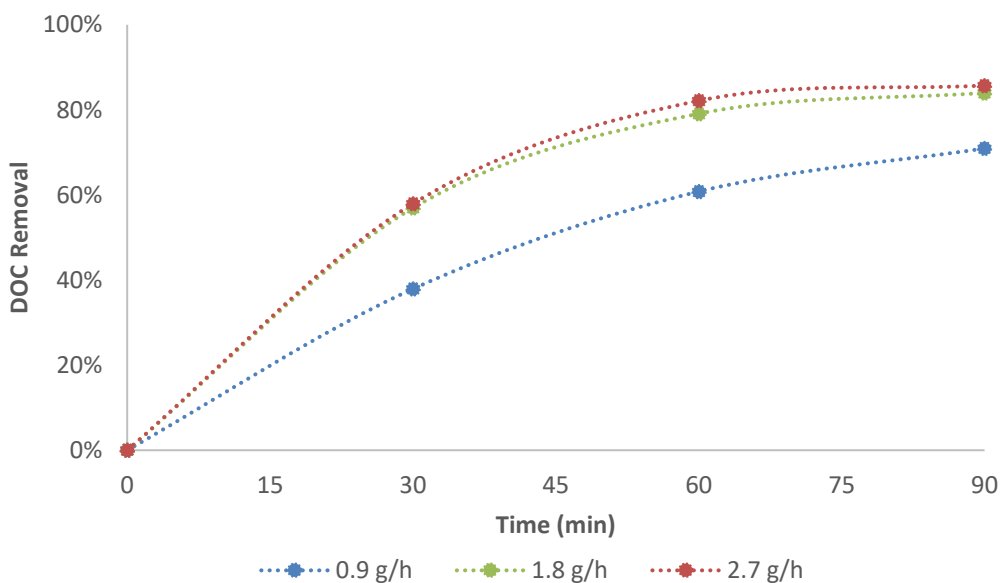


Figure 6.1 DOC removal efficiency by O_3/H_2O_2 treatment with varied production rates of O_3 and a constant H_2O_2/COD ratio of 2.

UV-C integration to O_3 -based treatments (**Figure 6.2**) enhanced the treatment efficiencies in great extent, allowing a shorter treatment time. This is likely due to the synergetic effect of the combined O_3 treatment with UV-C and/or H_2O_2 , which may form hydroxyl, peroxy and superoxide radicals increasing the reaction efficiencies, according to the literature [24,25]. Besides this, in-situ production of H_2O_2 from UV-C and O_3 can also occur, as reported before in several studies, favouring DOC removal by increased amounts of radicals [26,27]. After 90 min, DOC removal reached by single ozonation with 0.9 g/h and 1.8 g/h increased from 33% and 45% to 67% and 84%, respectively, solely due to its combination with UV-C. In the case of H_2O_2 addition to UV-C/ O_3 system, DOC removals after 90 min of treatment reached 87% and 98% for 0.9 g/h and 1.8 g/h O_3 production rates, respectively. Remarkably, this triple combination (i.e., $H_2O_2/O_3/UV-C$) conducted with 1.8 g/h of O_3 and H_2O_2/COD ratio of 2, already allowed a 65% and 92% of DOC removal in 30 min and 60 min, respectively.

Due to the improved results obtained by the use of a triple $H_2O_2/O_3/UV-C$ combination, the effect of H_2O_2 concentration has been studied further. The DOC removal trend after the triple $H_2O_2/O_3/UV-C$ combination (**Figure 6.3**) with $H_2O_2/COD=1.05$ and $H_2O_2/COD=2$ was very similar, reaching 83% and 87%,

respectively, after 90 min of treatment. Any decrease or increase of H_2O_2 dose caused a noticeable decrease in the removal efficiency either due to a lower radicals production (in the case of the lowest dose) or due to the scavenging effect of H_2O_2 itself (in the case of the highest dose) [28].

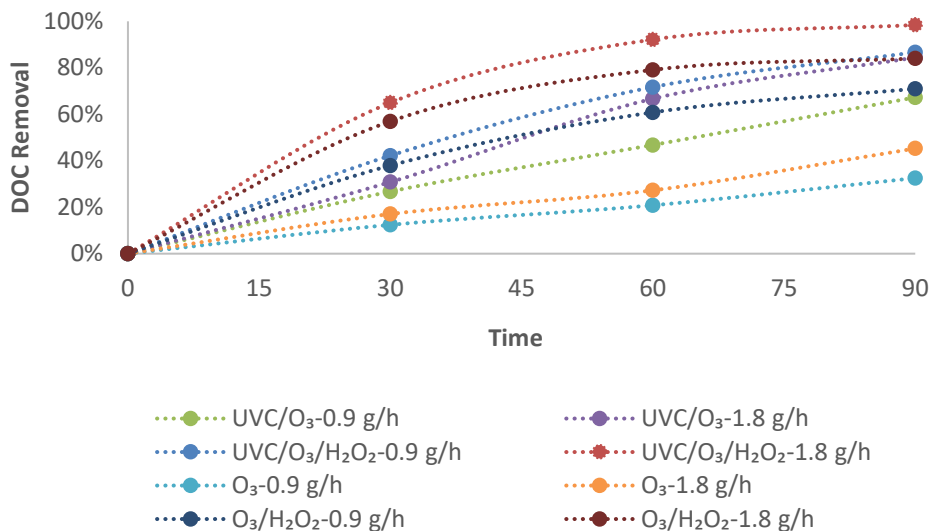


Figure 6.2. DOC removal efficiency by UV-C based treatments with varied production rates of O_3 with/without a constant H_2O_2/COD ratio of 2.

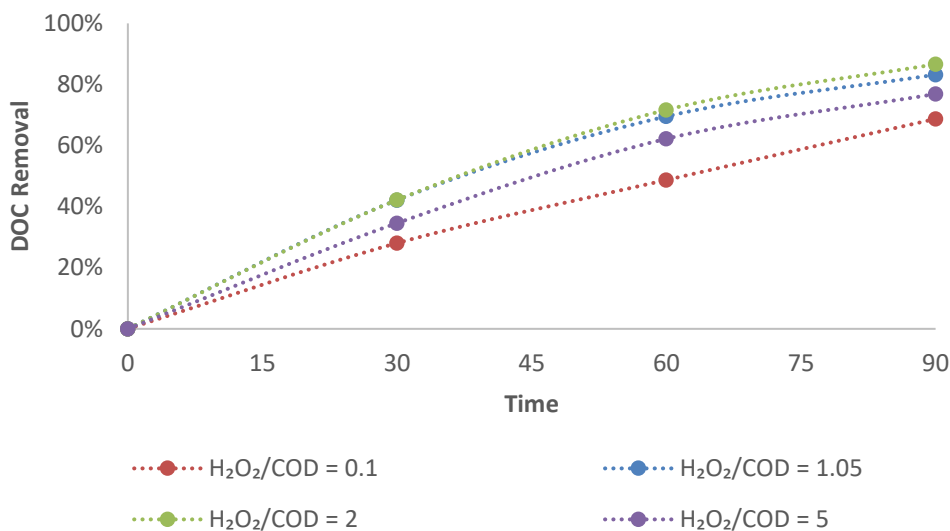


Figure 6.3 DOC removal efficiency by UV-C based treatments with varied ratios of H_2O_2/COD and a constant O_3 production rate of 0.9 g/h.

6.3.2 Toxicity evaluation

Toxicity of OSPW has been studied frequently as an indicator of effectiveness of the treatment. Raw OSPW present acute toxicity due to the presence of NAs and other organic components such as polycyclic aromatic hydrocarbons (PAHs), BTEX (benzene, toluene, ethyl benzene, and xylenes) and phenols [29]. Therefore, due to the complex nature of OSPW, toxicity is assessed for the entire OSPW composition or for its main constituents, such as NAs fractions or other organic fractions instead of individual components [29–31]. Accordingly, an effective treatment method that allows dischargement of OSPW safely by reducing its toxicity became a necessity unless treated effluent is reused in the plant.

Microtox is a rapid and relatively economic method commonly used to monitor acute toxicity of effluents like OSPW [17]. In the literature, values $EC_{50} < 25\%$ are defined as very toxic, while $25\% < EC_{50} < 75\%$ would be toxic and $EC_{50} > 75\%$ would be considered non-toxic [32]. Inhibition test is recommended for the effluents with low levels of toxicity, for which EC_{50} values are not calculable [33].

Toxicity tests on *V. fischeri* performed with the samples collected after the different treatments (**Table 6.2**) revealed that 90-min single O₃ treatment with the lowest O₃ production rate (i.e., 0.9 g O₃/h) already reduced the toxicity of OSPW, presenting a EC_{50} concentration of 42%, which would still be considered toxic, compared to EC_{50} of 19% for raw OSPW. Higher O₃ production rates decreased the toxicity to suitable ranges. Thus, the maximum inhibition effects found in those samples treated after 90 min of single ozonation with O₃ production rates of 1.8 g/h and 2/7 g/h were 33% and 37%, respectively. That is, the reduction of 50% in the luminescence intensity was not reached, which demonstrates the non-toxic features of the treated OSPW. In the case of combined treatments, acute toxicity also decreased significantly in accordance with the mineralization levels obtained, as shown by DOC analysis. After 90 min of treatment with the O₃/H₂O₂ system, with H₂O₂/COD=2 under dark conditions also resulted in 43% and 26% of maximum inhibition effect for the 0.9 g/h and 1.8 g/h O₃ production rate, respectively, improving the toxicity reduction as compared to those of single ozonation. After 90 min of combined treatment of UV-C/O₃/H₂O₂ the toxicity showed a maximum inhibition effect of 33% and 22% for the 0.9 g/h and 1.8 g/h O₃ production rate (with H₂O₂/COD=2), respectively, which would mean the lowest toxic properties.

Table 6.2 Toxicity tests on *V. fischeri* performed with the samples collected after the 90 min different treatments.

Process	Treatment Conditions			Toxicity Assessments	
	O ₃ (g/h)	H ₂ O ₂ /COD	UV-C	EC ₅₀ (%)	Inhibition Effect (%)
Raw OSPW				19	99
O ₃	0.9			42	62
	1.8				33
	2.7				37
O ₃ /H ₂ O ₂	0.9	2			43
	1.8	2			26
UV-C/O ₃	0.9		Applied		24
	1.8		Applied		41
UV-C/O ₃ /H ₂ O ₂	0.9	2	Applied		33
	1.8	2	Applied		22

The positive influence of ozone-based treatments on the toxicity of OSPW has also been reported in other studies [8,11]; however, the DOC reduction reported is quite small. Therefore, not only toxicity but a general assessment of all parameters must be considered for the most appropriate treatment method for OSPW including mineralization and economy.

6.3.3 O₃ consumption analysis

Beltran, reported in detail that when ozone dissolves in water decomposes to free radicals, and indirect reactions start beside the direct reactions. This decomposition mechanism is strongly dependant on the nature of the effluent including pH or the present components [16]. In a recent study, the treatment of a petroleum refinery wastewater effluent with the same ozonation system showed a reverse balance between O₃ and the H₂O₂ concentrations, suggesting that the highest TOC removals could be reached by an optimum ratio between O₃ and H₂O₂ [28]. Thus, the consumption tendency of the oxidants for treating OSPW was tried to be clarified as an example of case studies.

The mass balance of O₃ within the system was determined by *Eq. 1*. Here, although the dissolved O₃ concentrations of the collected samples were measured by indigo colorimetric method described by APHA [34], the residual dissolved O₃

concentrations were not taken into account due to the low detected concentrations (ranged between 3-8 mg/L) compared to those of inlet and outlet. However, it would be interesting to note that dissolved O₃ amount in samples after 90 min of treatment was as follows: UV-C/O₃/H₂O₂ < UV-C/O₃ < O₃ < O₃/H₂O₂. Lower dissolved amount of O₃ was observed in those experiments performed in the presence of UV-C light (approx. 3.8 mg/L for UV-C/O₃/H₂O₂ and UV-C/O₃). This is indeed in agreement with the consumed O₃ amount of those treatments as showed in **Figure 6.4b**. So that, O₃ consumptions of those systems including UV-C light (with an O₃ feed ratio of 1.8 g/h) were increased to ca. 2 g after 90 min compared to 0.5 g of O₃ consumed in the processes that do not include UV-C irradiation. The higher O₃ consumption shown by these UV-C based processes accounts for the photodecomposition of O₃ yielding H₂O₂ and subsequently hydroxyl radicals among other radicals [24]. Similarly, in addition, the O₃ consumption for O₃/H₂O₂ system (**Figure 6.4a**) was higher than that of single ozonation. This result was expected since H₂O₂ accelerates the ozone decomposition ratio that eventually leads to form hydroxyl radicals especially at alkaline pH [16].

$$\text{O}_3 \text{ consumption (reacted + dissolved) (g)} = \text{O}_3 \text{ (inlet) (g)} - \text{O}_3 \text{ (outlet) (g)} \quad (1)$$

The relationship between O₃ consumption and DOC removal (**Figure 6.5**) revealed that those treatments including the use of H₂O₂ - either with or without UV-C promoted efficient consumption of O₃ in terms of DOC removal. In the presence of H₂O₂, DOC removals of the treatments were almost two-fold, although the consumed O₃ amounts were almost the same for the treatments conducted in the absence of H₂O₂. In other words, when single ozonation is applied, O₃ consumption is mainly due to the transformation the OSPW components rather than mineralization likely due to the absence of the HO· degradation pathway. Also, the molar ratios of O₃(consumed)/DOC(removed) for the treatments conducted with 1.8 g/h O₃ production rates were calculated as 4, 6, 21 and 18 for the treatments of O₃, O₃/H₂O₂, UV-C/ O₃ and UV-C/O₃/H₂O₂, respectively, indicating that the O₃ was used more effectively in the O₃/H₂O₂ treatment considering also the DOC removal efficiency which was 45% and 84% for O₃ and O₃/H₂O₂ treatments, respectively. A previous study of another kind of petroleum refinery wastewater treatment by ozone-based processes also reported that the molar ratio of O₃(consumed)/DOC(removed) for the optimized O₃/H₂O₂ treatment was around 6 [28].

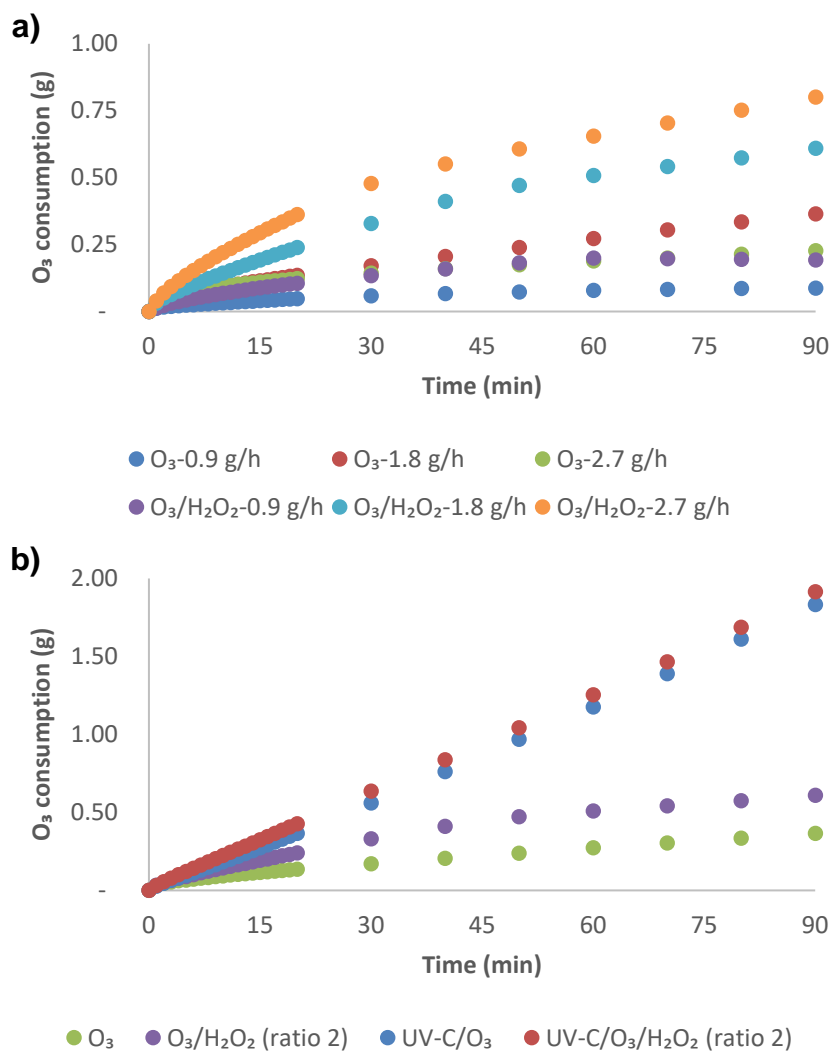


Figure 6.4 O_3 consumption during 90 min treatment by a) O_3 and O_3/H_2O_2 with $H_2O_2/COD=2$ and varied O_3 production rates b) different AOPs with O_3 production rate of 1.8 g/h.

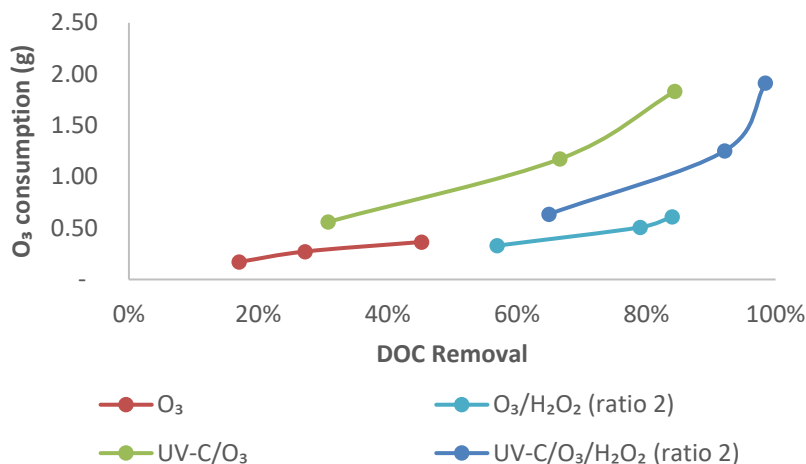


Figure 6.5 The relationship between O₃ consumption and DOC removal% for different AOPs with O₃ production rate of 1.8 g/h.

6.3.4 Operational comparison of applied treatments

The balance between operational costs and the treatment efficiencies becomes important for a feasible application of treatment processes. Although high mineralization degrees could be reached through the different combinations of UV-C, O₃ and H₂O₂, operational costs must be also considered to decide the most convenient alternative for the treatment of OSPW, also having in mind the final end of the treated effluent. The energy consumption comparison of the different treatments may help to make an approach on this question.

Energy consumption of the treatments can be assessed by the *Eq. 2*, reported by Bolton et al., based on the electrical energy per order (EEO) on a batch system [35].

$$EEO \left(\frac{kWh}{m^3} \right) = \frac{P(kW) * t(h) * 1000}{V(L) * \log \left(\frac{C_i}{C_f} \right)} \quad (2)$$

where P(kW), t(h), C_i and C_f and V(L) represent rated power, reaction time, initial and final concentration, and treated volume of OSPW, respectively.

In previous studies, this equation was slightly modified using initial and final TOC instead of a target compound concentration because of the complex nature of real

effluents [28,32]. In this study, calculations were made based on DOC removal expressed by the *Eq. 3*, since the first target was reaching higher DOC removal by mineralization.

$$EEO \left(\frac{kWh}{m^3} \right) = \frac{P(kW) * t(h) * 1000}{V(L) * \log \left(\frac{DOC_i}{DOC_f} \right)} \quad (3)$$

EEO of the applied processes were calculated considering the energy consumption of the current laboratory-scale system. P (kW) of magnetic stirrer, O₃ measurer and UV-C lights were 0.002, 0.008 and 0.06, respectively while that of O₃ generator was calculated depending on the produced O₃ amount (10 kW/kg O₃ according to the supplier). As shown in *Table 6.3*, it was observed that EEO corresponding to 90 min of single ozonation was pretty higher than the combined AOPs although the DOC removals were the lowest. Also, UV-C/O₃ treatment resulted in high energy demand. However, in the presence of UV-C, higher O₃ production rate resulted in lower EEO as the removal efficiency was higher at a given time. EEO values decreased to 177 kWh/m³ and 171 kWh/m³ for the O₃/H₂O₂ combination with O₃ production rates of 0.9 g/h and 1.8 g/h, respectively, and a H₂O₂/COD ratio of 2. This indicates a marked benefit of O₃/H₂O₂ treatment in mineralization that reached to 84% DOC removal, and economy obtained by applying 1.8 g/h of O₃ dosing in combination with H₂O₂ considering. Instead, the use of an O₃ feeding above 1.8 g/h increased the EEO significantly since DOC removal was not improved by applying higher O₃ production rate. The electrical energy need increased slightly to 243 kWh/m³ for the treatments conducted with the UV-C/O₃/H₂O₂ system with a O₃ production rate of 1.8 g/h and H₂O₂/COD ratio of 2, if compared with the EEO of O₃/H₂O₂ treatments. However, DOC removal% obtained by UV-C/O₃/H₂O₂ was remarkably high, 98%, which expands the range of reuse purposes in the plant. In contrast, decreasing the dose of O₃ to 0.9 g/h caused a great increase in EEO, up to 452 kWh/m³ for the same H₂O₂/COD ratio=2. Thus, it could be concluded that O₃/H₂O₂ system can offer an effective treatment with a better price, while UV-C/O₃/H₂O₂ system can provide an effluent with better quality that can increase its reuse rather than discharging.

Table 6.3 EEO comparison of different processes after 90 min treatment.

Process	Treatment Conditions				P (kW) for each unit			EEO (kWh/m ³)
	O ₃ (g/h)	H ₂ O ₂ /COD	UV-C	Magnetic Stirrer	O ₃ generator	O ₃ measurer	UV-C	
O ₃	0.9	-	-	0.002	0.009	0.008	-	556
	1.8	-	-	0.002	0.018	0.008	-	536
	2.7	-	-	0.002	0.027	0.008	-	568
O ₃ /H ₂ O ₂	0.9	2	-	0.002	0.009	0.008	-	177
	1.8	2	-	0.002	0.018	0.008	-	171
	2.7	2	-	0.002	0.027	0.008	-	219
UV-C/O ₃	0.9	-	Applied	0.002	0.009	0.008	0.06	827
	1.8	-	Applied	0.002	0.018	0.008	0.06	537
UV-C/O ₃ /H ₂ O ₂	0.9	2	Applied	0.002	0.009	0.008	0.06	452
	1.8	2	Applied	0.002	0.018	0.008	0.06	243
UV-C/O ₃ /H ₂ O ₂	0.9	0.1	Applied	0.002	0.009	0.008	0.06	782
	0.9	1.05	Applied	0.002	0.009	0.008	0.06	509
	0.9	5	Applied	0.002	0.009	0.008	0.06	621

It must be noted that EEO values were calculated for the laboratory scale system used in this study only to present how EEO would change by single or combined treatment methods. EEO of large-scale, optimized treatment systems, where a study of the best lamp type (if any) and O₃ production/injection systems would be performed, may be much lower than the presented values. Besides the process capacity, it is worthy to mention that EEO is highly dependent of the water features, eg. concentration of contaminants, turbidity, presence of recalcitrant components and radical scavengers. The effluent treated in this study is a real waste effluent with a very complex matrix that presents high concentrations of naphtenic acids, known by their high toxicity and resistance to mineralization. Thus, it is reasonable to expect higher energy demand than that needed in case studies where only one or few components are present in a pure water matrix.

6.4 Conclusions

This study explored an efficient and environmentally friendly treatment method that can add value to the industry's reclamation plan for the OSPW, which currently is stored in tailing ponds until it is treated properly. For this aim, ozone based AOPs including the different combinations of O₃, H₂O₂ and UV-C were investigated in detail as a candidate to treat OSPW. In contrast to many studies, mineralization rather than transformation of the recalcitrant components was targeted so as to reclaim the effluent after treatment, which could be then reused in the bitumen extraction or upgrading units without lowering the quality of the products or causing corrosion in the process units. Additionally, the treated effluent could be discharged safely to the environment.

Optimized O₃/H₂O₂ treatment can be considered as a feasible treatment method in terms of the mineralization degree, which decreased the final DOC down to ca. 15 mg C/L and eliminated the acute toxicity completely. These features make the effluent being discharged safely, after decreasing its alkalinity, or being reused in the extraction process since its quality is improved significantly. Thus, reusing improved quality of the treated effluent in extraction process can offer a remedy to the current problems due to the decreases in extraction efficiencies over time meanwhile increasing the pollution degree of OSPW in tailing ponds.

When UV-C light was irradiated during O₃/H₂O₂ treatment, final DOC was reduced down to 2 mg C/L with the consequent removal of toxicity. This method allows the treated water being used as cooling/boiling water in the units used for bitumen upgrading. However, in this case, it is expected that the operation costs would

increase slightly in the case of a large-scale application, based in our observations at lab-scale. Therefore, a global evaluation considering the costs of water processing or purchasing that is used for these systems should be performed.

The real effluent used in this study provides important information of the efficiency of the different AOPs tested in case of extrapolation to a larger scale. The efficiency showed by these treatment methods may bring the following benefits: i) the reduction of water use by decreasing the external water demand of the bitumen and heavy oils extraction plants in the search of a more resource efficient and environmental friendly processes; and ii) the opening up to the recovering and reclamation of land, decreasing the negative impact on the local fauna and possible seepage to surface water.

References

- [1] E.W. Allen, Process water treatment in Canada's oil sands industry: I. Target pollutants and treatment objectives, *J. Environ. Eng. Sci.* 7 (2008) 123–138. doi:10.1139/S07-038.
- [2] G. Boczkaj, M. Gałol, M. Klein, A. Przyjazny, Effective method of treatment of effluents from production of bitumens under basic pH conditions using hydrodynamic cavitation aided by external oxidants, *Ultrason. Sonochem.* 40 (2018) 969–979. doi:10.1016/j.ultsonch.2017.08.032.
- [3] L.D. Brown, A.C. Ulrich, Oil sands naphthenic acids : A review of properties, measurement, and treatment, *Chemosphere* 127 (2015) 276–290. doi:http://dx.doi.org/10.1016/j.chemosphere.2015.02.003.
- [4] G. Mannina, *Frontiers in Wastewater Treatment and Modelling*, Springer, Cham, 2017. doi:10.1007/978-3-319-58421-8.
- [5] R. Huang, Y. Chen, M.N.A. Meshref, P. Chelme-Ayala, S. Dong, M.D. Ibrahim, C. Wang, N. Klammerth, S.A. Hughes, J. V. Headley, K.M. Peru, C. Brown, A. Mahaffey, M. Gamal El-Din, Characterization and determination of naphthenic acids species in oil sands process-affected water and groundwater from oil sands development area of Alberta, Canada, *Water Res.* 128 (2018) 129–137. doi:10.1016/j.scitotenv.2018.07.111.
- [6] Z. Fang, R. Huang, P. Chelme-Ayala, Q. Shi, C. Xu, M. Gamal El-Din, Comparison of UV/Persulfate and UV/H₂O₂ for the removal of naphthenic acids and acute toxicity towards *Vibrio fischeri* from petroleum production process water, *Sci. Total Environ.* 694 (2019) 1–10. doi:10.1016/j.scitotenv.2019.133686.
- [7] J. V. Headley, D.W. McMartin, A Review of the occurrence and fate of naphthenic acids in aquatic environments, *J. Environ. Sci. Heal. Part A.* 39 (2004) 1989–2010. doi:10.1081/ESE-120039370.
- [8] M.N.A. Meshref, N. Klammerth, M.S. Islam, K.N. McPhedran, M. Gamal El-Din, Understanding the similarities and differences between ozone and peroxone in the degradation of naphthenic acids: Comparative performance for potential treatment,

- Chemosphere 180 (2017) 149–159. doi:10.1016/j.chemosphere.2017.03.113.
- [9] T. Leshuk, T. Wong, S. Linley, K.M. Peru, J. V. Headley, F. Gu, Solar photocatalytic degradation of naphthenic acids in oil sands process-affected water, *Chemosphere* 144 (2016) 1854–1861. doi:10.1016/j.chemosphere.2015.10.073.
- [10] J.S. Clemente, P.M. Fedorak, A review of the occurrence, analyses, toxicity, and biodegradation of naphthenic acids, *Chemosphere* 60 (2005) 585–600. doi:10.1016/j.chemosphere.2005.02.065.
- [11] A.K.H. Al jibouri, J. Wu, S.R. Upreti, Heterogeneous catalytic ozonation of naphthenic acids in water, *Can. J. Chem. Eng.* 97 (2018) 67–73. doi:10.1002/cjce.23209.
- [12] X. Xu, G. Pliego, J.A. Zazo, S. Sun, P. García-Muñoz, L. He, J.A. Casas, J.J. Rodriguez, An overview on the application of advanced oxidation processes for the removal of naphthenic acids from water, *Crit. Rev. Environ. Sci. Technol.* 47 (2017) 1337–1370. doi:10.1080/10643389.2017.1348113.
- [13] C. Wei, Z. Fengzhen, Y. Hu, C. Feng, Ozonation in water treatment : the generation, basic properties of ozone and its practical application, *Rev. Chem. Eng.* 33 (2017) 49–89. doi:10.1515/revce-2016-0008.
- [14] H. Karaca, Y.S. Velioglu, Ozone Applications in Fruit and Vegetable Processing, *Food Rev. Int.* 23 (2007) 91–106. doi:10.1080/87559120600998221.
- [15] A. Ried, J. Mielcke, A. Wieland, The Potential Use of Ozone in Municipal Wastewater, *Ozone Sci. Eng.* 31 (2009) 415–421. doi:10.1080/01919510903199111.
- [16] F.J. Beltran, Ozone reaction kinetics for water and wastewater systems, Lewis Publishers, Boca Raton, 2004.
- [17] A.C. Scott, W. Zubot, M.D. MacKinnon, D.W. Smith, P.M. Fedorak, Ozonation of oil sands process water removes naphthenic acids and toxicity, *Chemosphere* 71 (2008) 156–160. doi:10.1016/j.chemosphere.2007.10.051.
- [18] C. Wang, N. Klammerth, S.A. Messele, A. Singh, M. Belosevic, M. Gamal El-Din, Comparison of UV/hydrogen peroxide, potassium ferrate(VI), and ozone in oxidizing the organic fraction of oil sands process-affected water (OSPW), *Water Res.* 100 (2016) 476–485. doi:10.1016/j.watres.2016.05.037.
- [19] J.C. Anderson, S.B. Wiseman, N. Wang, A. Moustafa, L. Perez-Estrada, M.G. El-din, J.W. Martin, K. Liber, J.P. Giesy, Effectiveness of Ozonation Treatment in Eliminating Toxicity of Oil Sands Process-Affected Water to *Chironomus dilutus*, *Environ. Sci. Technol.* 46 (2012) 486–493. doi:dx.doi.org/10.1021/es202415g |.
- [20] M.H. El-Naas, M.A. Alhaija, S. Al-Zuhair, Evaluation of an activated carbon packed bed for the adsorption of phenols from petroleum refinery wastewater, *Environ. Sci. Pollut. Res.* (2017). doi:10.1007/s11356-017-8469-8.
- [21] Z. Xia, L. Hu, Treatment of Organics Contaminated Wastewater by Ozone Micro-Nano-Bubbles, *Water*. 11 (2019) 55. doi:10.3390/w11010055.
- [22] L. Chu, X. Xing, A. Yu, Y. Zhou, X. Sun, Enhanced ozonation of simulated dyestuff wastewater by microbubbles, *Chemosphere* 68 (2007) 1854–1860.

doi:10.1016/j.chemosphere.2007.03.014.

- [23] G. Boczkaj, A. Fernandes, P. Makos, Study of different advanced oxidation processes for wastewater treatment study of different advanced oxidation processes for wastewater treatment from petroleum bitumen production at basic pH, *Ind. Eng. Chem. Res.* 56 (2017) 8806–8814. doi:10.1021/acs.iecr.7b01507.
- [24] M.S. Lucas, J.A. Peres, G. Li Puma, Treatment of winery wastewater by ozone-based advanced oxidation processes (O₃, O₃/UV and O₃/UV/H₂O₂) in a pilot-scale bubble column reactor and process economics, *Sep. Purif. Technol.* 72 (2010) 235–241. doi:10.1016/j.seppur.2010.01.016.
- [25] B.W. Liu, M.S. Chou, C.M. Kao, B.J. Huang, Evaluation of Selected Operational Parameters for the Decolorization of Dye- Finishing Wastewater Using UV/Ozone, *Ozone Sci. Eng.* 26 (2004) 239–245. doi:10.1080/01919510490455557.
- [26] J.Y.U. Kim, G.G. Bessegato, B.C. de Souza, J.J. da Silva, M.V.B. Zanoni, Efficient treatment of swimming pool water by photoelectrocatalytic ozonation: Inactivation of *Candida parapsilosis* and mineralization of Benzophenone-3 and urea, *Chem. Eng. J.* 378 (2019) 1–10. doi:10.1016/j.cej.2019.122094.
- [27] S.T. Summerfelt, Ozonation and UV irradiation - An introduction and examples of current applications, *Aquac. Eng.* 28 (2003) 21–36. doi:10.1016/S0144-8609(02)00069-9.
- [28] H. Demir-Duz, A.S. Aktürk, O. Ayyildiz, M.G. Alvarez, S. Contreras, Reuse and recycle solutions in refineries by ozone-based advanced oxidation processes : A statistical approach, *J. Environ. Manage.* 263 (2020) 110346. doi:https://doi.org/10.1016/j.jenvman.2020.110346.
- [29] C. Li, L. Fu, J. Stafford, M. Belosevic, M. Gamal El-Din, The toxicity of oil sands process-affected water (OSPW): A critical review, *Sci. Total Environ.* 601–602 (2017) 1785–1802. doi:10.1016/j.scitotenv.2017.06.024.
- [30] E. Garcia-Garcia, J.Q. Ge, A. Oladiran, B. Montgomery, M.G. El-Din, L.C. Perez-Estrada, J.L. Stafford, J.W. Martin, M. Belosevic, Ozone treatment ameliorates oil sands process water toxicity to the mammalian immune system, *Water Res.* 45 (2011) 5849–5857. doi:10.1016/j.watres.2011.08.032.
- [31] E. Garcia-Garcia, J. Pun, L.A. Perez-Estrada, M.G. El Din, D.W. Smith, J.W. Martin, M. Belosevic, Commercial naphthenic acids and the organic fraction of oil sands process water downregulate pro-inflammatory gene expression and macrophage antimicrobial responses, *Toxicol. Lett.* 203 (2011) 62–73. doi:10.1016/j.toxlet.2011.03.005.
- [32] S. Jiménez, M. Andreozzi, M.M. Micó, M.G. Álvarez, S. Contreras, Produced water treatment by advanced oxidation processes, *Sci. Total Environ.* 666 (2019) 12–21. doi:10.1016/j.scitotenv.2019.02.128.
- [33] How to use the Microtox ® Acute Toxicity Test to perform an In-House Toxicity Reduction Evaluation (TRE), (2006). <http://foros.santafe-conicet.gob.ar/fotorreactores/archivos.php?action=downloadfile&filename=Mtx-TRE20Guide.pdf&directory=Procedimientos de uso de los equipos/Microtox> (accessed January 24, 2020).
- [34] APHA Method 4500-O3: Standard Methods for the Examination of Water and Wastewater,

1992.

- [35] J.R. Bolton, K.G. Bircher, W. Tumas, C.A. Tolman, Figures-of-merit for the technical development and application of advanced oxidation technologies for both electric- and solar-driven systems, *J. Adv. Oxid. Technol.* 1 (1996) 13–17. doi:10.1351/pac200173040627.

7

Main Conclusions

&

Future Works



UNIVERSITAT ROVIRA I VIRGILI

Application of Advanced Oxidation Processes in the Reclamation of Wastewaters from the Oil
& Gas Sector

Hande Demir Duz

This thesis aimed to contribute to the reclamation of wastewaters from the oil & gas industry that generates high amount of effluents, increasing the water stress worldwide. Different types of advanced oxidation processes were applied to upstream and downstream effluents collected from two petroleum related industries: a petroleum refinery located in Turkey and oil sand processing plant located in Canada. The efficiencies of photo-based and ozone-based treatments for the effluents compared and discussed in detail taking into account the objectives stated in Chapter 1.

The applied treatments for the petroleum refinery effluents included in Chapter 3 and Chapter 4 revealed that:

- ✓ Initial photo-based and ozone-based experiments conducted with a complex simulated synthetic refinery wastewater, containing a mixture of BTEX, PAHs and alkenes in a saline matrix, guided the treatment of real effluents in terms of identifying the initial parameters such as the amount of reactants and the reaction conditions on a stable medium, considering the known composition of the synthetic effluent. Detailed study of the real effluents showed that both higher amount of reactants and reaction time were necessary, comparing to synthetic refinery wastewater, due to more complex composition of the real effluents.
- ✓ Photo-Fenton was the most effective photo-based treatment for the treatment of RRW1 effluent (i.e., collected before biological treatment). Although photo-Fenton was performed by adding very low amount of Fe to the medium, this method was not appropriate when looking at the reuse of the treated effluents, considering the final TOC reached after treatment (ca. 20 mg/L). Even so, photo-Fenton can be used instead of biological treatment, which can prevent from the huge amount of sludge formation, since the amount of iron that will precipitate at the end of the treatment is quite low. In this sense, also, faster treatment than biological treatment would be possible. Heterogeneous photo-catalysis was found to be ineffective to treat RRW1 despite the high effectiveness showed in the treatment of SRW and RRW2. This demonstrates the high impact of turbidity on heterogeneous photo-catalysis. Contrarily to that found with RRW1 water, either photo-Fenton or heterogeneous photo-catalysis with TiO_2 made it possible to reuse treated RRW2 (i.e., collected after biological treatment) as cooling water or firewater. However, in both cases, the recovery of the catalysts (8 mg/L for

photo-Fenton, 500 mg/L for photo-catalysis with TiO_2) must be considered after the treatment.

- ✓ The application of $\text{O}_3/\text{H}_2\text{O}_2$ as a tertiary treatment was found to be the best option considering all effluents produced in the refinery, as well as no sludge production. The importance of the parameters optimization by experimental design has been demonstrated to reduce the operation costs while achieving high treatment efficiency that allow water reuse in the plant. It should be considered that the optimization has to be performed on a case-by-case analysis, since different properties of the effluents may effect the treatment efficiencies, and as a result, the optimized parameters.

The applied treatments for the oil sands process water included in Chapter 5 and Chapter 6 revealed that:

- ✓ Statistical approaches can be used for screening the effect of parameters on a response, which was the concentration removal in this thesis. This approach allowed selecting the best catalysts and knowing the significant parameters quickly and reliably. In Chapter 5, fractional factorial design was studied for different catalysts to observe the effects of O_3 dose, catalyst amount, pH and reaction time on the ACA concentration removal. An increase in the O_3 dose, catalyst amount and reaction time, increased the removal efficiency while the effect of the pH was varied depending on the catalyst (in some cases negatively).
- ✓ Considering both O_3 treatment and photo-based treatments applied in Chapter 5, GAC based materials were more effective when ozone or H_2O_2 were used as oxidant rather than PMS in terms of the final concentration of NAs and mineralization degree.
- ✓ The comparison between batch ozonation, UV/ H_2O_2 , UV/PMS and UV/Fenton suggested that UV/Fenton applied at pH 3 with 5 mg/L Fe^{2+} was more effective to obtain high mineralization rather than transformation of components, which would allow the discharge of the effluent after treatment or increasing its reuse opportunity in the plant.
- ✓ When the interests are directed toward mineralization by ozone-based treatments, which was not possible to reach by batch mode with low amount of O_3 dose, $\text{O}_3/\text{H}_2\text{O}_2$ treatment applied in semi-batch mode was found to be the most effective treatment of OSPW considering the mineralization degree reached after 90 min treatment and economic comparisons. In addition to $\text{O}_3/\text{H}_2\text{O}_2$ process, the use of UV-C with $\text{O}_3/\text{H}_2\text{O}_2$ can allow to obtain a good

quality of effluent to reuse it in the plant for several purposes, since the final DOC was ca. 2 mg/L after treatment.

In general, considering all the applied treatments within this thesis, O_3/H_2O_2 treatment was found as the best process to be used in oil & gas sector since it resulted suitable for both upstream and downstream process effluents, according also to previous studies of the research group performed on produced water. Through this treatment it was obtained a high mineralization degree at mild conditions (natural temperature and pH as well as atmospheric pressure), which results in high quality water after treatment. The treatment system can be optimized to reduce residual ozone that escapes in gas phase without reacting in liquid phase. Thus, the cost of the treatment system can be reduced significantly.

However, in some cases, photo-based treatments could be more interesting considering the possibilities of using sun as the energy source. In that case, photo-Fenton system can be a suitable candidate to treat the effluents from oil & gas sector with lower cost, according to the results obtained at lab scale treatment that was performed in a solar light simulator. Some more improvements to reduce the cost, such as increasing the operation pH, could be studied, since this treatment at pH 3 reached high efficiencies for both effluents with very low amount of catalyst, which decreased down to 5 mg/L in this thesis. The discharging limit for Fe is ranged between 2-10 mg/L depending on the policies of different countries.

8

Publications & Communications



UNIVERSITAT ROVIRA I VIRGILI

Application of Advanced Oxidation Processes in the Reclamation of Wastewaters from the Oil
& Gas Sector

Hande Demir Duz

8.1 Published Articles

Demir-Duz, H., Ayyildiz. O., Akturk, A. S., Álvarez, M. G., Contreras, S. (2020). Reuse and recycle solutions in refineries by ozone-based advanced oxidation processes: A statistical approach. *Journal of Environmental Management* Vol. 263, pp.110346 (<https://doi.org/10.1016/j.jenvman.2020.110346>).

Demir-Duz, H., Ayyildiz. O., Akturk, A. S., Álvarez, M. G., Contreras, S. (2019). Approaching zero discharge concept in refineries by solar-assisted photo-Fenton and photo-catalysis processes. *Applied Catalysis B: Environmental*, Vol 248, pp. 341-348 (<https://doi.org/10.1016/j.apcatb.2019.02.026>).

8.2 Articles to Be Submitted

Demir-Duz, H., Messele, S. A., Álvarez, M. G., Contreras, S., El-Din, M. G. (2020). Comparison of Catalytic Ozone, UV/H₂O₂, UV/PMS and UV/Fenton in Degrading the Naphthenic Acid Fraction in Oil Sands Process Water.

Demir-Duz, H., Pérez-Estrada, L., Messele, S. A., Álvarez, M. G., El-Din, M. G., Contreras, S. (2020). Synergetic Effect of O₃/H₂O₂ and UV-C Light Irradiation for the Treatment of Oil Sands Process Water.

8.3 Oral Communications

Demir-Duz, H., Messele, S. A., Álvarez, M. G., Contreras, S., El-Din, M. G. (October, 2019). Comparison of UV/Fenton, UV/H₂O₂, UV/Oxone and Ozone in degrading the naphthenic acids in oil sands process water. Oral presentation at IOA24 Ozone World Congress & Exhibition, Nice, France.

Demir-Duz, H., Ayyildiz. O., Akturk, A. S., Álvarez, M. G., Contreras, S. (June, 2019), Reuse and recycle solutions in refineries by Ozone/H₂O₂: A real case study by Box-Behnken experimental design. Oral presentation at 6th European Conference on Environmental Applications of AOPs, Portoroz, Slovenia.

Demir-Duz, H. (May, 2019), Application of advanced oxidation processes in the reclamation of wastewaters from the oil & gas sector. Oral presentation at 16th Doctoral Day, URV, Tarragona, Spain.

Demir-Duz, H., Messele, S. A., Álvarez, M. G., Contreras, S., El-Din, M. G. (May, 2019) Catalytic ozone-based treatment of oil sands process water by heteroatom

doped Fe/GAC. Oral presentation at CAWQ-11th Western Canadian Symposium on Water Quality Research, Edmonton, Canada.

Demir-Duz, H., Álvarez, M. G., Contreras, S. (June, 2018) Petroleum refinery wastewater treatment by photo-Fenton and photo-catalysis under solar light irradiation. Oral presentation at 10th European Meeting on Solar Chemistry and Photocatalysis: Environmental Applications (SPEA10), Almeria, Spain

8.4 Poster Presentation

Demir-Duz, H., Messele, S. A., Álvarez, M. G., Contreras, S., El-Din, M. G. (May, 2019) Granular activated carbon-based catalysts for treatment of oil sands process water by advanced oxidation processes. Poster presentation at University of Alberta Energy week, FES Colloquium, Edmonton, Canada.

Demir-Duz, H., Álvarez, M. G., Contreras, S. (June, 2018) Petroleum refinery wastewater treatment by photo-Fenton and photo-catalysis under solar light irradiation. Poster presentation at 10th European Meeting on Solar Chemistry and Photocatalysis: Environmental Applications (SPEA10), Almeria, Spain.

Demir-Duz, H., Álvarez, M. G., Contreras, S. (May, 2018), Refinery wastewater treatment solutions by advanced oxidation processes. Poster presentation at 15th Doctoral Day, URV, Tarragona, Spain

Demir-Duz, H., Álvarez, M. G., Contreras, S. (July, 2017), Application of Fenton-based processes in the reclamation of refinery wastewater, Poster presentations at 2nd Summer School on Environmental Applications of Advanced Oxidation Processes, Porto, Portugal

Demir-Duz, H., Álvarez, M. G., Contreras, S. (May, 2017), Application of advanced oxidation processes in the reclamation of wastewaters from the oil & gas sector. Poster presentation at 14th Doctoral Day, URV, Tarragona, Spain

APPENDICES

Appendix A: Additional Figures and Tables from Chapter 3

Table Appx. A1 Summary of experimental conditions tested, and main results obtained with the SRW.

Synthetic Refinery Wastewater					
Photo-Fenton increasing Fe²⁺ with constant H₂O₂			TiO₂-photo-catalysis increasing catalyst amount		
H₂O₂/COD	H₂O₂/Fe²⁺	TOC Removal % at 90 min	TiO₂ (mg/L)	TOC Removal % at 360 min	
2	5	72	100	64	
2	10	76	250	80	
2	50	81	500	81	
Photo-Fenton increasing H₂O₂ with constant Fe²⁺			pH effect on TiO₂-photo-catalysis with 250 mg/L catalyst		
H₂O₂/COD	H₂O₂/Fe²⁺	TOC Removal % at 90 min	pH	TOC Removal % at 360 min	
1	50	75	3	67	
2	50	81	5	91	
4	50	77	8	80	

Table Appx. A2 Summary of experimental conditions tested, and main results obtained with the RRW1.

Photo-Fenton			
H₂O₂/COD	H₂O₂/Fe²⁺	TOC removal at 90 min (%)	TOC removal at 180 min (%)
2	50	58	-
2	100	67	70
4	100	65	74
4	10	63	68
4	50	67	-
10	50	75	76
TiO₂-photo catalysis (pH free)			
Catalyst amount (mg/L)		TOC removal at 90 min (%)	TOC removal at 360 min (%)
100		24	26
250		26	27
500		24	30
Combination of photo-Fenton/photo-catalysis			
"One after the other" mode			TOC removal (%)
1. Step: photo-Fenton (180 min) H ₂ O ₂ /COD=4; H ₂ O ₂ /Fe ²⁺ =100			74
2. Step: photo-catalysis (360 min) 500 mg/L TiO ₂			63
Total treatment (540 min)			90
"Synchronous" mode			TOC removal (%)
1. Step: Combination (90 min) 100 mg/L TiO ₂ ; H ₂ O ₂ /Fe ²⁺ =100; H ₂ O ₂ /COD=2			71
100 mg/L TiO ₂ ; H ₂ O ₂ /Fe ²⁺ =100; H ₂ O ₂ /COD=4			79
100 mg/L TiO ₂ ; H ₂ O ₂ /Fe ²⁺ =100; H ₂ O ₂ /COD=10			84

Table Appx. A3 Summary of experimental conditions tested, and main results obtained with the RRW2.

Photo-Fenton			
H₂O₂/COD	H₂O₂/Fe²⁺	TOC removal at 90 min (%)	TOC removal at 180 min (%)
2	50	46	-
4	50	58	69
4	10	64	78
10	50	69	78
2	10	50	62
10	10	65	73
TiO₂-photo catalysis (pH free)			
Catalyst amount (mg/L)		TOC removal at 90 min (%)	TOC removal at 360 min (%)
100		0.1	33
250		20	70
500		27	73
TiO₂-photo catalysis (pH 5)			
Catalyst amount (mg/L)		TOC removal at 90 min (%)	TOC removal at 360 min (%)
500		56	92

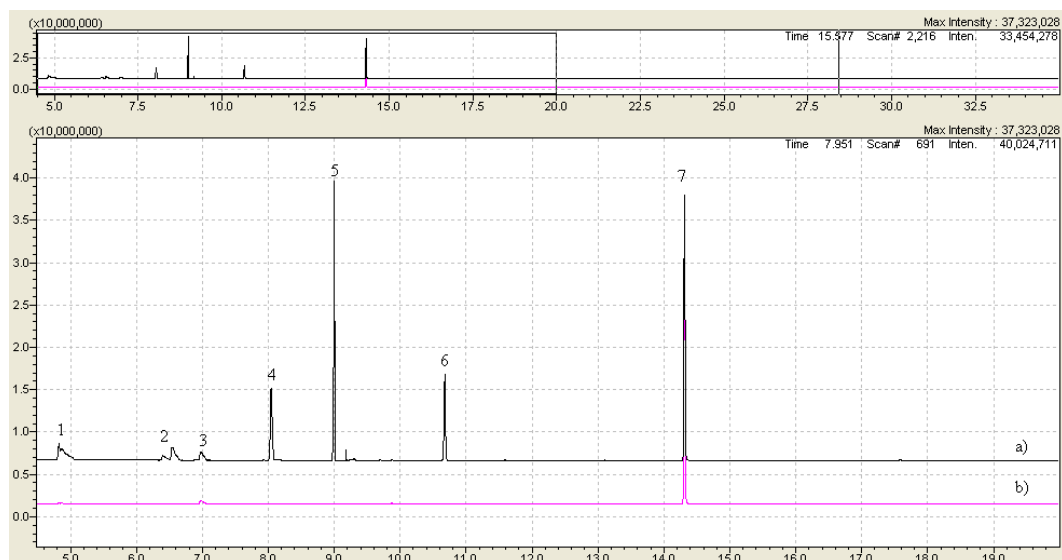


Figure Appx. A1 GC-MS chromatogram after photo-Fenton test with the $\text{H}_2\text{O}_2/\text{COD}$ ratio of 2 and the $\text{H}_2\text{O}_2/\text{Fe}^{2+}$ ratio of 50. a) Initial SRW; b) after 1.5h: 1) toluene; 2) xylene; 3) nonane; 4) phenol; 5) o-cresol; 6) naphthalene; 7) hexadecane.

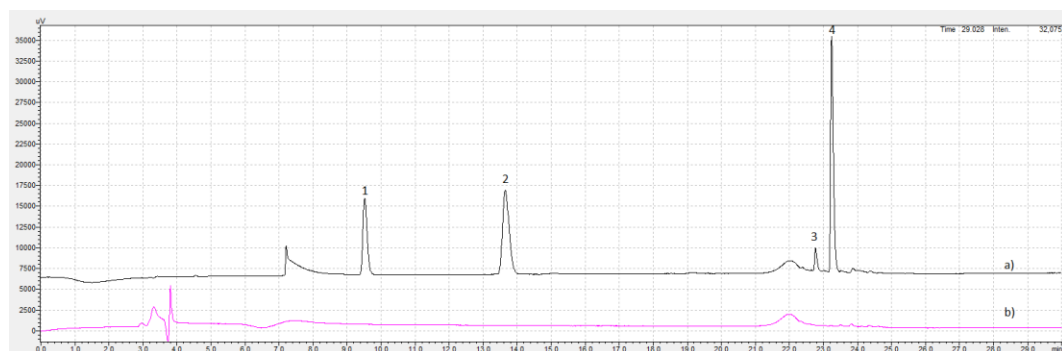


Figure Appx. A2 HPLC chromatogram after photo-Fenton with the $\text{H}_2\text{O}_2/\text{COD}$ ratio of 2 and the $\text{H}_2\text{O}_2/\text{Fe}^{2+}$ ratio of 50. a) Initial SRW; b) after 1.5h: 1) phenol; 2) o-cresol; 3) toluene; 4) naphthalene.

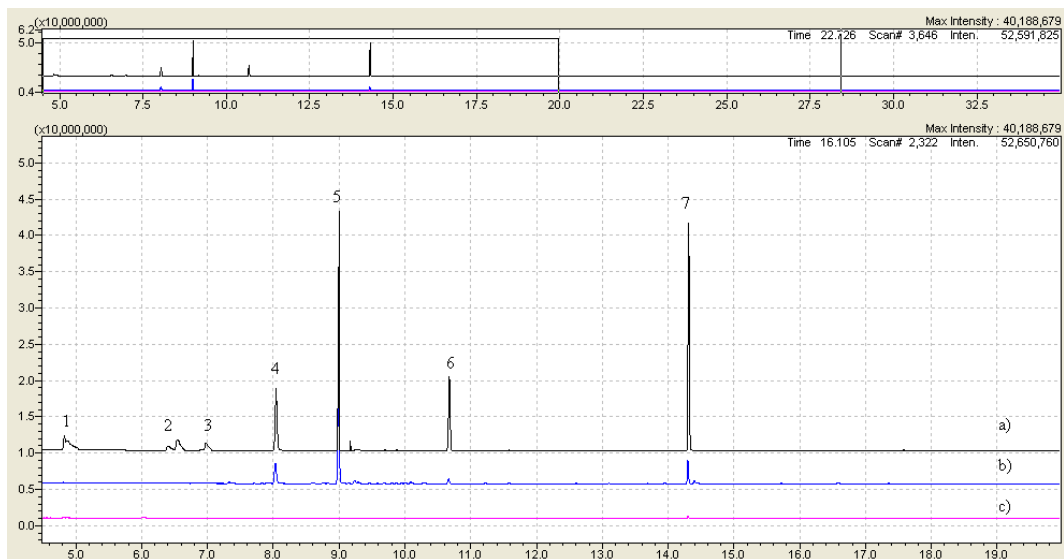


Figure Appx. A3 GC-MS chromatogram after photo-catalysis with 250 ppm catalyst a) Initial SRW; b) after 1.5h; c) after 6h: 1) toluene; 2) xylene; 3) nonane; 4) phenol; 5) o-cresol; 6) naphthalene; 7) hexadecane.

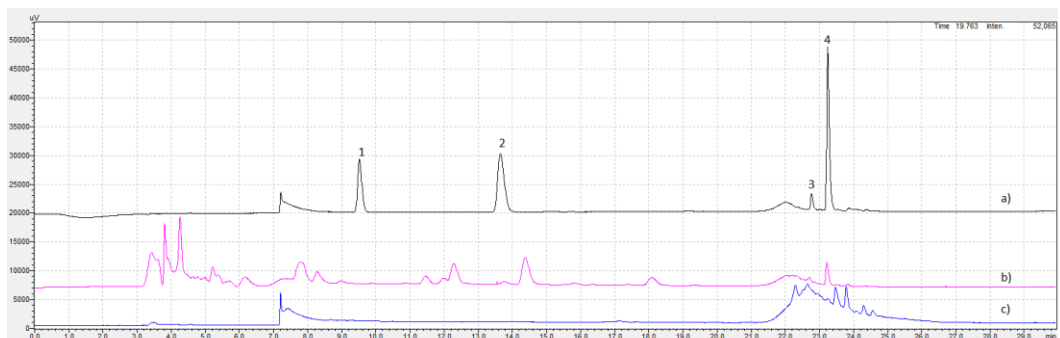


Figure Appx. A4 HPLC chromatogram after photo-catalysis with 250 ppm catalyst a) Initial SRW; b) after 1.5 h; c) after 6 h: 1) phenol; 2) o-cresol; 3) toluene; 4) naphthalene.

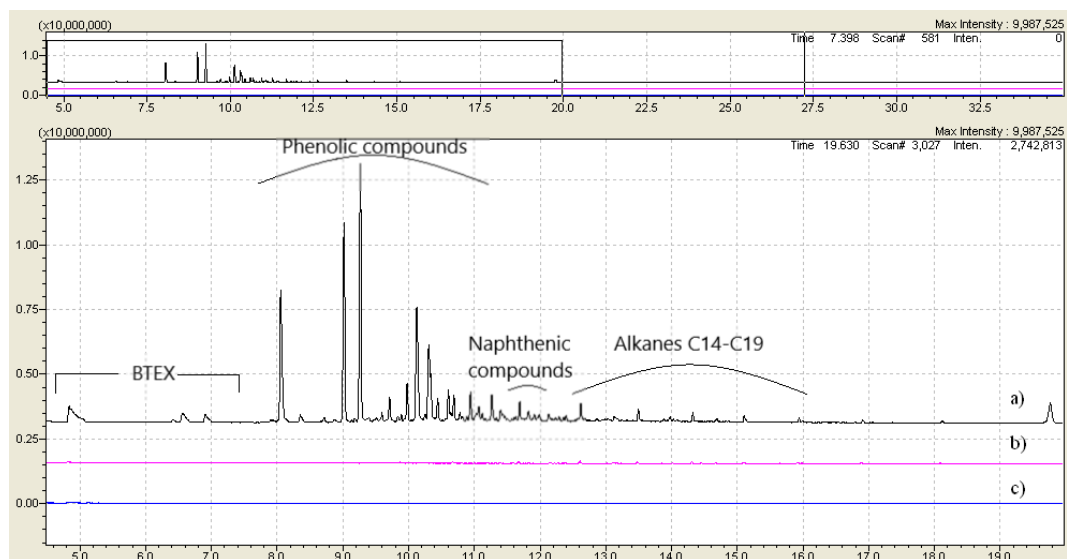


Figure Appx. A5 GC-MS chromatogram of a)Initial RRW and after 1.5h synchronous photo-Fenton/photo catalysis treatment b) $H_2O_2/COD=4$, $H_2O_2/Fe=100$, $TiO_2=100ppm$, $pH=3$; c) $H_2O_2/COD=10$, $H_2O_2/Fe=100$, $TiO_2=100ppm$, $pH=3$.

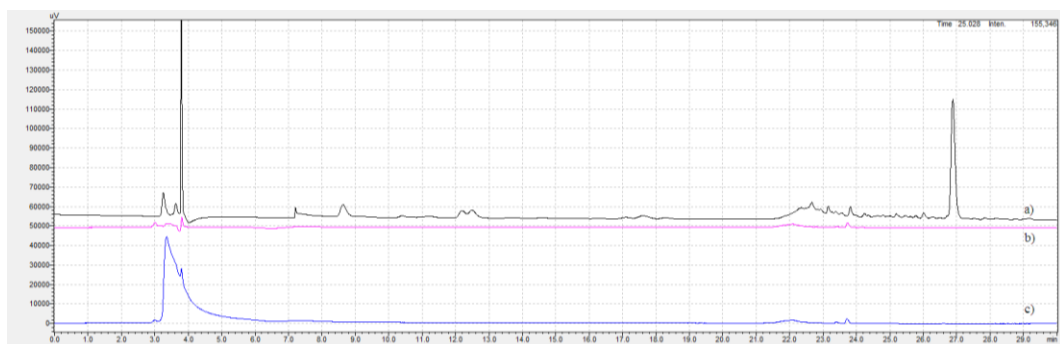
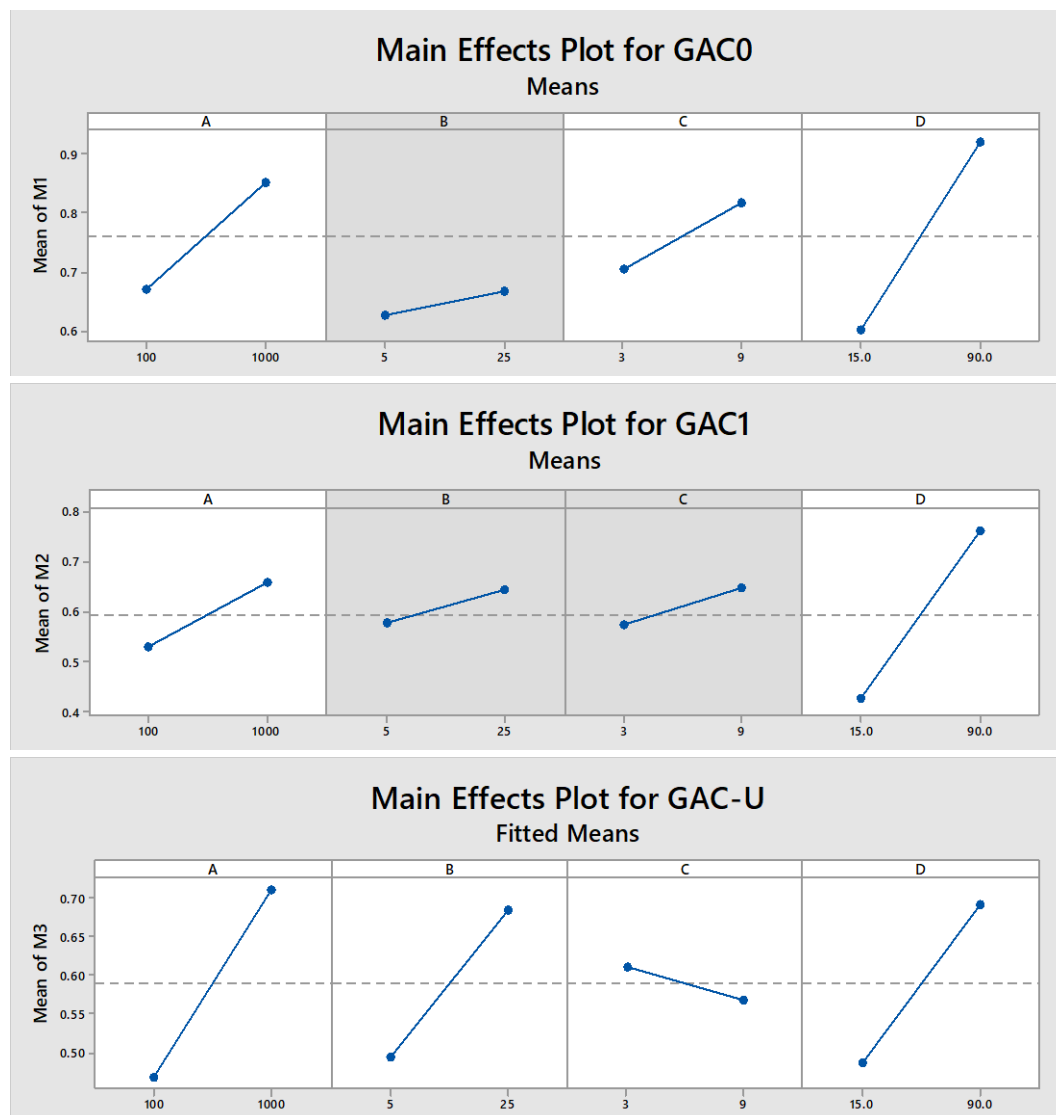
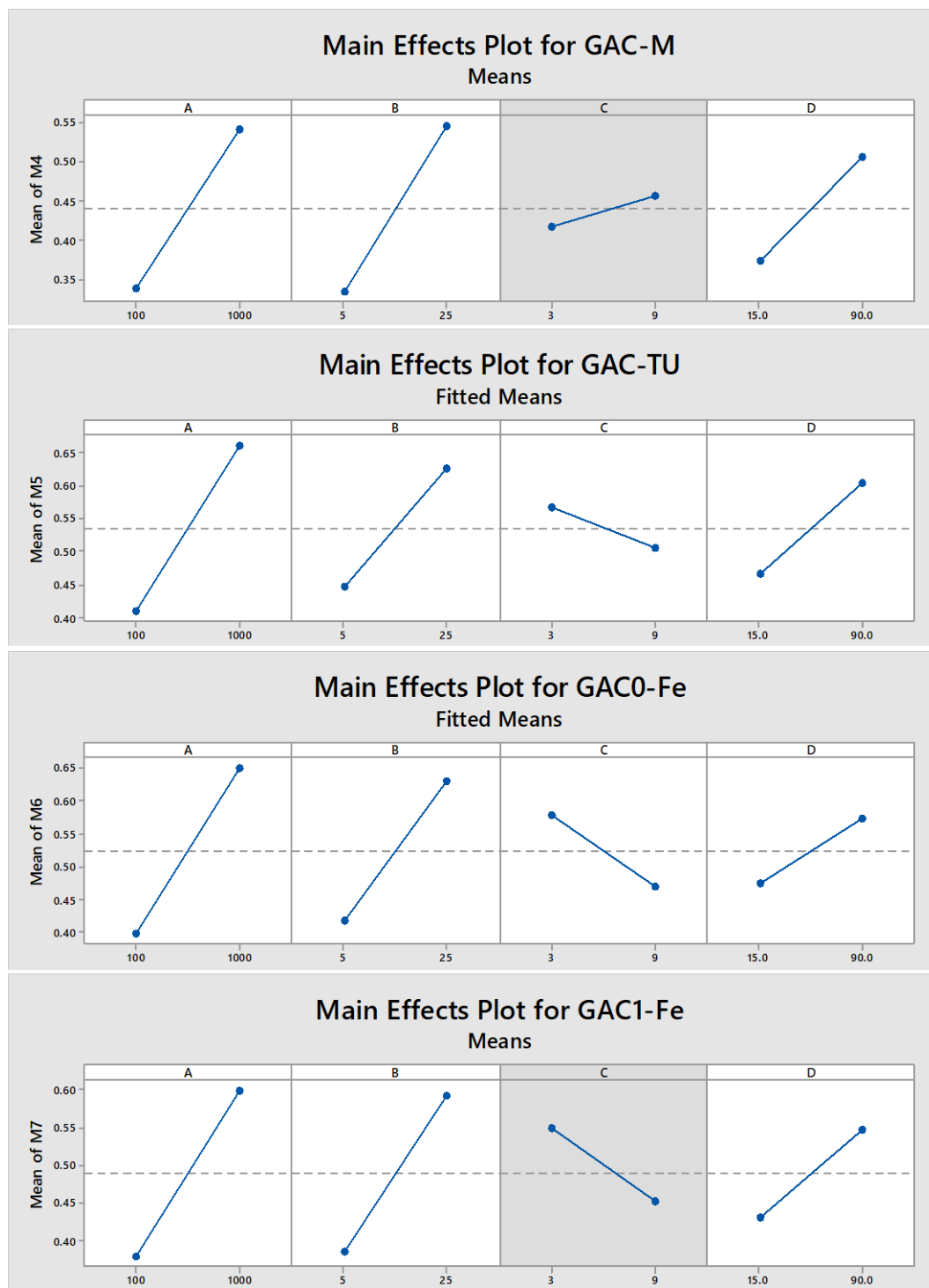


Figure Appx. A6 HPLC chromatogram of a) initial RRW and after 1.5h synchronous photo-Fenton/photo catalysis treatment b) $H_2O_2/COD=4$, $H_2O_2/Fe=100$, $TiO_2=100ppm$, $pH=3$; c) $H_2O_2/COD=10$, $H_2O_2/Fe=100$, $TiO_2=100ppm$, $pH=3$

Appendix B: Additional Figures and Tables from Chapter 5

Main Effects of the parameters on the catalytic ozone treatment of effluent prepared with ACA:





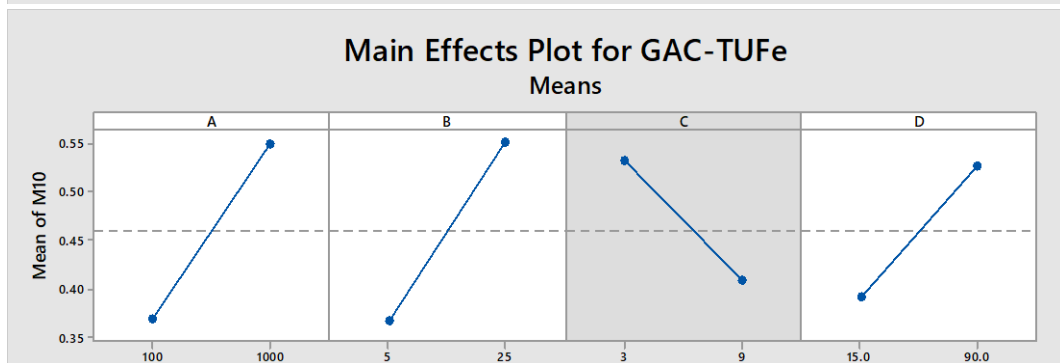
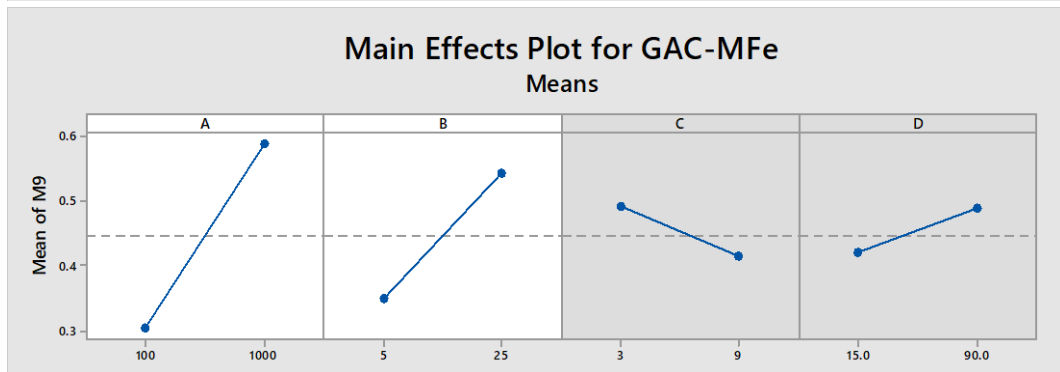
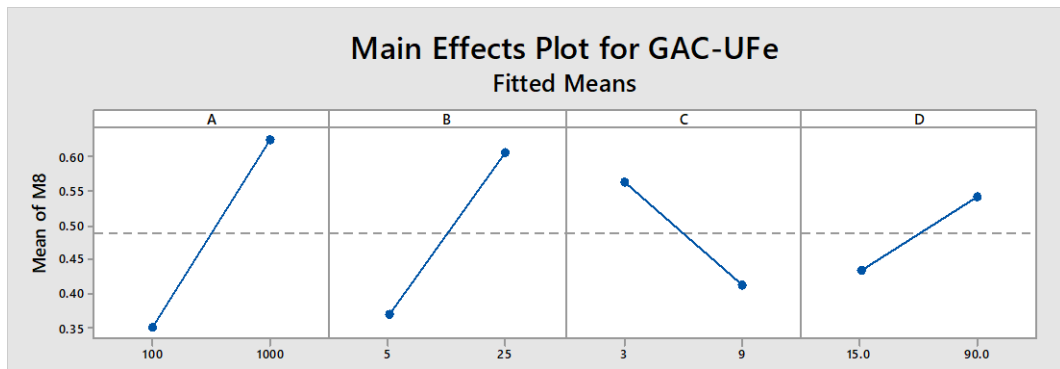


Table Appx. B1 Summary of ozone-based treatments.

Treatment	Catalyst	Catalyst Amount (g/L)	O ₃ amount (mg/L)	DOC	NAs
Adsorption	GAC0	0.5	-	25%	49%
	GAC-U	0.5	-	33%	60%
	GAC-TU	0.5	-	21%	41%
	GAC-UFe	0.5	-	27%	56%
	GAC-TUFe	0.5	-	33%	63%
Ozonation	GAC0	0.5	25	11%	93%
	GAC-U	0.5	25	6%	95%
	GAC-TU	0.5	25	15%	96%
	GAC-UFe	0.5	25	11%	95%
	GAC-TUFe	0.5	25	7%	93%
	Single	-	25	0%	91%
	GAC0	0.5	10	21%	92%
	GAC-U	0.5	10	17%	85%
	GAC-TU	0.5	10	18%	86%
	GAC-UFe	0.5	10	6%	81%
	GAC-TUFe	0.5	10	17%	84%
	GAC0	0.1	10	0%	78%
	GAC-U	0.1	10	0%	79%
	GAC-TU	0.1	10	2%	79%
	GAC-UFe	0.1	10	1%	77%
	GAC-TUFe	0.1	10	0%	78%
	Single	-	10	0%	63%

Table Appx. B2 Summary of photo-based treatments.

Treatment	Catalyst	Catalyst Amount (g/L)	Oxidant	Oxidant/ COD (w/w)	pH	DOC	NAs
photo-Fenton	Fe ²⁺	0.005	H ₂ O ₂	1	3	26%	90%
		0.005	H ₂ O ₂	2	3	51%	99%
		0.005	H ₂ O ₂	2.5	3	63%	95%
		0.005	H ₂ O ₂	5	3	64%	82%
Fenton-like	GAC0	0.1	H ₂ O ₂	2.5	3	15%	77%
	GAC-U	0.1	H ₂ O ₂	2.5	3	14%	73%
	GAC-TU	0.1	H ₂ O ₂	2.5	3	14%	77%
	GAC-UFe	0.1	H ₂ O ₂	2.5	3	14%	70%
	GAC-TUFe	0.1	H ₂ O ₂	2.5	3	0%	60%
	GAC0	0.1	H ₂ O ₂	2.5	8.45	27%	98%
	GAC-U	0.1	H ₂ O ₂	2.5	8.45	29%	99%
	GAC-TU	0.1	H ₂ O ₂	2.5	8.45	28%	98%
	GAC-UFe	0.1	H ₂ O ₂	2.5	8.45	29%	99%
	GAC-TUFe	0.1	H ₂ O ₂	2.5	8.45	31%	98%
PMS	GAC0	0.1	PMS	2.5	8.45	12%	N/A
	GAC-U	0.1	PMS	2.5	8.45	14%	N/A
	GAC-TU	0.1	PMS	2.5	8.45	11%	N/A
	GAC-UFe	0.1	PMS	2.5	8.45	9%	N/A
	GAC-TUFe	0.1	PMS	2.5	8.45	10%	N/A

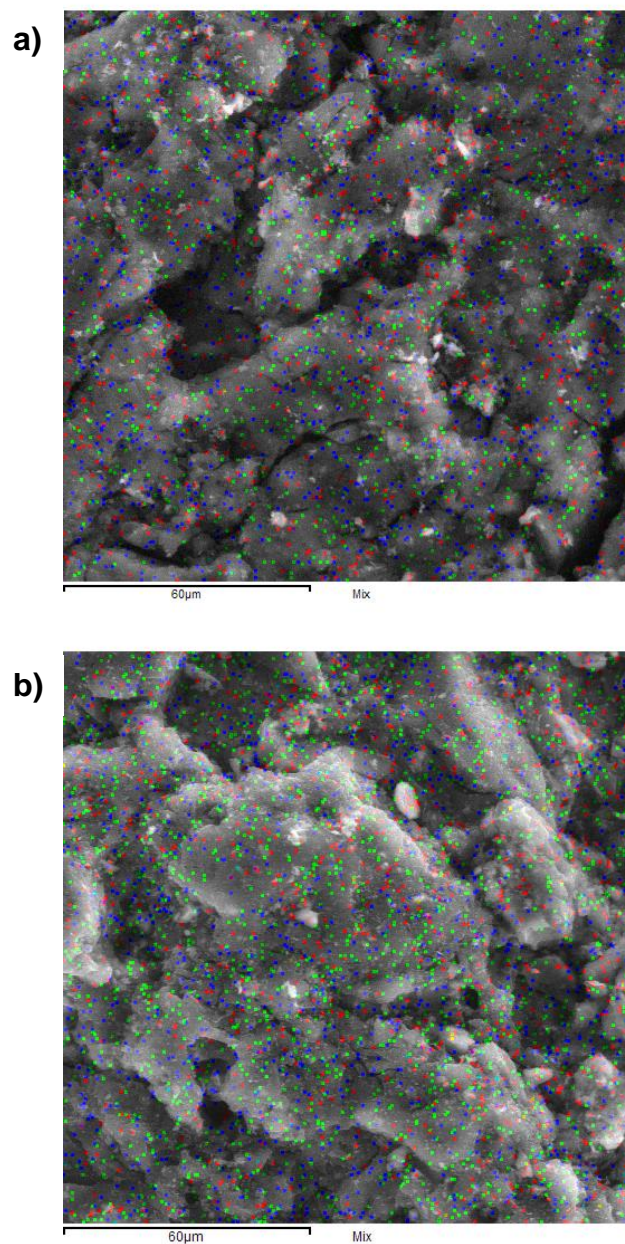


Figure Appx. B1 SEM-EDX mapping images and elemental distribution (O-red, S-green, Fe-blue) of Fe-based catalysts a)GAC-UFe, b)GAC-TUFe.

UNIVERSITAT ROVIRA I VIRGILI

Application of Advanced Oxidation Processes in the Reclamation of Wastewaters from the Oil
& Gas Sector

Hande Demir Duz